EFFICACY OF GREEN SYNTHESISED ZINC OXIDE NANOPARTICLES AGAINST MULTI-DRUG RESISTANT NON-TYPHOIDAL *SALMONELLA* SPP.

VARSHA UNNI

(19-MVP-33)

THESIS

Submitted in partial fulfilment of the requirement for the degree of

MASTER OF VETERINARY SCIENCE

(Veterinary Public Health)

2021

Faculty of Veterinary and Animal Sciences

Kerala Veterinary and Animal Sciences University

DEPARTMENT OF VETERINARY PUBLIC HEALTH

COLLEGE OF VETERINARY AND ANIMAL SCIENCES

POOKODE, LAKKIDI P.O., WAYANAD-673 576

KERALA, INDIA

EFFICACY OF GREEN SYNTHESISED ZINC OXIDE NANOPARTICLES AGAINST MULTI-DRUG RESISTANT NON-TYPHOIDAL *SALMONELLA* SPP.

VARSHA UNNI

(19-MVP-33)

THESIS

Submitted in partial fulfilment of the requirement for the degree of

MASTER OF VETERINARY SCIENCE

(Veterinary Public Health)

2021

Faculty of Veterinary and Animal Sciences

Kerala Veterinary and Animal Sciences University

DEPARTMENT OF VETERINARY PUBLIC HEALTH

COLLEGE OF VETERINARY AND ANIMAL SCIENCES

POOKODE, LAKKIDI P.O., WAYANAD-673 576

KERALA, INDIA

DECLARATION

I hereby declare that this thesis entitled **"Efficacy of green synthesised Zinc oxide nanoparticles against multi-drug resistant non-typhoidal *Salmonella* spp."** is a bonafide record of research done by me during the course of research and that the thesis has not previously formed the basis for the award of any degree, diploma, fellowship or other similar title, of any other University or Society.

Pookode **VARSHA UNNI**

Date: **(19-MVP-33)**

Dr. Jess Vergis
Assistant Professor
Department of Veterinary Public Health
Kerala Veterinary and Animal Sciences University
Pookode, Wayanad, Kerala – 673576

CERTIFICATE

Certified that this thesis, entitled **"Efficacy of green synthesised Zinc oxide nanoparticles against multi-drug resistant non-typhoidal *Salmonella* spp."** is a record of research work done independently by **Varsha Unni (19-MVP -33)** under my guidance and supervision and that it has not previously formed the basis for the award of any degree, diploma, fellowship or associateship to her.

Pookode
Date:

Dr. Jess Vergis
Chairperson
Advisory Committee

CERTIFICATE

We, the undersigned, members of the Advisory Committee of **Varsha Unni (19-MVP-33)**, a candidate for the degree of Master of Veterinary Science in Veterinary Public Health agree that the thesis entitled **"Efficacy of green synthesised Zinc oxide nanoparticles against multi-drug resistant non-typhoidal *Salmonella* spp."** may be submitted by **Varsha Unni (19-MVP-33),** in partial fulfilment of the requirement for the degree.

Dr. Jess Vergis
Assistant Professor
Department of Veterinary Public Health
College of Veterinary and Animal Sciences
Pookode, Wayanad, Kerala-673 576
(Chairperson)

Dr. Latha C.
Professor and Head
Department of Veterinary Public Health
College of Veterinary and Animal Sciences, Mannuthy
Thrissur, Kerala-673 576
(Member)

Dr. Prejit
Assistant Professor and Head (i/C)
Department of Veterinary Public Health
College of Veterinary and Animal Sciences, Pookode, Wayanad,
Kerala-673 576
(Member)

Dr. Lijo John
Assistant Professor
Department of Veterinary Biochemistry
College of Veterinary and Animal Sciences
Pookode, Wayanad, Kerala-673 576
(Member)

EXTERNAL EXAMINER

ACKNOWLEDGMENT

I feel a great sense of satisfaction and pride in submitting this research work to the vast ocean of human knowledge. Completion of this dissertation would not have been possible without the support and guidance of many people. I would like to take this opportunity to extend my deepest sense of gratitude and words of appreciation towards those, who dedicated their valuable time and energy for me.

I take this opportunity to sincerely acknowledge ***Dean****, CV & AS, Pookode for granting the necessary infrastructure and resources to accomplish my research work*

I do hereby express most sincere gratitude and thankfulness to my guide, ***Dr. Jess Vergis,*** *Assistant Professor, Department of Veterinary Public Health, College of Veterinary and Animal Sciences, Pookode, Wayanad for his meticulous guidance, personal care, persuasion and motivation rendered in all possible ways, which was the prime factor that led me to accomplish this endeavour. The constant guidance and encouragement that you delivered on me even in the midst of your tight work schedule were inevitably the motive for completion of this study. Words are inadequate to express my gratitude.*

I am extremely indebted to the members of my advisory committee ***Dr. Prejit,*** *Assistant Professor, Department of Veterinary Public Health, CV & AS, Pookode,* ***Dr. Latha C,*** *Professor and Head, Department of Veterinary Public Health,College of Veterinary and Animal Sciences, Mannuthy,* ***Dr. Lijo John,*** *Assistant Professor, Department of Veterinary Biochemistry, CV & AS, Pookode for their assiduous guidance, constant support, valuable advice and, wholeheartedcooperation on the present investigation and enquiring the progress of work from time to time.*

I owe my sincere gratitude to ***Dr.V.K.Vinod,*** *Assistant Professor, Department of Veterinary Public Health, CV & AS, Pookode****, Dr. Asha K****, Assistant Professor, Department of Veterinary Public Health, CV & AS, Pookode, and* ***Dr. Sanis Juliet****, Associate Professor, Department of Veterinary Pharmacology and Toxicology, CV & AS, Pookode,* ***Dr. Deepa C.K*** *&* ***Dr. Anju****., Assistant Professor, Department of Veterinary Parasitology, CV & AS, Pookode, for their creative suggestions, sustained interest, valuable and wholehearted help during my course of work.*

I am greatful to the financial support for my Master's research from ***KVASU*** *Pookode.*

With exquisite pleasure, I express my deep thanks to ***ICAR-NASF*** *Project co-ordinator, investigators and research staff for granting the necessary fund, and resources to accomplish my research work.*

I am extremely grateful to ***Mr. Abishad P.M****, Senior Research Fellow, Department of Veterinary Public Health, Pookode for his selfless help rendered during the course of my research.*

I am short of words in expressing my deep sense of obligation to my seniors ***Dr Hema Persis Andrews, Dr. Hamna Hakim, Dr. Akarsh K.L.****, my colleagues* ***Dr. Manoj M, Dr. Anjitha G.S, Dr. Vidyavarsha, Dr. Gatchandra Shravan Kumar, Dr. Prabodh Kumar Hembram, Dr. Dhanya Thomas, Dr. Elizabeth, Dr. Merin Sneha, Dr. Jishnu Haridas P*** *and juniors* ***Dr. Arya P. R. and Dr. Anjusha K. M.*** *for their honestbacking, untiring support and constant inspiration which instilled in me the confidence to tackle many hurdles during the study.*

No phrase or words can ever express my deep sense of love and gratitude to my parents ***Mrs. V. Usha Devi*** *and* ***Mr. V. Unnikrishnan Nair****. I also owe gratitude to my beloved sister* ***Mrs. Reshma Unni,*** *and my better half* ***Mr. Athul G.R****, for being with me and also assisting me during difficult times throughout the*

work. Without their help, love and backing, my efforts would not have been met with success. I will always treasure the generous help, concern, encouragement, suggestions and moral support by them.

Above all, I bow before ***God*** *for all the blessings showered on me and being with me always and for his abundant grace, blessings, mercy and unfathomable love showered on me for completion of this study.*

VARSHA UNNI

TABLE OF CONTENTS

LIST OF TABLES

LIST OF FIGURES

LIST OF ABBREVIATIONS

%	: Per cent
µg	: Microgram
µL	: Microliter
Å	: Angstrom
AMP	: Ampicillin
AMC	: Amoxicillin
ANNOVA	: Analysis of variance
ATCC	: American type culture collection
AMR	: Antimicrobial resistance
AZM	: Azithromycin
bp	: Base pair
CA-MH	: Cation adjusted muller hinton
CAC	: Ceftazidime- clavulanic acid
CAZ	: Ceftazidime
CDC	: Centres for Disease Control and Prevention
CEC	: Cefotaxime- clavulanic acid
CFU	: Colony forming unit
CIP	: Ciprofloxacin
CL	: Chloramphenicol
CLSI	: Clinical Laboratory Standards Institute
CO	: Colistin sulphate
COT	: Co-trimoxazole
Cm	: Centimeter
CTR	: Ceftriaxone
CTX	: Cefotaxime

CuO	: Copper oxide
DNA	: Deoxyribonucleic acid
DO	: Doxycycline
DTA	: Differential thermogravimetric analysis
DMEM	: Dulbecco's Modified Eagle Medium
EDAX	: Energy dispersive X-ray analysis
et al.,	: etalii/Alia (any other people)
ETEC	: Enterotoxigenic *E. coli*
Fig	: Figure
FTIR	: Fourier transform infrared spectroscopy
g	: Gram
GDP	: Gross domestic product
GEN	: Gentamicin
h	: Hour
HEK	: Human embryonic kidney
HR TEM	: High resolution transmission electron microscopy
ICAR	: Indian Council of Agricultural Research
JCPDS	: Joint Committee on Powder Diffraction Standards
M	: Molar
min	: Minute
MH	: Muller hinton
mL	: Milliliter
MDR	: Multi-drug-resistant
MBC	: Minimum Bactericidal Concentration
MIC	: Minimum Inhibitory Concentration
mm	: Millimeter
m*M*	*:* Millimolar
MRP	: Meropenem

MRS	: de Mann- Rogosa- Sharpe
MTT	: Dimethylthiazole diphenyl tetrazolium bromide
NA	: Nalidixic acid
NaCl	: Sodium chloride
NASF	: National Agricultural Science Fund
nm	: nanometer
$MgCl_2$	: Magnesium chloride
MTCC	: Microbial type culture collection
NCCLS	: National Committee for Clinical Laboratory Standards
No.	: Number
NTS	: Non- typhoidal *Salmonella*
O.D	: Optical Density
PBS	: Phosphate buffer saline
PCR	: Polymerase chain reaction
PEG	: Polyethylene glycol
pH	: Log hydrogen ion concentration
PXRD	: Powder x-ray diffraction
rpm	: Revoluton per minute
^oC	: Degree Celsius
SAED	: Selected area electron diffraction
sec	: Second
SEM	: Scanning electron microscopy
spp.	: Species
SPR	: Surface plasmon resonance
TAE	: Tris acetate EDTA
Taq	: *Thermus aquaticus*
TBE	: Tris buffer EDTA
TGA	: Thermogravimetric analysis

θ	: Theta
TEM	: Transmission electron microscopy
UV-Vis	: Ultraviolet visible
V	: Voltage
WHO	: World Health Organization
XPS	: X-ray photoelectron spectroscopy
XRD	: X-ray diffraction
XLD	: Xylose Lysine Deoxycholate
ZnO	: Zinc oxide

Dedicated to my Family

1. Introduction

1. INTRODUCTION

Food-borne illnesses constitute a growing public health concern, as they are associated with considerable global morbidity, disability and mortality, and a significant impediment to socio-economic development. The contamination of the food supply chain with the pathogens of public health significance, further its persistence, growth, multiplication and toxin production has emerged as an important public health threat. Foods may get contaminated at any stage from production until consumption. World Health Organization (WHO) estimated that food-borne illnesses were responsible for nearly 600 million cases and 4,20,000 deaths worldwide (Al-mohaithef *et al*., 2019). Of the 31 identified food-borne hazards, seven were documented as diarrhoeal bacterial agents (WHO, 2017); salmonellosis is one of the listed priority pathogens.

Salmonella is a diverse genus of gastrointestinal bacterial pathogens that cause a wide spectrum of diseases ranging from self-limiting gastroenteritis (pain, vomiting and diarrhoea), bacteraemia, extra-intestinal localized infections, myocarditis to systemic enteric fever (Chiu ans Su, 2019; Nair *et al*., 2020). Non- typhoidal *Salmonella* (NTS) serovars constitute a major food-borne hazard and comprise one of the leading causes of gastrointestinal zoonotic infection worldwide. Globally, NTS is responsible forapproximately 153 million cases of gastroenteritis and 57,000 deaths annually (Sharma *et al*., 2019). Further, NTS is reported to infect and colonize both the intestinal and reproductive tract or could be a part of the normal intestinal floraof many food-producing and wild animals, constituting the environmental reservoirs (Gal-Mor, 2019). The NTS serovars are commonly associated with foods of animal origin (milk, meat and egg) and are responsible for transmission to humans. Poultry serves as one of the most significant carriersof NTS serotypes, among many food-producing animals which can persist in the intestinal tract of birds asymptomatically and shed in their faeces. Of the

serotypes, *S.* Enteritidis and *S.* Typhimurium are the most frequently encountered serovars from poultry and poultry products. The most important route of transmission of NTS serovars from poultry to humans includes contaminated poultry products *i.e.*, eggs and meat (Wang *et al*., 2020). Hence, NTS- contaminated poultry products are often regarded as the major source of food-borne salmonellosis outbreaks in humans.

On the therapeutic front, antibiotics have widely been used in human medicine and as prophylaxis or growth promoters in the food animal industry. The level and complexity of resistance mechanisms exhibited by bacterial pathogens have increased with indiscriminate therapeutic and prophylactic use of antimicrobial agents. Due to its broad-spectrum antimicrobial activity, fluoroquinolones and cephalosporins are widely employed in both human and veterinary medicine for treating salmonellosis (Forouhar and Harzandi, 2019; Sharma *et al*., 2019). In recent times, WHO announced antimicrobial resistance (AMR) as one of the major threats to humankind and the environment. It is reported that AMR is responsible to cause mortality among 7,00,000 individuals every year around the globe (Ghosh *et al.,* 2019). It has also been estimated that the death toll by way of AMR would increase to 10 million by the year 2050, which would further decrease the gross domestic product (GDP) by 3.50 per cent, with a fall in livestock by three to eight per cent, resulting in an overall global economic loss to the tune of USD 100 trillion (Taneja and Sharma, 2019; Rezasoltani *et al*., 2020). Lately, an unusual emergence of ciprofloxacin-resistance as well as multi-drug-resistant (MDR)- carbapenem resistance observed in *S.* Kentucky serovars were noticedas a serious public health concern along with MDR strains of *S.* Kentucky, *S.* Virchow and *S.* Typhimurium recovered from the chicken meat and faecal samples (Alghoribi *et al*., 2019; Sharma *et al.,* 2019). Moreover, WHO (2017) included fluoroquinolone-resistant *Salmonella* spp. as one of the 12 antibiotic- resistant ‘priority pathogens that pose a high risk to human health, while recent

Centres for Disease Control and Prevention (CDC, 2019) reports categorised drug-resistant NTS serotypes as a serious threat.

Of late, the focus has primarily been shifted towards alternative therapeutic strategies to combat AMR apart from the routinely employed antibiotics. The alternative therapeutic strategies devised include phytobotanicals and phytochemicals, synthetic peptides, probiotics, polyclonal antibodies and nanoparticles (Alam *et al.*, 2019; Ghosh *et al.*, 2019; Ali *et al.*, 2020; Chee and Brown, 2020; Kumar *et al*., 2021). Recently, nanoparticles (NPs) have emerged as a novel alternative approach to overcome bacterial drug resistance encountered globally. The potential anti-bacterial activity of NPs is mainly due to their large surface area to volume ratio than their bulk material which allows the binding of a large number of ligands on the surface of NPs and hence its complexation with receptors present on the bacterial cell surface (Alavi and Rai, 2019; Aquib *et al*., 2019; Kumar *et al*., 2020; Varghese *et al*., 2020). Since they act directly on the cell wall and the action is primarily microbicidal, NPs could be a better choice to overcome bacterial resistance and have the potential to be developed into antimicrobial theragnostic in medicine (Fernando *et al*., 2018). The metals and metal oxide NPs could be an effective alternative in this regard. Recently, metal (silver, gold, copper, iron) NPs and metal oxide (such as zinc oxide, copper oxide, titanium oxide and iron oxide) NPs have also been widely used as antimicrobial agents, as they possess unique physical and chemical characteristics linked to their nanometer size ranging from 1 to 100 nm.

Metal oxide NPs have got unique physicochemical and optoelectronic properties with various biomedical applications (Kumar *et al*., 2020). Zinc, being a micronutrient, plays a pivotal role in the management of infectious diarrhoea. Zinc oxide (ZnO) has got a comparatively higher photocatalytic efficiency and biocompatibility than other inorganic photocatalytic materials; possess greater selectivity, heat resistance and durability, and most importantly broad-spectrum antiviral, antifungal and antibacterial activity (da Silva *et al*.,

2019). The antimicrobial property of ZnO NPs is mainly due to their smaller size and large surface area which involves effective electrostatic interaction between NPs and microbial cell surfaces by way of which it could create pores on the microbial cell surface, leading to leakage of cytoplasmic contents and eventually, cell death (Akbar *et al*., 2020).

It is well established that the nanostructures could be synthesized effectively by physical (microwave irradiation, electrochemical method and ultra-sonication), chemical (metallic precursors, reducing and stabilizing agents) as well as biological means. Physical and chemical methods may cause several stress on the environment because of the release of toxic metabolites; besides, the high cost of materials used, chances of failure and difficulties in characterization are considered as the major drawbacks of these techniques (Gour and Jain, 2019; Yusof *et al*., 2019; Akbar *et al*., 2020). However, the use of organic sources in the biological method would eliminate the need for using toxic chemicals as reducing agents in the biosynthesis of NPs. Additionally, as the plants harbour a wide range of metabolites that act both as reducing and stabilizing agents, they are considered as one of the most useful sources for the green synthesis of NPs as it is safe, relatively easy to handle and inexpensive. Hence, the physical and chemical methods for the synthesis of NPs have greatly been replaced recently by green synthesis methods employing the use of various plant parts, bacteria, fungi and algae, as they provide ergonomic nanomaterials (Vijilvani *et al*., 2020). Nevertheless, there exists a dearth of systematic studies employing NPs against NTS, especially, MDR strains of NTS serovars.

Piper longum L. (Family Piperaceae), commonly known as Indian long pepper or pippali, has widely been used as a herbal antibacterial, analgesic, counter-irritant and anti-inflammatory agent in India. Owing to its antioxidant and antimicrobial properties, the roots, fruits and the thicker part of the stem of *P. longum* is widely used as an important medicinal remedy (Sultana *et al*., 2019; Huang *et al*., 2020). Further, *P. longum* extract is rich in alkaloids,

flavonoids, tannins, sesamim, iso-butyl deca-trans-2-trans-4-dienamide and several other phytoconstituents with medicinal properties (Jayapriya *et al*., 2019), that prompted this study to investigate the efficacy of green synthesized ZnO NPs employing the dried spike extract of *P. longum* against MDR-NTS serovars.

Under these circumstances, the present study was undertaken with the following objectives:

1. Synthesis and characterization of green synthesized ZnO NPs.
2. Antibacterial activity of green synthesized ZnO NPs against MDR-NTS.

2.Review of literature

2. REVIEW OF LITERATURE

Food-borne illnesses have been emerged as a leading cause of mortality and morbidity especially in developing countries creating a serious impact on economic and public health worldwide. There were several reports of food-borne outbreaks which produce illnesses ranging from mild symptoms like vomiting, diarrhoea, abdominal pain, nausea, respiratory difficulties to severe health issues and sometimes death (Gupta, 2020; Wilson *et al*., 2020; Al-seghayer and Al- Sarraj, 2021; Li *et al*., 2021). The frequency of occurrence of food-borne illnesses largely depends on the interaction between pathogen, food, host, and the environment (Gourama, 2020). World Health Organisation (WHO, 2020) reportedthat nearly 4,20,000 deaths with diseases among one in ten humans and a loss of
33 million life-years annually indicate the potential public health hazards of consuming contaminated food and the need for possible intervention and addressing the threat immediately.

2.1. Salmonellosis

Salmonellosis is an important food-borne disease caused by *Salmonella enterica*, a Gram-negative intracellular facultative pathogenic bacterium that comprises more than 2600 serovars (Pulford *et al.,* 2019). It is estimated that *Salmonella* causes about 1.35 million infections, 26,500 hospitalizations, and 420 deaths in the United States every year (CDC, 2020).

Among the enteric bacterial pathogens, 99 per cent of the animal and human infections are caused by *Salmonella enterica* serovars and produce about 94 million infections and 155,000 deaths worldwide every year (Yanagimoto *et al.*, 2020). Among non-typhoidal *Salmonella* (NTS) serotypes, *S.* Typhimurium and *S.* Enteritidis are commonly associated with human infections in North America, Latin America, Europe, Asia, and Africa. Alghoribi *et al*. (2019) documented the occurrence of *Salmonella* in Saudi Arabia from 200 clinicalisolates of which *S.* Enteritidis and *S.* Typhimurium were reported to be the predominant serotypes. However, in Europe, 41.3 per cent of cases were caused

by *S*. Enteritidis, followed by *S*. Typhimurium, with a prevalence rate of 22.1 per cent, and both were identified as the most common serovars among the identified NTS isolates (Macdonald *et al*., 2019).

In the United States, *S. enterica* serovar Heidelberg was identified as the twelfth most common serovar of *S. enterica* responsible for salmonellosis and it produces systemic infection than NTS serotypes (Etter *et al*., 2019). Moreover, *S*. Panama, a frequently isolated serovar producing public health threat for the past 70 years globally, has been recognized as the eleventh most frequently isolated *Salmonella* serovars in humans between 2001 and 2007 in Asia (Pulford *et al*., 2019). The most frequently detected serovar from food and animal sources in Europe isolated from human cases of salmonellosis over the past few decades was *S*. Infantis after *S*. Enteritidis, and *S*. Typhimurium (Gymoese *et al*., 2019; Mughini-Gras *et al*., 2021). Nonetheless, *S*. Typhi and *S*. Paratyphi have been associated with systemic enteric fever, bacteremia, and self-limiting gastroenteritis resulting in invasive salmonellosis in humans of Sub-Saharan Africa (Park *et al*., 2019).

2.2 Sources

Contaminated meat products, poultry, and eggs have been recognized as the important sources of NTS serovars (Morgado *et al*., 2021). Poultry act as an asymptomatic carrier for various serovars of *Salmonella* spp. and increases the risk of dissemination throughout the farm premises and to the public via contaminated products (Dewi *et al*., 2021). Further, the consumption of egg and poultry products results in infection with *S*. Enteritidis, while various other products such as chicken, pork, beef, and close contact with animals cause *S*. Typhimurium infection. The domesticated and wild animals have been identified as the natural reservoirs of *Salmonella* spp. Consumption of contaminated water, contact with animals and pet food, travel to foreign countries are the other causes for contracting salmonellosis (Macdonald *et al*., 2019). One or multiple strains of NTS could be associated with a single source within a particular geographical

area, which may alter over a period, thereby changing the dynamics of salmonellosis (Bloomfield *et al.*, 2021).

Yanagimoto *et al*. (2020) documented the occurrence of *Salmonella* spp.in wastewater treatment plants. In their study, the source of infection was traced from those humans who consume poultry-associated products. Among egg, beef, poultry, pork, and other food of animal origin, the highest prevalence of *Salmonella* spp. was reported from the poultry meat. Contaminated water, feed, pastures act as an important source of *Salmonella* spp. which in turn produces infection in humans. The most important source of NTS is the food of animal origin (Pal *et al*., 2020).

2.3 Clinical manifestations

The most common clinical symptom of salmonellosis is gastroenteritis, which often ranges from mild to severe illness. Mild symptoms of gastroenteritis constitute headache, vomiting, dehydration, diarrhoea, nausea, and abdominal cramps (Vidayanti *et al*., 2021); severe infections may occur due to septicaemia which might lead to death. Some individuals may also develop meningitis, appendicitis, and arthritis when the disease becomes chronic (Pal *et al*., 2020). Being a self-limiting illness, salmonellosis ceases normally within one week; however, if the disease becomes chronic, it may advance to appendicitis, meningitis, and arthritis in some individuals (Ehuwa *et al*., 2021).

A rare case of neonatal epididymo-orchitis was reported in Canada which is important, however, an unusual manifestation of salmonellosis, and the serotype responsible for the condition was *S*. Javiana (Trecarten *et al*., 2019). Myocarditis, pericarditis, and myopericarditis were found to be serious complications of NTS infections in addition to gastrointestinal symptoms, and the most frequently reported serotypes causing the condition were *S*. Typhimurium and *S*. Enteritidis (Jin *et al*., 2020).

Mohan *et al*. (2019) conducted a retrospective study from 2011 to 2016 among children less than 15 years of age and found pneumonia as the most

common clinical manifestation of invasive NTS along with other symptoms like meningitis, arthritis, and gastroenteritis. In addition to osteomyelitis and septic arthritis, infectious endarteritis is an important complication of salmonellosis in adults. There were also reports of patients with inflammatory bowel disease developing toxic megacolon on the invasion of *S.* Enteritidis (Chiu ans Su, 2019; Ali *et al*., 2020). Further, gastrointestinal symptoms can also occur secondarily as identified in an exclusive case of salmonellosis with initial symptoms of erythema nodosum and breast abscess (Hassan *et al*., 2019).

2.4. Non-typhoidal Salmonellosis (NTS)

Salmonellosis is a self-limiting disease caused by NTS which is mainly characterized by vomiting and diarrhea. The severity of infection is high in immunocompromised individuals, elder persons, and children. In addition to bacteremia, it may also result in extra-intestinal localized infections (Ouali *et al*., 2021)

According to the recent report of the global burden of diseases, injuries, and risk factors study, 95.10 million cases of NTS-associated enterocolitis and 50,771 related deaths were estimated worldwide (Stanaway *et al*., 2019). Furthermore, gastrointestinal illnesses associated with the NTS serovars may progress further to bacteraemia in nearly five per cent of individuals, especially in infants and immune-compromised individuals (Lee and Yoon, 2021). Moreover, NTS has also been recognized as an important illness that would result in 1.35 million infections, 26,500 hospitalizations, and 420 deaths every year in the United States. CDC published an antibiotic resistance threat report in the United States and identified drug-resistant NTS as a serious threat to human health (CDC,2019).

The identified NTS serovars, *S.* Typhimurium and *S.* Enteritidis accounted for over 80 per cent of serovars responsible for invasive NTS (Marchello *et al*., 2021). They were the most predominant serotypes isolated from humans in Asia, Africa, Europe, and America and the common serotypes among NTS that cause

bloodstream infection worldwide (Albert *et al*., 2019; Chiu ans Su, 2019). It is widely accepted that poultry acts as the most important reservoir for these serotypes (Chiu ans Su, 2019). In sub-Saharan Africa, the most important cause of bloodstream infection was found to be NTS and the predominant serovars associated with the disease are *S*. Typhimurium and *S*. Enteritidis. Moreover, the most susceptible populations were immunocompromised individuals and children less than 3 years of age (Aldrich *et al*., 2019; Park *et al.*, 2021). *S*. Typhimurium and *S*. Enteritidis are the most predominant serovars among the 13 different NTS serovars isolated from patients in Kuwait. The disease was mostly seen in patients with chronic diseases over 50 years of age (Albert *et al*., 2019).

The clinical manifestations of NTS were usually self-limiting with fever, abdominal cramps, and diarrhoea (Lee *et al*., 2019). Ingestion of contaminated feed and water were the main sources of infection with NTS. A bacterial load of nearly 10^6 to 10^8 organisms must be ingested by a healthy individual to produce symptoms in NTS infections (Chiu and Su, 2019).

2.5. Antimicrobial resistance (AMR)

As the development of antimicrobial-resistant bacteria is increasing at a rapid rate, AMR became an important public health issue that should be addressed and demands essential intervention. Haphazard use of antimicrobial agents in both animals and humans reduced the effectiveness of antibiotics against microorganisms.

2.5.1. Global scenario

A fall in GDP by 1.10 per cent and 3.80 per cent could be expected by 2050 in low impact and high impact AMR scenarios, respectively, owing to the emergence of antimicrobial-resistant strains worldwide (Ahmad and Khan, 2019). The recent reports of WHO suggested that the AMR was producing critical public health emergencies and has emerged as an important reason for premature mortality in Nepal (Adhikari *et al*., 2019). Of late, it was also reported that the world population might fall between 11 million and 444 million by 2050, which

would be far below the actual population if AMR was absent (Ahmed *et al.*, 2019).

A low level of fluoroquinolone resistance has been reported among *Salmonella* spp., *E. coli,* and *Campylobacter* spp. in Australia, as the country restricted the usage of these antibiotics in food animals. Though the interaction between companion animals is very high, researches have been conducted so far in the country regarding the transmission of AMR (Hill-Cawthorne *et al*., 2019).A global action plan was formulated in the year 2015 to tackle AMR by promoting a 'one health' approach, thereby preventing the spread of AMR among humans and animals (Raina, 2019; Shrivastava *et al*., 2019). Vietnam became the topmost nation amid the 5 top countries (Myanmar, Indonesia, Nigeria, Peru) out of the 50 countries studied with the highest usage of antimicrobial agents in animals and has the highest predictable percentage rise in antimicrobial usage by 2030 (Thapa *et al*. 2020). The presence of antimicrobial-resistant genes in *K. pneumoniae* isolates was obtained from South and Southeast Asia through a retrospective genomic epidemiology study confirming the presence of hypervirulent AMR strains (Wyres *et al*., 2020).

2.5.2. Indian scenario

The anticipated rise in the consumption of antibiotics between 2010 and 2030 was reported to be 67 per cent in India, wherein animal houses have been emerged as an important source for the dissemination of antimicrobial-resistant bacteria due to the extensive usage of antimicrobials for growth promotion and disease prevention (Sivagami *et al*., 2020).

Sanjukta *et al*. (2019) documented the occurrence of multidrug-resistant (MDR) *E.coli* strains from the swine of northeast India and reported that all the recovered isolates were resistant to amoxicillin, ceftazidime, and polymyxin- B. Mandakini *et al*. (2019) also reported the occurrence of MDR- *E.coli* strains from swine in Arunachal Pradesh and the highest resistance to cephalexin (83.56 per

cent) and lowest to imipenem (0.34 per cent). Further, the antimicrobial resistance pattern observed in northwestern Punjab among livestock and poultry revealed that all the isolates exhibited resistance to at least one antibiotic, and high resistance was observed among isolates of *E. coli*, *Pseudomonas,* and *Staphylococcus* spp. (Ralte *et al*., 2019). Similarly, a multidrug resistance pattern was confirmed in *Campylobacter* spp. isolated from a slaughterhouse environmentand broiler chicken in India (Suman Kumar *et al*., 2021). Moreover, the study conducted by Saharan *et al*. (2020) to determine the occurrence of AMR in *E.coli, Salmonella,* and *S.aureus* isolates recovered from poultry farms and poultry retail shops in Rajasthan reported high resistance to amikacin, azithromycin, cefazoline, ceftazidime, colistin, streptomycin and trimethoprim and moderate resistance to vancomycin and levofloxacin. Antimicrobial resistance profiles of *C. jejuni* isolated from crows of India and the United States were analyzed and confirmed their role as an indicator and potential environmental reservoirs of antibiotic- resistant determinants that were supposed to circulate among the human population (Sen *et al*., 2021).

The scoping report on AMR in India (2017) suggested that the resistance to third-generation cephalosporins and fluoroquinolones was seen in more than 70 per cent of isolates of *Acinetobacter baumannii, K. pneumoniae,* and *E. coli.* Although the colistin resistance documented in India was less than one per cent, colistin-resistant *K. pneumoniae* accounted for more than 70 per cent of death. Colistin has become the last resort antimicrobial agent for treating *A. baumanii* infections since the organism became resistant to carbapenem (Taneja and Sharma, 2019; Gourkhede *et al*., 2021).

2.5.3. Causes of AMR

The dissemination of antimicrobial-resistant genes among bacteria occurs by horizontal gene transfer through plasmid DNA and also by using genetic elements like bacteriophages, transposons, and integrons. Once the cells containing antimicrobial-resistant genes get destroyed, the DNA will be released into the environment thereby passing on the resistance (Sivagami *et al*., 2020).

Moreover, Yang *et al*. (2019) reported that the plasmids and transposons serve as the mobile genetic elements responsible for the transmission of AMR genes. Inappropriate use of antimicrobial agents in the poultry industry and feed, widespread use in patients suffering from various disease conditions, gene transfer, mutation, and selective pressure has been reported as the major causes of AMR. Another major contributor to the spread and occurrence of new MDR strains includes improper handling of meat and meat products in slaughterhouses (Adhikari *et al*., 2019).

2.5.4. AMR among NTS strains

The AMR associated with various strains of NTS can be acquired from contaminated food and water, from various environmental sources, during international travel, and also through contact with animals. In the United States, the most commonly isolated anti-microbial resistant serotypes are Typhimurium, Enteritidis, Newport, I 4,[5],12:i:- and Heidelberg (Medalla *et al*., 2021).

A study conducted in Taiwan among the paediatric patients with non-typhoidal salmonellosis suggested that the strains were highly resistant to third-generation cephalosporins and the resistance rate has significantly increased in 2018 than 2010. Besides, the isolates also exhibited resistance to ampicillin, ciprofloxacin, and trimethoprim-sulfamethoxazole (Lee and Yoon, 2021). Additionally, the recovered NTS strains (*S*. Typhimurium and *S*. Enteritidis) were reported widely to be multidrug-resistant and the resistance rate was high towards cephalosporins (Albert *et al*., 2019). Rodregues *et al*. (2020) reviewed studies of AMR in NTS isolates from humans and swine in Brazil, wherein among 920 swine isolates the most predominant serovar identified was *S*. Typhimurium and 20 per cent of the isolates exhibited resistance towards tetracycline, followed by sulphonamides, ampicillin, streptomycin, and nalidixic acid. The lowest rates in the AMR were exhibited by *S*. Heidelberg, *S*. Cerro, *S*. Anatum, and S. Enteritidis. Additionally, *S*. Typhimurium, *S*. Infantis, and *S*. Enteritidis were the most predominant serovars isolated from a human source and most of the serovars were resistant to ampicillin, followed by tetracycline. This study revealed that both

swine and human isolates were resistant to most of the therapeutically relevant antimicrobials and swine acts as a possible source for transmission of NTS to humans.

The antimicrobial susceptibility profiles of NTS among swine isolates of Argentina suggested that among the most prevalent serovar, *S.* Anatum and *S.* Typhimurium, two isolates of *S.* Typhimurium were found to be multidrug- resistant and exhibited comparatively higher resistance (four per cent) to enrofloxacin. (Vico *et al.*, 2020). In Africa, NTS was considered one of the most common pathogens associated with bacteraemia. The ceftriaxone-resistant invasive NTS isolates prevalent in western Kenya also exhibited co-resistance with other antimicrobial agents (Luvsansharav *et al*., 2020).

Viana *et al*. (2019) reported the occurrence of multidrug-resistant NTS isolates in Brazil; *S.* Typhimurium was the most common serotype among the 41 recovered *S. enterica* isolates of swine-origin; 91.20 per cent of the isolates exhibited resistance to streptomycin, 87.80 per cent to tetracycline, 80.50 per cent to ampicillin, 70.70 per cent to chloramphenicol, and 51.20 per cent to ciprofloxacin. Chang *et al.* (2021) evaluated the prevalence of AMR in the NTS strains among children of Taiwan. In the study, 26.90 per cent of the isolates were found to be resistant either to ceftriaxone or ciprofloxacin. Additionally, NTS serotypes were detected from the retail meats (94.10 per cent) which indicated the potential spillover of AMR strains of NTS from animal-based food to humans.

2.6. Alternative therapeutics

Indiscriminate use of conventional antibiotics as a mode of empirical therapy has led to the emergence of MDR as well as extensively drug-resistant (XDR) pathogens, thereby making AMR an imminent threat to public health. As more and more antibiotics have rendered unsuccessful against such untreatable infections, and the development of new antibiotics is time-consuming, emphasis shall be given to adjuvant therapies to combat this nagging public health threat (Borrelli *et al*., 2021). Of late, cationic antimicrobial peptides (AMPs),

bacteriophages, endolysins, photodynamic light therapy, and nanoparticles (NPs) have been used as some of the alternative strategies (Boone *et al*., 2021; Basavegowda and Baek, 2021; Samir, 2021). These promising therapeutic approaches can be used either alone or in combination with conventional therapeutic agents (Ghosh *et al*., 2019; Mulani *et al*., 2019; Salama *et al*., 2021).

Gondil and Chhibber (2021) reviewed studies on endolysins and recognized that it could be used as a suitable alternative for conventional antibiotics due to its host specificity, synergistic action, safety against normal microflora of the host, and lower chance of developing resistance against bacteria. Similarly, cationic AMPs have drawn recent public health attention, as they are potent antimicrobial agents with minimal toxicity to eukaryotic cells (Lu *et al*., 2020). Moreover, antibacterial activity and biofilm disrupting activity of AMPs against drug-susceptible as well as drug-resistant *P. aeruginosa* and *S. aureus* strains indicated its potential as a novel therapeutic agent (Park *et al*., 2019).

In yet another study, Anand *et al*. (2020) published the first reported case of intranasal administration of phages as an alternative approach for treating *K. pneumoniae* infection in a mouse model. Phage therapy has been reported as a novel approach for treating infections as high efficacy was observed in XDR *A. baumanni* infected mouse models than untreated ones (Leshkasheli *et al*., 2019; Gondil and Chhibber, 2021).

Phytochemicals such as terpenoids, at sub-inhibitory concentrations, could exhibit potential antibiofilm activity against *S.* Typhimurium and *S.* Enteritidis (Sakarikou *et al*., 2020). Situmeang *et al*. (2019) documented the antibacterial efficacy of kesambi plant (*Schleichera oleosa*) against *E. coli* and *S. aureus*.

The antimicrobial resistant genes present in the avian pathogenic *E. coli* (APEC) strain O23:H52 isolated from the chicken underwent missense mutation in presence of phytochemicals, carvacrol, and oregano (Al-mnaser and Woodward, 2020). Besides, previous studies revealed that various phytochemicalspresent in the plant extracts have resulted in appreciable antimicrobial activity

against MDR pathogens in humans in terms of clinical trials, safety and toxicity studies, and affordability (Kebede *et al*., 2021; Ude *et al*., 2021)

2.7. Nanotechnology as an alternative therapeutic approach

In recent times, nanotechnology has developed as an alternative strategyfor combating AMR and has widely been employed against MDR bacterial infections (Gupta *et al*., 2019; Al-Fahad *et al*., 2021). The unique physicochemical characteristics of NPs such as large surface- to- volume ratio, shape, zeta potential, surface chemistry, direct contact with the bacterial cellmembrane, and better biofilm penetration has enhanced the interaction of NPs with target organisms and further enabled them as a promising tool to combat AMR (Allaker and Yuan, 2019; Lee *et al*., 2019; Ojemaye *et al*., 2020; Al-Fahad*et al*., 2021). Nanoparticles could also possess the ability to act as drug delivery vehicles and possess intrinsic antimicrobial activity making them a better replacer of contemporary antimicrobial agents (Makvandi *et al*., 2020). Moreover, NPs act by alteration of the microbial cell wall and pathway of nucleic materials, enzyme pathway blockade, and through the destruction of cell membranes (Angel Villegas*et al*., 2019).

2.7.1. Metal oxide NPs

Though different types of nanomaterials such as mesoporous silica particles, liposomes, metal/metal oxides, carbon nanotubes, magnetic NPs arewidely used as a tool for drug delivery in order to combat microbial pathogens, the metal NPs are the most studied and widely accepted ones due to its intrinsic antimicrobial capability (Viswanathan *et al*., 2019; Tewabe *et al*., 2021). Moreover, NPs are widely used in the field of biomedicine, owing todistinguishing features such as larger surface-area-to-volume ratio, enhanced particle surface reactivity, small dimensions, thermal stability, outstanding surfaceplasmon resonance (SPR), and photoelectrochemical activity (Alavi and Rai, 2019; Basavegowda and Baek, 2021; Xu *et al*., 2021). Various metals and metal oxides NPs like gold (Au), silver (Ag), silicon dioxide (SiO2), Ag oxide (Ag_2O),

calcium oxide (CaO), copper oxide (CuO), titanium dioxide (TiO_2), magnesium oxide (MgO) and ZnO have been developed and evaluated (Angel Villegas *et al*., 2019).

Metal NPs mainly acts through surplus production of reactive oxygen species inside the microorganisms, antioxidant depletion, destruction of the plasma membrane of the microbes, thereby damaging the vital enzymes in the respiratory pathway, metal ion accumulation in the microbial membrane,disrupting metabolic activities through electrostatic attraction between microbial cell, alteration of signal transduction by dephosphorylation of peptides and by inhibition of microbial enzymes (Nisar *et al*., 2019; Zohra *et al*., 2021). Merah *et al*. (2019) evaluated the antibacterial efficacy of both ZnO and CuO NPs and reported that the Gram-positive bacteria are more sensitive to ZnO, while Gram- negative bacteria were more sensitive to CuO.

2.7.1.1. ZnO NPs

The ZnO NPs were found to exhibit numerous antibacterial properties and have been extensively studied for the development of next-generation therapeutics against a wide range of pathogenic microorganisms including Gram-negative and Gram-positive bacteria in order to combat multi-drug resistance identified recently (Mohd Yusof *et al*., 2021). The unique physicochemical characteristics ofZnO NPs i.e., crystallinity, size, extensive surface area, shape, biodegradability, biocompatibility, semiconductor behavior, and porosity have broadened their application in various fields including biomedicine. Besides, they can be combined with conventional antibiotics and anti-inflammatory drugs to enhance antimicrobial potential against pathogenic microorganisms (Jin and Jin, 2021; Mohd Yusof *et al*., 2021).

The formation of ROS has been proposed to produce antibacterial potential of ZnO NPs by Mohd Yusof *et al*. (2021). In this study, an excessive ROS generation inside the bacterial cell of poultry- associated food borne pathogens was observed in a concentration- and time-dependent manner upon

incubation with biosynthesised ZnO NPs. Akbar *et al*. (2019) demonstrated that a very low concentration (1.33 millimolar) of ZnO NPs was found effective against *S. aureus* and *S*. Typhimurium. The study has also reported that these NPs could successfully be used to prevent food-borne infections owing to their low cost, safety, and effectiveness. The effect of carvacrol and ZnO NPs was studied on *C. jejuni* and found that the ZnO NPs exhibited a synergistic effect on carvacrol and caused physical disruption by interacting with the cell membrane of the bacteria (Windiasti *et al*., 2019). Besides, this study also revealed the importance of a synergistic antimicrobial approach for combating AMR successfully. Moreover, ZnO NPs also revealed excellent antimicrobial activity against drug-resistant enterotoxigenic *E. coli* (ETEC) isolates recovered from the drinking water. Additionally, the guava (*Psidium guajava*) leaf extract was found to potentiate the antimicrobial effect of ZnO NPs (Jyothi *et al*., 2020). Further, Prasad and Sivakumar (2020) documented an effective antibacterial efficacy of ZnO NPs against food-borne pathogens and their remarkable applications in the biomedical field.

2.8. Synthesis of NPs

The synthesis of NPs could effectively be attained by using various physical, chemical, photochemical, and biological methods (Aygun *et al*., 2019). The physical and chemical methods for the synthesis of NPs include vaporization, condensation, sol-gel, interferometric lithography, solvent evaporation, physical fragmentation, and precipitation from microemulsion (Sepasgozar *et al.*, 2021).

Often, the physical methods are usually tedious and require high temperature, pressure, and energy. Besides, the chemical methods of synthesis involve the use of highly hazardous and toxic chemicals which results in environmental pollution and health issues to the persons handling the chemicals. Moreover, in the photochemical approach, the photoreduction of NPs was commonly employed but required a suitable environment and high-cost equipment (Miri *et al*., 2019; Yaqoob *et al*., 2019; Yosuf *et al*., 2019; Umavathi *etal*., 2021).

Ali *et al*. (2021) compared the effect of chemically and biologically synthesized ZnO NPs from the leaf extracts of *Azadirachta indica* (neem) and reported that the biologically synthesized NPs were more effective in inducing antimicrobial activity against food-borne pathogens (*E. coli* and *S. aureus*). Besides, this study reported that the biologically synthesized ZnO NPs were foundto exhibit better antifungal properties in comparison to the ZnO NPs synthesized chemically. Likewise, green synthesized NPs were found to be more stable and crystalline than chemically synthesized ones and found to have better antioxidant potential due to the surface modification by phytochemicals present in the plant extract (Mahmoud *et al.,* 2021).

2.8.1. Green synthesis and characterization of NPs

Recently, green synthesis of NPs has been widely accepted and becoming increasingly popular, as they are eco-friendly, non-toxic, cost-effective, easily reproducible, thereby overcoming the disadvantages of the other methods of synthesis (Gour and Jain, 2019; Pan *et al*., 2020). Microbes such as fungi, yeast, bacteria, and plant extracts derived from seeds, leaves, stems, fruits, and gum are usually employed for the bio-based components for green synthesis (Aygun *et al*., 2020). Since microbe-based synthesis requires an aseptic environment and careful maintenance, plant-mediated synthesis is far more feasible and advantageous as the biological risk are minimal (Ghotekar, 2019).

The phytoconstituents present in the plant extract are coated over thesurface of NPs, thereby imparting the properties of both phytochemicals and NPs. The resulting synergistic effect could therefore be attributed to the increased antibacterial activity of green synthesized NPs. Bioactive compounds possessing unique characteristics of the plant material play an important role in treating various ailments. Furthermore, the shape and size of the NPs are strongly influenced by the type of plant extract used (Rajendran *et al*., 2021). Moreover, metallic NPs synthesized by employing plant extract have been extensively used for numerous applications including antidiabetic, antimicrobial, cancer therapy, and tissue engineering (Iqbal *et al*., 2021).

Arya *et al*. (2019) used vanillin-capped gold NPs for the treatment of *P. aeruginosa* and demonstrated that it potentiated the action of meropenem and trimethoprim, which are reported to be the last line of antibiotics used and could successfully be used against XDR clinical isolates of *P. aeruginosa*. The antimicrobial efficacy of silver NPs synthesized using reishi mushroom suggested a higher antibacterial activity against both Gram-positive and Gram-negative bacteria and potential antifungal activity against *C. albicans* (Aygun *et al*., 2020). Besides, copper nanoparticles were synthesized using a mixture of *Zingiber officinale, Piper nigrum* and *P. longum*. The synthesised NPs were reported to exhibit excellent antibacterial efficacy against *Bacillus subtilis, E. coli, P. aeruginosa* and *S. aureus* (Shah *et al*., 2019).

2.8.2 Green synthesis and characterization of ZnO NPs

The ZnO NPs synthesized using the extract of *Portulaca oleracea* (regla seeds) exhibited good antibacterial as well as antioxidant activity against methicillin- resistant *Staphylococcus aureus* (MRSA) and *Helicobacter pylori* (ATCC 700392). Besides, the synthesized ZnO NPs demonstrated high anticancer activity for HCT-116 cells (Mohamed *et al*., 2021). Further, Awwad *et al*. (2020) recognized potential antimicrobial activity for the ZnO NPs fabricated using the aqueous fruit extracts of *Ailanthus altissima* against *E. coli* and *S. aureus.* The green synthesis of ZnO NPs using neem gum demonstrated to exhibit significant antimicrobial activity against *P. aeruginosa* biofilms than the ZnO NPssynthesized by the chemical method (Vijayakumar *et al*., 2020).

P. longum L. (Family Piperaceae), commonly known as Indian long pepper or pippali, is a well-known herbal antibacterial, analgesic, counter-irritant and anti-inflammatory agent found widely in India (Subramaniam *et al*., 2021). The extract of *P. longum* is a rich source of bioactive compounds like terpenines, tannins, piperidine alkaloids, dihydro stigmasterol, isobutyl deca-trans-2-trans-4-dienamide, and various other phytoconstituents with medicinal properties. They also have anti-inflammatory, anti-cancerous, and anti-oxidant properties (Jayapriya *et al*., 2019; Yadav *et al*., 2020). Owing to its antimicrobial and

antioxidant properties, the catkin, roots, and thicker part of the stem of *P. longum* are widely used as a home remedy for several ailments (Jamila *et al*., 2020).

The antimicrobial efficacy of ZnO NPs is affected widely by variousfactors such as particle size, surface area, porosity, morphology, and crystallinity. Hence, the physicochemical characterization of ZnO NPs is warranted and could provide valuable information about the biochemical as well as microbiological effects against pathogens (Czyzowska *et al*., 2021). The key parameter is the particle size or particle size distribution, which would greatly influence the uptake of NPs into the cell membrane thereby determining its antimicrobial efficacy (Jin and Jin, 2021). The UV- Vis spectroscopy, Fourier transform infrared spectroscopy (FTIR), Thermogravimetric analysis (TGA), X-ray diffraction (XRD), Energy dispersive X-ray analysis (EDAX), scanning electron microscopy (SEM) and transmission electron microscopy (TEM), X-ray photoelectron spectroscopy (XPS) analysis are some of the reported characterization methods employed for confirming the formation of ZnO NPs (Vinay and Chandrasekhar, 2021; Ramya *et al*., 2021).

The primary technique used for the characterization of ZnO NPs is powder XRD, which reveals information about the lattice parameters, average crystalline size, crystalline structure, and nature of the phase (Mourdikoudis *et al*., 2018; Jayappa *et al*., 2020). Moreover, UV- Vis spectroscopy provides sufficient data regarding the optical parameters of ZnO NPs, while the associated surface functional groups were analyzed by FTIR (Naseer *et al*., 2020). Besides, SEM and TEM verify the shape, surface morphology, and crystalline nature of the synthesized NPs (Alkasir *et al*., 2020; Nityasree *et al*., 2021). The TGA is a technique performed to determine the thermal stability and thermal degradation of green synthesized ZnO NPs under constant heating (Thi *et al*., 2020).

3.Materials and Methods

3. MATERIALS AND METHODS

3.1. MATERIALS

3.1.1. Chemicals and reagents

The chemicals and reagents used in this study were of Analytical Grade procured from MeRCK® (Germany), Invitrogen® (USA), Sigma-Aldrich chemicals® (India), SRL® (Sisco, India), Loba Chemie® (India), HiMedia® (India), Takara Bio® (India) and other reputed national and international firms.

3.1.2. Plasticware and glassware

The plasticware and glassware were procured from Tarsons, JSGW, and Borosil (India). The washing and sterilization of glassware were carried out by observing standard procedures.

3.1.3. Scientific Instruments and Equipment

The scientific equipment used in the study includes probe sonicator (Hielscher Ultrasonics, Germany), digital ultrasonic sonicator (Labman Scientific Instruments, India), T100^{TM} thermal cycler (Bio-Rad, USA), gel Doc^{TM} EZ gel documentation system (Bio-Rad, USA), cyclomixer (REMI Equipments, India), hot air oven (Roteck, India), water bath (Labline, India), laboratory centrifuge (REMI Equipments, India), laminar airflow system (Labline, India), bacteriological incubator (Labline, India), submarine horizontal electrophoresis system (Bio-Rad, USA), electronic weighing machine (Shimadzu, Japan), pH meter (Eutech Instruments, India) and micropipettes (ThermoFisher Scientific, Eppendorf, Germany).

3.1.4. Reference strains

The reference strains of MDR- NTS isolates namely, *S.* Typhimurium and *S.* Enteritidis (n= 3 for each serotype), the quality control strain (*E. coli* ATCC 25922), *Lactobacillus acidophilus* MTCC 10307, and *L. plantarum* MTCC 5690

used in this study were maintained in the Zoonoses laboratory of the Department of Veterinary Public Health, College of Veterinary and Animal Sciences, Pookodeas a part of the ongoing ICAR- NASF funded research project.

3.1.5 Oligonucleotides

The details of oligonucleotide primers used for the validation of MDR- NTS isolates are presented in Table 1. All the primers used in this study were synthesised from Sigma Aldrich Pvt. Ltd., India.

3.1.6 Antibiotic discs

The commercial antibiotic discs used in the present study for determining the antibiotic susceptibility testing were procured from HiMedia Laboratories Pvt. Ltd.

Table 1. Details of oligonucleotides used in the present study

Target organism	Gene	Sequence (5'-3')	Amplicon size(bp)	References
Salmonella spp.	*invA*	F: TCGTGACTCGCGTAAATGGCGATA R: GCAGGCGCACGCCATAATCAATAA	423	Nair *et al.*, 2015
Salmonella Enteritidis	*SdfI*	F: TGTGTT TTATCTGATGCAAGAGG R: TGAACTACGTTCGTTCTTCTGG	301	
Salmonella Typhimurium	*Spy*	F: TTGTTCACTTTTTACCCCTGAA R: CCCTGACAGCCGTTAGATATT	401	

3.2. METHODS

3.2.1. Validation of MDR- NTS isolates

The MDR- NTS isolates (n= 3) maintained in the laboratory repository (as described in section 3.1.4) were revived and re-validated by employing PCR assay (Nair *et al*., 2015). Further, the MDR-NTS isolates were screened to determine their multi-drug resistance pattern by antibiotic susceptibility testing employing the disc diffusion method (CLSI, 2019).

3.2.1.1. PCR based validation

The MDR-NTS isolates were re-validated by employing standardized PCR targeting genus-specific *invA* gene for *Salmonella* spp., and serovar-specific *sdfI* and *spy* genes for *S*. Enteritidis, and *S*. Typhimurium, respectively (Nair *et al*., 2015).

The standardized PCR protocol for all the genes (*invA*, *sdfI*, and *spy*) involves a reaction volume of 20 µL which included 10 µL of 2X master mix (PCR reaction buffer, dNTPs, Taq DNA polymerase, gel loading dye), 10 µM of aprimer set containing each forward and reverse primers (final concentration of 0.40 µM of each primer), 2.50 µL of the DNA template (approximately 100 ng) and sterilized Milli-Q water to make up the reaction volume.

The cycling conditions for the PCR- based detection of all the genesincluded an initial denaturation of DNA at 94 ^{o}C for 5 min, followed by 35 cycles each of 30 sec denaturation at 95 ^{o}C, 1 min annealing at 56 ^{o}C, and an extension at72 ^{o}C for 1 min 30 sec, followed by a final extension of 10 min at 72 ^{o}C and hold at 4 ^{o}C.

PCR amplified DNA was analyzed by 1.20 per cent agarose (Invitrogen, USA) as per the procedure described by Sambrook (2001). An appropriate quantity of agarose was boiled in 15ml of 0.5 x TBE buffer to obtain uniform molten agarose of the desired per cent which was cast in an appropriate gel- casting tray fitted with an acrylic comb and left for setting after adding ethidium

bromide (0.5 µg/mL final concentration). Solidified gel transferred into electrophoresis tank containing Tris–Acetate–EDTA (TAE) buffer. DNA to be analyzed was mixed with an appropriate volume of DNA loading buffer (6X) and loaded into wells alongside 100 bp DNA molecular weight marker (Takara). Electrophoresis was carried out at 5 V/cm until the tracking dye has just passed out of the gel. The DNA bands were visualized and documented under a gel documentation system (Gel doc^{TM} EZ imager, BioRad). The molecular sizes of the DNA bands were analyzed in comparison with the molecular weight marker.

The materials contaminated with ethidium bromide were disposed off according to the local guidelines.

3.2.1.2. Antibiotic susceptibility testing

The antibiotic susceptibility testing of the revived MDR-NTS isolates was determined as per the guidelines provided by Clinical Laboratory Standards Institute (2019).

In brief, the MDR- NTS isolates were subjected to disc diffusion assay as per the method described by Bauer *et al.* (1966). The revived isolates were tested for their susceptibility against gentamicin (GEN, 10 µg), ampicillin (AMP, 2 µg), chloramphenicol (CL, 10 µg), colistin sulphate (CO, 30 µg), azithromycin (AZM, 15 µg), meropenem (MRP, 10 µg), ciprofloxacin (CIP, 5 µg), doxycycline (DO, 30 µg), ceftriaxone (CTR, 30 µg), co-trimoxazole (COT, 25 µg), amoxicillin (AMC, 10 µg), nalidixic acid (NA, 30 µg), ceftazidime (CAZ, 30 µg), ceftazidime-clavulanic acid (CAC, 30/10 µg), cefotaxime (CTX, 30 µg) and cefotaxime-clavulanic acid (CEC, 30/10 µg).

In brief, log-phase cultures of each of the test isolates grown on nutrient broth were centrifuged at 10,000 rpm for 10 min. Later, the supernatant was discarded and the bacterial pellet was mixed with sterile phosphate-buffered saline (PBS; pH 7.40) to achieve 0.50 McFarland standard tube turbidity (approximately 1.50×10^8 CFU/mL) for each test isolate. This culture was then evenly spread on

Mueller Hinton (MH) agar plate using a sterile cotton swab and allowed to dry for five min.

The commercial antibiotic discs were placed about two to three cm apart on the inoculated agar surface. Each disc was then pressed down to ensure complete contact with the agar surface. The plates were inverted and kept for overnight incubation at 37 °C. The zones of inhibition (diameter in mm) were measured for each antibiotic, initially for the quality control strain (*E. coli* ATCC 25922) and also for all the test strains.

The obtained data were compared with an interpretative chart furnished by the manufacturer to grade the test isolates as sensitive, intermediate, and resistant to respective antibiotics.

3.2.2. Preparation of aqueous extract of *P. longum* catkin

The catkins of *P. longum* were purchased from a local grocery shop. The aqueous extract of the *P. longum* catkins purchased was prepared as described by Khoobchandini *et al*. (2019) and Jayapriya *et al*. (2019).

In brief, the *P. longum* catkins were cleaned thoroughly in running tap water to remove the visible dirt and debris, air-dried in shade, and ground properly to make it into powder. This powdered catkin (10 g) was then transferred into a round bottom flask containing nanopure water (100 ml) and heated up to 60 °C for one h. Later, the solid particulates were filtered using Whatman No. 1 filter paper. The filtrate, thus obtained, was stored at 4 °C until the synthesis of ZnO NPs.

3.2.3. Green synthesis of ZnO NPs

The ZnO NPs were green synthesised using the aqueous extract of *P. longum* catkin. The graphical representation of the green synthesis of ZnO NPs is illustrated in Fig. 1.

Briefly, the *P. longum* catkin filtrate (20 mL) was added to 0.10 *M* Zinc acetate dihydrate solution (80 mL) and kept for continuous stirring in a magnetic stirrer (300 rpm) at 60 °C for two h. A colour change of the reaction mixture from colourless to light brown indicated the formation of ZnO NPs (Fig. 1). Later, the

ZnO NPs formed were washed thrice with methanol, followed by nanopure water to remove the impurities. Finally, the ZnO NPs were air-dried at 80 °C overnight and stored at 4 °C until further use.

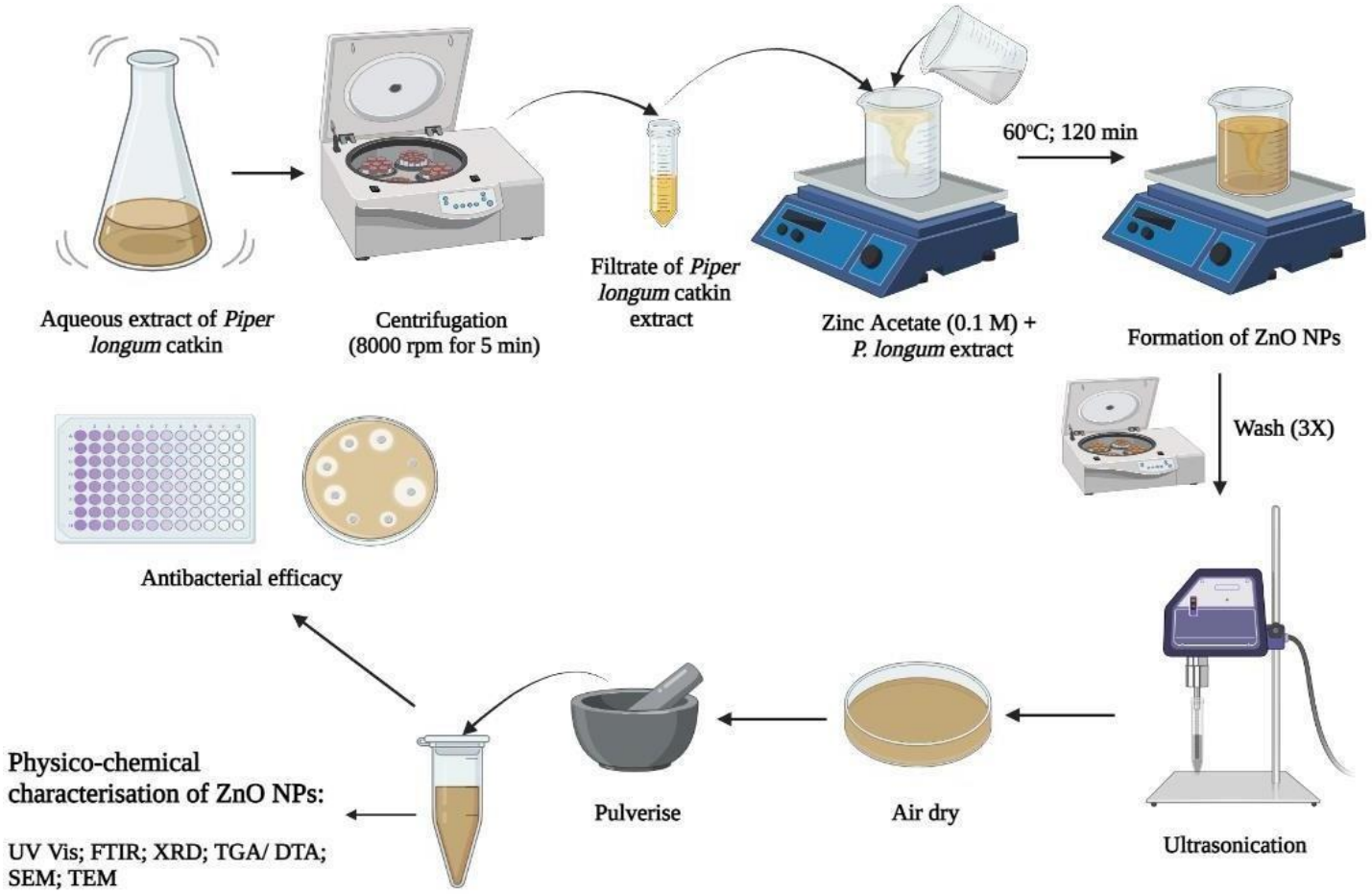

Fig. 1 Green synthesis of ZnO NPs using aqueous extract of *P. longum* catkin

3.2.4. Characterisation of green synthesised ZnO NPs

The green synthesised ZnO NPs was characterised by UV- Vis spectroscopy, Fourier transform infra-red spectroscopy (FTIR), thermogravimetric analysis (TGA) and differential thermal analysis (DTA), powder X-ray diffraction (PXRD), scanning electron microscopy (SEM) as well as transmission electron microscopy (TEM).

Initially, the obtained ZnO NPs were dissolved in ultrapure water at a final concentration of 1 mg/mL and scanned within the range of 250 to 450 nm using UV- Vis spectrophotometer (ThermoFisher Scientific, USA), keeping water as the blank.

The Fourier transform infra-red (FTIR) spectra were used to evaluate the presence of unknown functional groups on the biosynthesised ZnO NPs within the range of 4000 to 400 cm^{-1} at a resolution of 4 cm^{-1} (PerkinElmer C94012, USA).

The TGA- DTA of ZnO NPs was then carried out by heating around 12.473 mg of samples in a nitrogen atmosphere at the rate of 40 ℃ per min in the range of 40 to 1300 ℃ (Perkin Elmer STA 600, USA).

For structural investigations of the biosynthesised ZnO NPs, PXRD (Bruker D8 Advance, USA) operated at CuKα radiation using 40 KeV and 40 mA with a scanning step size of 0.02° (ƛ= 1.54060Å) was employed. The average crystalline size of the green synthesised ZnO NPs was then estimated from the Debye Scherrer formula, $D= k\lambda/\beta Cos\theta$ (Sali *et al*., 2021), wherein D denotes average crystallite size (in nm), k indicates shape factor (0.90), λ is the incident radiation, β is the full width at half maximum, whereas θ denotes Bragg diffraction angle.

Finally, the morphology of ZnO NPs was carried out by examining the samples using SEM (Jeol 6390LV, Japan) at different magnifications and high-resolution transmission electron microscope (HR-TEM; JEM 2100, Jeol, Japan).

3.2.5. *In vitro* antimicrobial efficacy of green synthesised ZnO NPs

The *in vitro* antimicrobial efficacy of green synthesised ZnO NPs was carried out against the MDR-NTS isolates (*S*. Typhimurium and *S*. Enteritidis; n= 3 for each serotype).

3.2.5.1. Determination of Minimum Inhibitory Concentration (MIC) and Minimum Bactericidal Concentration (MBC)

To evaluate the *in vitro* antimicrobial efficacy of green synthesised ZnO NPs, the MIC and MBC values were determined against the characterised MDR-field strains of *S.* Typhimurium and *S.* Enteritidis by micro broth dilution technique (CLSI, 2019).

In brief, 100 µL of the individual test cultures (at a final concentration of 1 x 10^7 CFU/mL) were co-incubated with decreasing concentrations of ZnO NPs (500 to 0.244 µg/ mL) in 100 µL of cation- adjusted Mueller Hinton broth (CA- MH; HiMedia) in a 96- well flat- bottom microtiter plate. After the incubation at 37 ^oC for 18 to 24 h, 20 µL of the resazurin dye (0.015 per cent) was added to all the wells to determine the dye reduction (from purple to pink) and thereby the bacterial inhibition. The lowest concentration of ZnO NPs without visible growth was designated as MIC.

Later, the MBC of ZnO NPs was estimated by plating 10 µL aliquots drawn from each well (Miles *et al*., 1938) revealing no visible growth in 96- well flat-bottom microtiter plate onto Xylose Lysine Deoxycholate (XLD) agar (HiMedia) supplemented with 100 µg of ampicillin, since all the six test strains used in this assay were resistant to ampicillin. The lowest concentration of the ZnO NPs which revealed 99.90 per cent killing of the test cultures in the XLD agar was determined to be its MBC (NCCLS, 1999).

3.2.5.2. In vitro stability assays of ZnO NPs

The green synthesised ZnO NPs were individually explored for their *in vitro* stability assays by subjecting them to high-end temperatures, protease enzymes, the physiological concentration of cationic salts as well as pH, as described below.

3.2.5.2.1. Effect of high-end temperatures

In order to determine the thermal stability of green synthesised ZnO NPs, the ZnO NPs were subjected to high-end temperatures (70 ^oC and 90 ^oC) for 5, 15,

and 30 min. Subsequently, the antimicrobial activity (MIC and MBC values) of the green synthesised ZnO NPs was determined against each of the MDR- NTS test strains, corresponding to each time interval, as described in section 3.2.5.1. The untreated ZnO NPs, kept at room temperature, were used as a control for eachtime interval (Ebbensgaard *et al*., 2015).

3.2.5.2.2. Effect of protease enzymes (trypsin, lysozyme, and proteinase-K)

The effect of protease enzymes (trypsin, lysozyme, and proteinase- K) on the antimicrobial activity of green synthesised ZnO NPs were investigated by co-incubating with the respective proteases at 37 ^{o}C for 30 sec, 5, 15, and 30 min (Ebbensgaard *et al*., 2015).

The protease to ZnO NP ratio used in this assay was 1:100 (w/w). Each of the protease- untreated ZnO NP was used as a control to rule out the antimicrobial activity. After incubation at respective time intervals, the samples were heated at 90 ^{o}C for 10 min to inactivate the protease activity and then the antimicrobial activity (MIC and MBC values) was determined as described in 3.2.5.1.

3.2.5.2.3. Effect of physiological concentration of cationic salts

To investigate the stability of green synthesised ZnO NPs in the presence of a physiological concentration of cationic salts, the NPs were tested against MDR-NTS isolates (*S*. Typhimurium and *S*. Enteritidis; n= 3 for each serotype)in a CA-MH broth with added concentrations of NaCl (150 mM). Subsequently, the MIC and MBC values were identified as described in 3.2.5.1.

A similar procedure was employed for studying the effect of added concentrations of $MgCl_2$ (2 mM) on green synthesised ZnO NPs (Mohamed *et al*., 2016). In this assay, the green synthesised ZnO NPs untreated with aphysiological concentration of cationic salts (150 mM NaCl and 2 mM $MgCl_2$) served as controls.

3.2.5.2.4. Effect of pH

In order to investigate the stability of green synthesised ZnO NPs at different pH, the NPs were tested against the individual serotypes of both *S.* Typhimurium and *S.* Enteritidis in CA-MH broth maintained at pH four, six and eight. Subsequently, the MIC and MBC values were identified as described in section 3.2.5.1.

3.2.5.3. In vitro safety assay

The *in vitro* safety of green synthesised ZnO NPs on the host cells were determined using a haemolytic assay employing chicken erythrocytes as well as cytotoxicity assay employing epithelial human embryonic kidney (HEK) cell lines.

3.2.5.3.1. Haemolytic Assay

To determine the safety of green synthesised ZnO NPs (to ensure their activity specifically against the MDR-NTS isolates and not the mammalian cells), the haemolytic assay based on the release of haemoglobin from chicken erythrocytes was performed in polystyrene microtitre plates (Ebbensgaard *et al.*, 2015).

In brief, the aseptically collected fresh defibrinated chicken blood was washed thrice with PBS, centrifuged for 15 min at 1000 xg and resuspended at 10 per cent (v/v) in PBS containing 10 mM DL-Dithiothreitol (DL- DTT). Thechicken erythrocytes (100 µL) were then transferred to a 96- well microtiter plate and mixed with 100 µL of ZnO NP solution kept at different MIC (1X, 5X and 10X) levels. Sterile PBS (100 µL) was used as a negative control, whereas 0.20 per cent Triton X-100 (100 µL) was used as the positive control. The microtiter plates were then incubated at 37°C for 60 min and further centrifuged at 1300 xg for 10 min. The supernatant was transferred to a flat-bottom 96-well polystyrene microtiter plate and the haemoglobin release was monitored by measuring the absorbance at 540 nm. The per cent of haemolysis was calculated as,

$$\textbf{Haemolysis} = 100 \times (A_{sample} - A_{PBS}) / (A_{TritonX\text{-}100} - A_{PBS})$$

wherein, A_{sample} is the experimental absorbance of the NP sample, A_{PBS} is the control absorbance of untreated erythrocytes and $A_{TritonX\text{-}100}$ is the absorbance of 0.20 per cent Triton X-100 lysed cells.

3.2.5.3.2. MTT cytotoxicity assay

The *in vitro* effect of green synthesised ZnO NPs on the viability of eukaryotic cells was evaluated using MTT assay [3-(4,5-dimethylthiazole-2-yl)-2,5-diphenyl tetrazolium bromide] (Mosmann, 1983). In this study, the viability of ZnO NPs was tested against eukaryotic HEK cell lines.

In brief, the HEK cells were pre-cultured in tissue culture flasks containing Dulbecco's Modified Eagle Medium (DMEM, pH 7.20) until the formation of a monolayer at the bottom of the flasks. The adherent HEK cells were then transferred to another 96-well plate at a density of $1x10^5$ cells per well and allowed to attach overnight. The monolayers of cells were treated with 200 µL of ZnO NPs at different MIC (1X, 5X and 10X) levels diluted in DMEM; the treated cells were maintained for 24 h at 37 °C in a humidified incubator with 5 per cent CO_2 atmosphere. The cells incubated with fresh DMEM served as the negative control. The supernatant was then removed and proceeded further using the MTT cell proliferation assay kit (Abcam, USA). Accordingly, 50 µL of MTT reagent mixed with 50 µL of media was added to each well and incubated at 37 °C for three h. After incubation, MTT solvent (150 µL) was added to each well, mixed thoroughly and the cytotoxicity was monitored by measuring the absorbance at 590 nm. The per cent of cytotoxicity was calculated as,

Cytotoxicity = 100 x (Control– Sample)/ (Control)

wherein, the control denotes experimental absorbance of the untreated cell control and the sample represents the control absorbance of the treated cell lines.

3.2.5.4. Effect of ZnO NPs on commensal gut lactobacilli

The adverse effect of green synthesised ZnO NPs was further explored on commensal gut lactobacilli (*L. acidophilus* MTCC 10307 and *L. plantarum* MTCC 5690).

In brief, de Mann- Rogosa- Sharpe (MRS) broth medium (100 µL) containing 1X MIC levels of ZnO NPs was inoculated with a defined number of each commensal bacteria ($1x10^7$ CFU/mL) in 96-well microtiter plates. Each plate included a positive growth control (untreated individual commensal lactobacilli) and negative control (sterile MRS broth). After incubation at 37 °C for 48 h, the effect of ZnO NPs on commensal lactobacilli was determined by drawing two samples (10 µL) from each well and plated onto MRS agar plates.

3.2.5.5. In vitro dose- and time-dependent extracellular growth kinetics of MDR-NTS with ZnO NPs

The antibacterial activity of green synthesised ZnO NPs was determined against MDR- strains of *S.* Enteritidis and *S.* Typhimurium by an *in vitro* dose- and time-dependent extracellular growth kinetics (Vergis *et al*., 2019).

Briefly, the log-phase cultures of each of the test isolates grown on nutrient broth were centrifuged at 10,000 rpm for 10 min. Later, the supernatant was discarded and the bacterial pellet was mixed with sterile phosphate-buffered saline (PBS; pH 7.40) to achieve 0.50 McFarland standard tube turbidity (approximately 1.50×10^8 CFU/mL) for each test isolate. The bacterial cultures were then diluted to attain a concentration of 1×10^7 CFU/mL using sterile CA-MH broth.

The green synthesised ZnO NPs with MIC (1X) and MBC (1X) levels were then added and the following groups were formed:

Group 1: $1x\ 10^7$ CFU of MDR- NTS (100 µL) + 1X MIC ZnO NPs (100 µL);

Group 2: $1 x\ 10^7$ CFU of MDR- NTS (100 µL) + MBC ZnO NPs (100 µL);

Group 3: $1x\ 10^7$ CFU of MDR- NTS (100 µL) + Meropenem (10 µg/mL; 100 µL) taken as positive treatment control; and

Group 4: 1x 10^7 CFU of MDR- NTS (100 µL) + CA-MH Broth (100 µL) taken as untreated control.

Similar groups were also processed for the other five MDR-NTS isolates. The respective groups along with the appropriate controls were incubated at 37 ℃ up to 24 h.

To enumerate the antibacterial effect of green synthesised ZnO NPs on MDR-NTS isolates, an aliquot of 10 µL from all the four groups were drawn at 0, 30, 60, 120, 180, 240, and 360 min and finally at 24h. At each time point, an aliquot (10 µL) from each respective group were serially diluted with 90 µL of sterile PBS and 10 µL was plated on XLD agar plates supplemented with 100 µg of ampicillin (Miles *et al*., 1938). After the incubation period at 37 ℃ for 18 to 24 h., the individual MDR- NTS colonies were counted and expressed as MDR-NTS $\log_{10}$CFU/mL.

3.2.6. Statistical Analysis

All experiments were analyzed as triplicates in three independent assays. The results were represented as means ± standard deviations of the three independent experiments performed using GraphPad Prism version 5.01 (GraphPad Sotware Inc., California, USA).

A one-way analysis of variance (ANOVA) with Bonferroni multiple comparison post-test was used to compare the differences between cytotoxicity of control and ZnO NPs-treated cell lines. The association of ZnO NPs on commensal gut lactobacilli was measured by paired two-tailed ‘t’ test. Moreover,a two-way (repeated measures) ANOVA with Bonferroni multiple comparison post-test was used to compare the differences between control and ZnO NPs - treated tests for the *in vitro* dose- and time-dependent extracellular growth kinetics of MDR-NTS.

A *P*-value of ≤ 0.01 was considered highly significant, while a *P*-value ≤ 0.05 was considered statistically significant.

4. Results

4. RESULTS

In the present study, three isolates of each MDR- *S*. Typhimurium and *S*. Enteritidis serotypes maintained in the laboratory repository of the Department of Veterinary Public Health, College of Veterinary and Animal Sciences, Pookode were revived and re-validated by employing genus- as well as serotype-specific PCR assays. Later, the antibiotic susceptibility testing of the confirmed MDR- NTS isolates was performed to determine their MDR pattern and to investigate the *in vitro* antimicrobial efficacy of green synthesized ZnO NPs. The green synthesis of ZnO NPs was achieved using the aqueous extract of the *P. longum* catkin from zinc acetate dihydrate solution. The physicochemical characterization of the green synthesized ZnO NPs was performed by UV- Vis spectroscopy, FTIR, TGA/ DTA, PXRD, SEM and TEM. Further, the *in vitro* antimicrobial activity, safety aswell as stability assays of the characterized green synthesized ZnO NPs was carried out. The obtained results are presented systematically as follows.

4.1 RE-VALIDATION OF MDR-NTS ISOLATES

4.1.1. PCR- based re-validation

The revived cultures of NTS isolates were re-validated by employing a standardized PCR assay targeting genus-specific *invA* gene for *Salmonella* spp., and serovar-specific *sdfI* and *spy* genes for *S*. Enteritidis, and *S*. Typhimurium, respectively (Nair *et al*., 2015). The results are presented in Fig. 2.

4.1.2. Antibiotic susceptibility testing

The MDR pattern of the confirmed NTS isolates was evaluated by antibiotic susceptibility testing using disc diffusion assay. The results are tabulated in Table 2.

All the confirmed NTS strains were found to be MDR in nature, as the isolates exhibited resistance to three or more classes of antibiotics tested (Table 2).

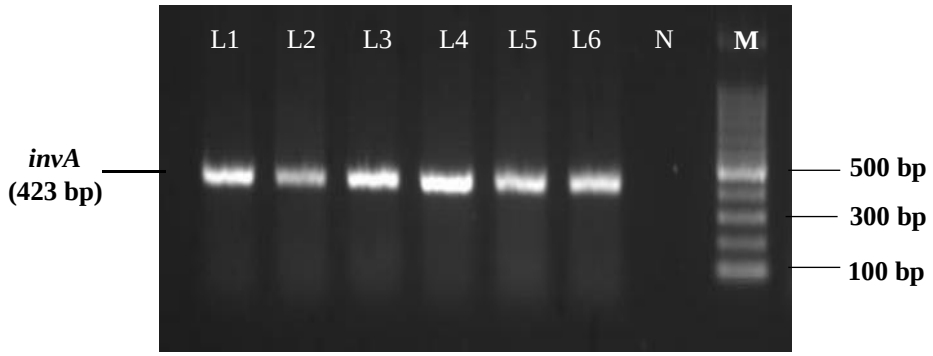

Fig. 2A. PCR- based confirmation of *Salmonella* spp.
M- DNA Marker ladder (100 bp); L1- L3: *S.* Enteritidis; L4-L6: *S.* Typhimurium;
N: Negative Control

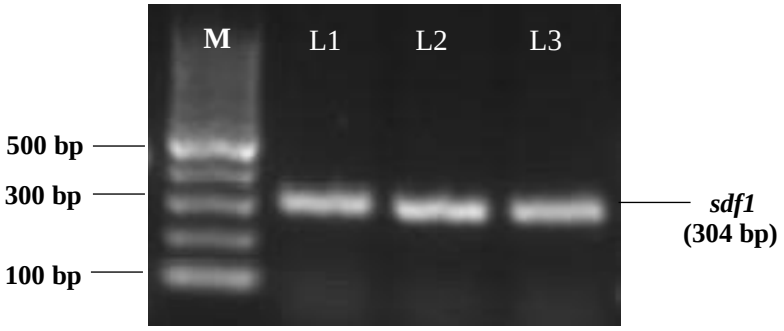

Fig.2B. PCR- based revalidation of *S.* Enteritidis
M- DNA Marker ladder (100 bp); L1- L3: *S.* Enteritidis

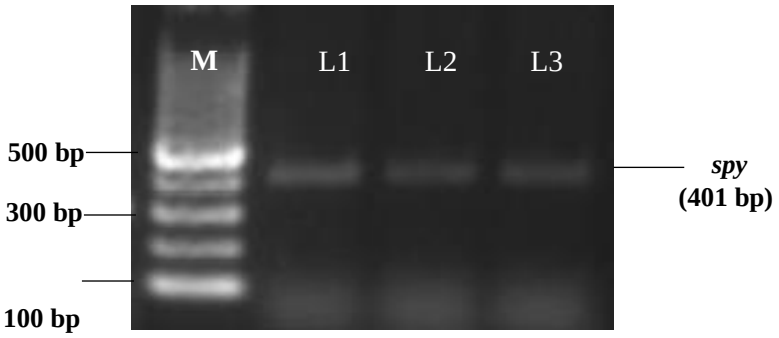

Fig.2C. PCR- based revalidation of *S.*Typhimurium
M- DNA Marker ladder (100 bp); L1- L3: *S.* Typhimurium

Table 2. Antibiotic susceptibility testing of MDR-NTS isolates used in the present study

ISOLATE ID		GEN (10mcg)	AMP (2mcg)	C (30mcg)	CL (10 mcg)	AZM (15mcg)	MRP (10mcg)	DO (30 mcg)	CIP (5 mcg)	CTR (30mcg)	COT (25mcg)	AMC (10mcg)	NA (30 mcg)	ESBL	
														CAZ (30 mcg)/CAC (30/10 mcg)	CTX (30 mcg)/CEC (30/10 mcg)
***S*. Enteritidis**	S1	**R**	**R**	**R**	S	I	S	**R**	**R**	S	**R**	**R**	**R**	S	S
	S2	**R**	**R**	**R**	S	I	S	**R**	**R**	S	**R**	**R**	**R**	S	S
	S3	**R**	**R**	S	S	I	S	**S**	**S**	S	**R**	**R**	**R**	S	S
***S*. Typhimurium**	ST1	**R**	**R**	I	S	S	S	**R**	**R**	S	**R**	**R**	**R**	S	S
	ST2	**R**	**R**	**R**	S	I	S	**R**	**R**	I	**R**	**R**	**R**	**R**	S
	ST3	**R**	**R**	S	S	I	S	**R**	**R**	S	**R**	**R**	**R**	S	S

(GEN- Gentamicin, AMP- Ampicillin, C- Colistin sulphate, CL- Chloramphenicol, AZM- Azithromycin, MRP- Meropenem, DO- Doxycycline, CIP- Ciprofloxacin, CTR- Ceftriaxone, COT- Co-trimoxazole, AMC: Amoxycillin, NA- Nalidixic acid, CAZ- Cefotaxime, CAC- Cefotaxime/ clavulanic acid, CTX- Ceftazidime, CEC- Ceftazidime/ clavulanic acid)

4.2. GREEN SYNTHESIS OF ZnO NPs

In the present study, the aqueous extract of *P. longum* catkin was used for the green synthesis of ZnO NPs.

The aqueous extract of *P. longum* catkins reduced the aqueous solution of 0.10 *M* Zinc acetate dihydrate (at a ratio of 1:4) to ZnO NPs at 60 ^{o}C under constant stirring for two h. The formation of brown coloured precipitate at the bottom of the beaker indicated the formation of ZnO NPs (Fig. 1).

The green synthesized ZnO NPs, thus obtained, were then subjected to physicochemical characterisation.

4.3. CHARACTERIZATION OF ZnO NPs

Initially, UV- Vis spectroscopic pattern confirmed the formation of green synthesized ZnO NPs. The obtained green synthesized ZnO NPs, in this study, revealed a progressive surface plasmon resonance (SPR) band between 320 nm to 350 nm, confirming its formation. The maximum absorbance peak was obtained at 340 nm (Fig. 3).

The chemical and functional groups present in the green synthesized ZnO NPs were estimated by FTIR spectrum analysis (Fig. 4). In this study, peaks were observed at 3640 cm^{-1}, 2850 cm^{-1}, 2100 $cm^{-1,}$ 1739 cm^{-1}, 1490 cm^{-1}, 870 cm^{-1}, 915 cm^{-1} and 620 cm^{-1} (Fig. 4). The obtained peaks in the FTIR spectra were compared with the standard chart to interpret the functional groups present in the green synthesised ZnO NPs.

In order to determine the thermal stability and thermal degradation of green synthesized ZnO NPs under constant heating, TGA/ DTG was performed. The TGA data obtained in this study revealed an initial weight loss of around six per cent from 40 ^{o}C to 100 ^{o}C, supported by the DTG graph, with an exothermic peak observed at 200 ^{o}C. Further, progressive thermal degradation of the green synthesized ZnO NPs was observed between 250 ^{o}C and 400 ^{o}C that corresponded with a narrow endothermic peak at 330 ^{o}C (Fig. 5). Furthermore, good thermal

stability was noticed for annealing temperatures between 900^{o}C and 1300^{o}C (Fig. 5).

The PXRD analysis was carried out to confirm the formation of ZnO NPs, to verify their crystallinity and to determine the size. The peaks were observed in the PXRD pattern of the green synthesised ZnO NPs at 2θ values of 31.85^{o}, 34.50^{o}, 37.1^{o}, 51^{o}, 59^{o}, 64^{o}, 67.1^{o} and 77^{o} (Fig. 6). Later, the PXRD diffractogram obtained was compared with the standard powder diffraction card of the Joint Committee on Powder Diffraction Standards (JCPDS), ZnO file No. 36-1451 and the crystallinity of green synthesized ZnO NPs was verified. The observed intense sharp peaks in the PXRD pattern of green synthesized ZnO NPs exhibited a hexagonal wurtzite crystalline structure. Additionally, an average crystallite sizeof 14.54 nm was estimated for the green synthesised ZnO NPs from the Debye- Scherrer formula.

In order to determine the shape and surface morphology of the green synthesised ZnO NPs, SEM imaging was carried out. The green synthesised ZnO NPs obtained in this study appeared uniformly, predominantly hexagonal and a few of them in the form of cubes (Fig. 7).

The TEM and selected area electron diffraction (SAED) imaging were performed to determine the shape and crystalline nature of the green synthesised ZnO NPs. The green synthesized ZnO NPs exhibited an almost hexagonal shape with a slight variation in thickness (Fig. 8). Moreover, some of the particles were found agglomerated (Fig. 8). Besides, the SAED patterns (Fig. 8) demonstrated hexagonal wurtzite crystallinity of ZnO NPs. Further, the HR TEM image (Fig. 8) demonstrated a spacing of lattice fringes for the green synthesised ZnO NPs in the range of 0.24 nm.

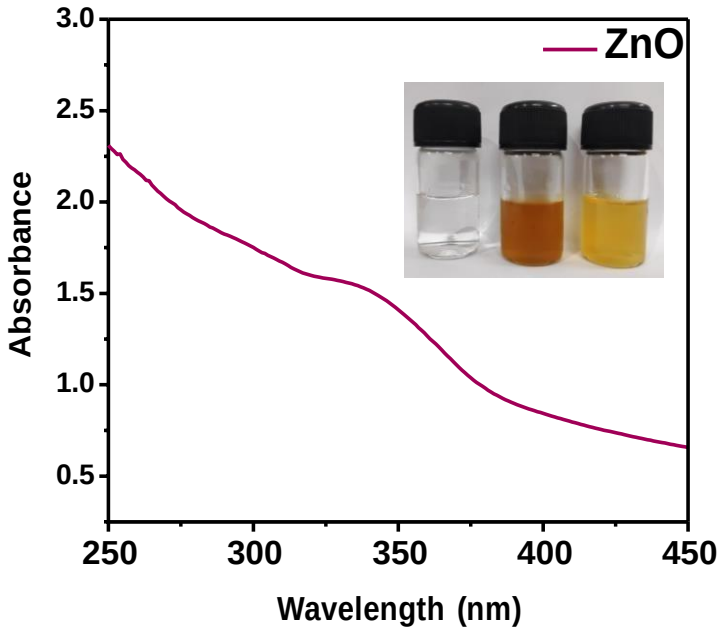

Fig. 3. UV-Vis spectroscopic characterisation of green synthesised ZnO NPs

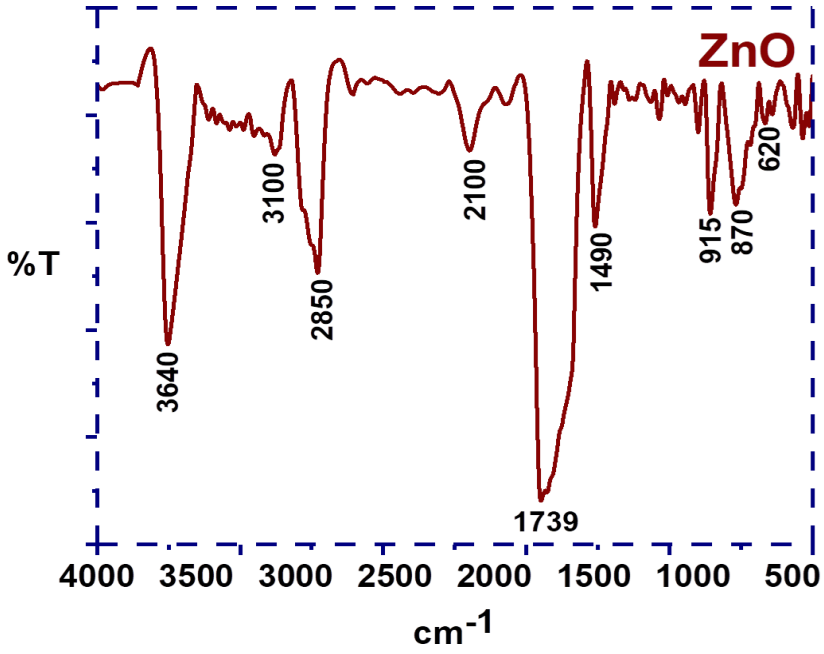

Fig. 4. FTIR spectra of green synthesised ZnO NPs

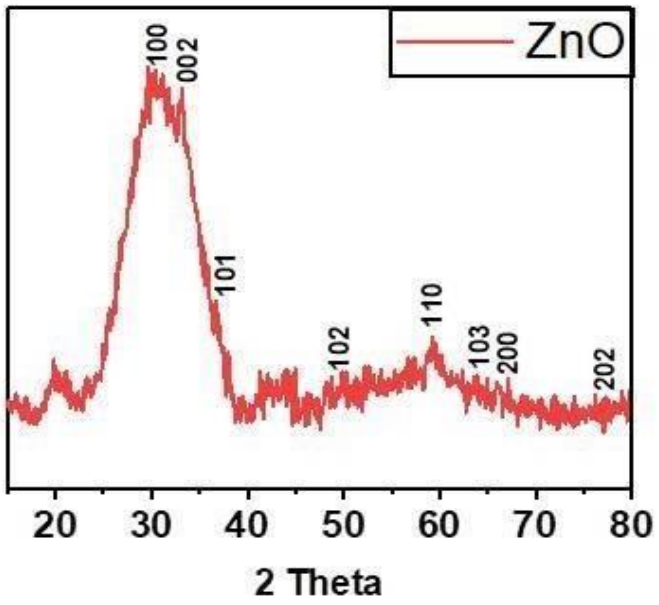

Fig. 5. PXRD pattern of green synthesised ZnO NPs

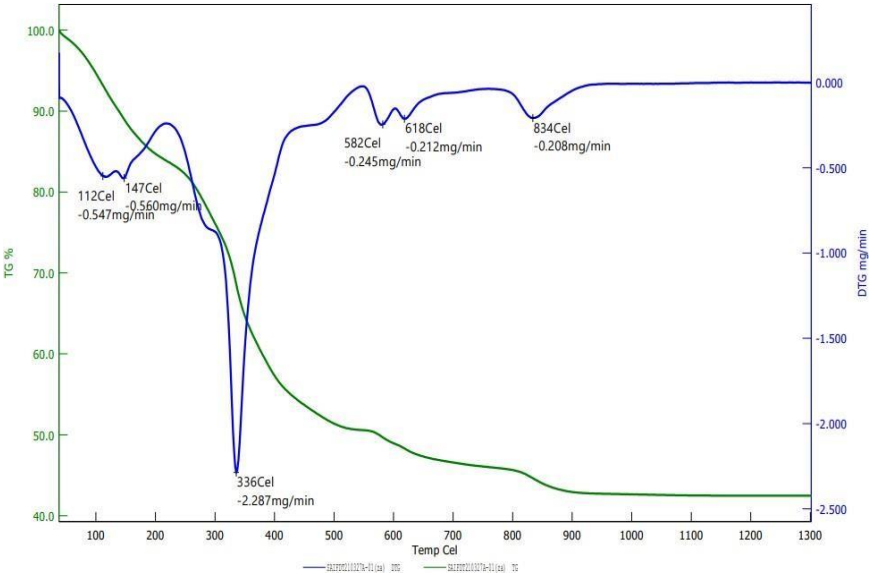

Fig. 6. TGA/DTG of green synthesised ZnO NPs

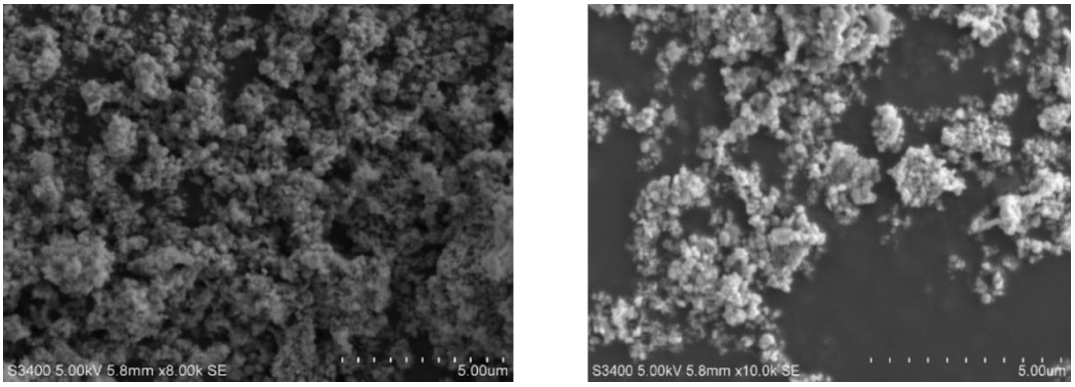

Fig. 7. SEM image of green synthesised ZnO NPs

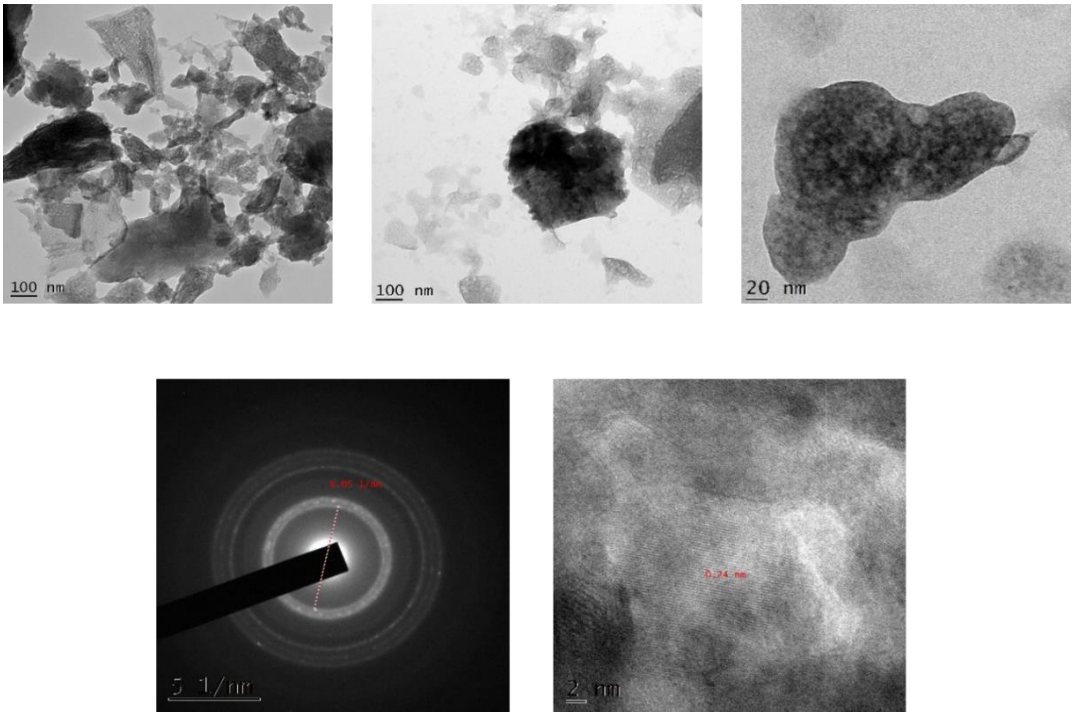

Fig. 8. TEM and SAED images of green synthesised ZnO NPs

4.4. *IN VITRO* ANTIMICROBIAL EFFICACY OF GREEN SYNTHESISEDZnO NPs

4.4.1 Determination of MIC and MBC of green synthesized ZnO NPs against MDR-NTS

The MIC and MBC values of the green synthesized ZnO NPs against MDR-NTS strains, as a measure of *in vitro* antibacterial activity, were determined according to the CLSI (2018) guidelines. The results obtained are presented in Table 3.

The MIC and MBC values of green synthesised ZnO NPs against the MDR-*S.* Typhimurium and *S.* Enteritidis strains were found to be 125 µg/mL and 250 µg/mL, respectively. In general, the MBC values of ZnO NPs obtained were twice greater than the MIC values.

Table 3. MIC and MBC values of green synthesized ZnO NPs against MDR-NTS isolates

ISOLATES		MIC/MBC (µg/mL)
***S.* Enteritidis**	**S1**	125/250
	S2	125/250
	S3	125/250
***S.* Typhimurium**	**ST1**	125/250
	ST2	125/250
	ST3	125/250

4.4.2. *In vitro* stability assays of green synthesized ZnO NPs

The green synthesized ZnO NPs were investigated for their stability to high-end temperatures (70 °C and 90 °C), proteases (trypsin, lysozyme and proteinase-K), the physiological concentration of cationic salts (150 m*M* NaCl and 2 m*M* $MgCl_2$) and pH (four, six, and eight).

4.4.2.1. *Effect of high-end temperatures*

The stability of green synthesized ZnO NPs at high-end temperatures was measured by determining their antimicrobial activity after incubation at 70 °C and 90 °C for five, 15 and 30 min. The results are presented in Table 4 .

At MIC levels, the antimicrobial activity of ZnO NPs remained the same at 70 °C for S3 and S2. However, a two-fold increase in the MIC levels was observed with all the remaining test strains (S1, ST1, ST2, and ST3).Additionally, a three- to four-fold increase in the MBC values was observed for ZnO NPs until 30 min (Table 4).

In contrast, the green synthesized ZnO NPs were found stable even after incubation at 90 °C, since they retained their MIC values with the tested MDR- NTS strains. Alike at 70 °C, a three to four-fold increase in the MBC values was observed upon incubation at 90 °C for five, 15 and 30 min (Table 4).

Table 4. *In vitro* stability of green synthesized ZnO NPs at high-end temperatures (70 °C and 90 °C)

	MIC/MBC (µg/mL)					
ISOLATES	**70 °C**			**90 °C**		
	5 min	**15 min**	**30 min**	**5 min**	**15 min**	**30 min**
S1	250/750	250/1000	250/1000	250/1000	250/750	250/750
S2	250/750	250/750	125/1000	125/750	125/750	125/1000
S3	125/750	250/750	125/1000	125/1000	125/750	125/750
ST1	250/500	250/750	250/750	125/1000	125/750	125/750
ST2	250/500	250/1000	250/1000	250/1000	125/750	125/750
ST3	250/500	250/1000	250/750	250/500	125/750	125/750

4.4.2.2. *Effect of enzymes*

The residual antimicrobial activity of green synthesized ZnO NPs on exposure to protease enzymes (trypsin, lysozyme and proteinase-K) at different incubation intervals is summarised in Table 5.

In this study, the MIC value of green synthesized ZnO NPs was halved (62.50 µg/mL) up to 15 min of incubation with trypsin; thereafter, remained the same for the rest of the exposure period (Table 5). Similarly, on exposure to lysozyme, the MIC values of ZnO NPs were reduced to half, in general; however, strain-wise variation was observed (Table 5). Moreover, a three- to four-fold increase in the MBC values of ZnO NPs was noticed upon exposure to trypsin and lysozyme throughout the incubation period (Table 5).

Further, the green synthesized ZnO NPs when exposed to proteinase- K, MIC values remained the same throughout the exposure period, except for the isolate S1. Nonetheless, a two-fold increase in the MBC values was observed against the isolates ST2 and ST3 up to 30 sec, while for S1 and S2 until exposure for 30 min. However, a three- to four-fold increase in the MBC values wasobserved for all the remaining isolates throughout the exposure period.

4.4.2.3. *Effect of physiological concentration of cationic salts*

The stability of green synthesized ZnO NPs at physiological concentrations of cationic salts (150 m*M* NaCl and 2 m*M* $MgCl_2$) was determined (Table 6).

Irrespective of the cationic salts (150 m*M* NaCl and 2 m*M* $MgCl_2$), the green synthesized ZnO NPs tested retained their antimicrobial activity (MIC and MBC values) throughout the incubation period (Table 6).

4.4.2.4. *Effect of pH*

The stability of green synthesized ZnO NPs at varying pH (four, six and eight) was measured by determining their antimicrobial activity against the MDR strains of both *S.* Typhimurium and *S.* Enteritidis (Table 7).

In the present study, the green synthesized ZnO NPs tested were found to be stable at different pH, as they retained their antimicrobial activity (MIC and MBC values). However, the MIC value of ZnO NPs was reduced to half at pH eight (Table 7).

Table 5. *In vitro* stability of green synthesized ZnO NPs on exposure to trypsin, lysozyme, and proteinase- K

ISOLATES	MIC/MBC (µg/mL)											
	PROTEINASE- K				LYSOZYME				TRYPSIN			
	30 sec	5 min	15 min	30 min	30 sec	5 min	15 min	30 min	30 sec	5 min	15 min	30 min
S1	250/1000	125/750	125/1000	125/1000	250/1000	125/750	125/1000	125/1000	250/750	250/1000	250/750	250/500
S2	62.5/1000	62.5/1000	125/1000	125/1000	62.5/1000	62.5/1000	125/1000	125/1000	125/750	125/750	125/750	125/500
S3	62.5/1000	62.5/750	62.5/750	125/1000	62.5/750	62.5/750	62.5/750	125/1000	125/750	125/1000	125/1000	125/750
ST1	62.5/750	62.5/1000	62.5/750	125/750	62.5/1000	62.5/1000	62.5/750	125/750	125/750	125/750	125/1000	125/750
ST2	62.5/1000	62.5/1000	62.5/750	125/1000	62.5/750	125/1000	62.5/750	125/1000	125/500	125/750	125/750	125/750
ST3	62.5/1000	125/750	125/750	125/1000	62.5/750	125/750	125/750	125/1000	125/500	125/750	125/750	125/750

Table 6. *In vitro* stability of green synthesized ZnO NPs on exposure to the physiological concentration of cationic salts (150 m*M* NaCl and 2m*M* $MgCl_2$)

ISOLATES	MIC/MBC (µg/mL)	
	NaCl (150 m*M*)	$MgCl_2$ (2 m*M*)
S1	125/250	125/250
S2	125/250	125/250
S3	125/250	125/250
ST1	125/250	125/250
ST2	125/250	125/250
ST3	125/250	125/250

Table 7. *In vitro* stability of green synthesized ZnO NPs on exposure to different pH (four, six, eight)

ISOLATES	MIC/MBC (µg/mL)		
	pH : 4	pH : 6	pH : 8
S1	125/250	125/250	62.5/250
S2	125/250	125/250	62.5/250
S3	125/250	125/250	62.5/250
ST1	125/250	125/250	62.5/250
ST2	125/250	125/250	62.5/250
ST3	125/250	125/250	62.5/250

4.4.3. *In vitro* safety assays of green synthesized ZnO NPs

In vitro safety studies of green synthesized ZnO NPs were estimated by a haemolytic assay using chicken erythrocytes as well as HEK cell line-based MTT cytotoxicity assay. Besides, the ZnO NPs were tested for their adverse effects on the commensal gut lactobacilli, if any.

4.4.3.1. *Haemolytic assay*

The haemolytic activity of green synthesized ZnO NPs (2X, 5X and 10X MIC levels) observed against the chicken erythrocytes are presented in Table 8 and Fig. 9.

In this study, minimal haemolysis (less than two per cent) was noticed for the green synthesized ZnO NPs at 2X, 5X and 10X MIC levels (Table 8; Fig. 9).

4.4.3.2. *MTT cytotoxicity assay*

The *in vitro* cytotoxicity effect of green synthesized ZnO NPs on the viability of HEK cell lines was evaluated using the MTT assay.

Overall, the green synthesized ZnO NPs did not exhibit any cytopathic effect at 1X, 5X and 10X MIC levels.

Table 8. *In vitro* haemolytic activity of green synthesized ZnO NPs on poultry RBCs

Concentration of ZnO NPs	Haemolysis (%)
MIC (2X)	1.04
MIC (5X)	1.23
MIC (10X)	1.34

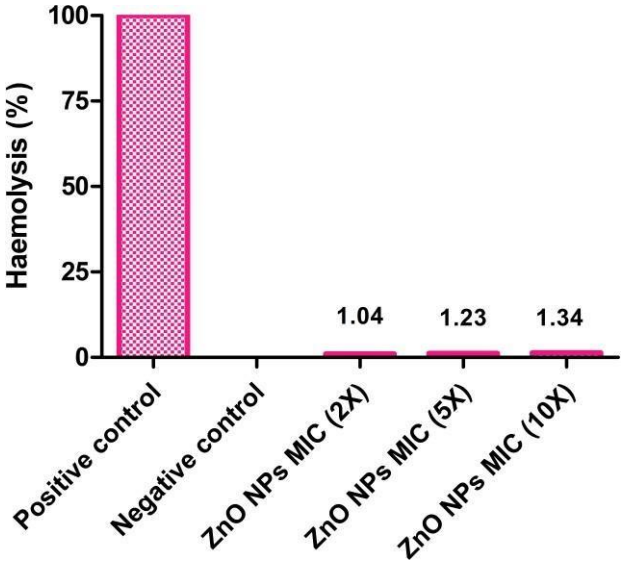

Fig 9. *In vitro* haemolytic activity of green synthesized ZnO NPs on poultry RBCs

4.4.3.3. Effect of green synthesized ZnO NPs on commensal gut lactobacilli

The adverse effect of green synthesized ZnO NPs on the commensal gut lactobacilli were investigated by the microbroth dilution method employing *L. acidophilus* MTCC 10307 and *L. plantarum* MTCC 5690. The observed results are graphically presented in Fig.10.

The commensal lactobacilli tested (*L. acidophilus* and *L. plantarum*) revealed a similar growth pattern in both treatment control (treated with green synthesized ZnO NPs) and the untreated control. Overall, a non-significant (*P*>

0.05) antimicrobial efficacy was observed for the green synthesized ZnO NPs against the tested strains of *L. acidophilus* and *L. plantarum.*

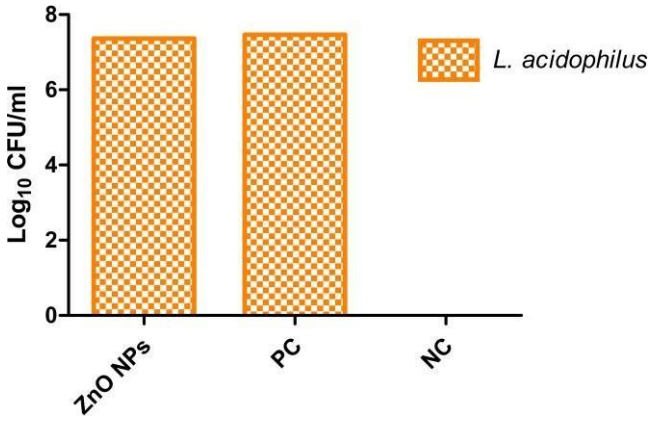

Fig. 10A. *In vitro* efficacy of green synthesized ZnO NPs on *L. acidophilus* MTCC 10307
PC: Positive control, NC: Negative control

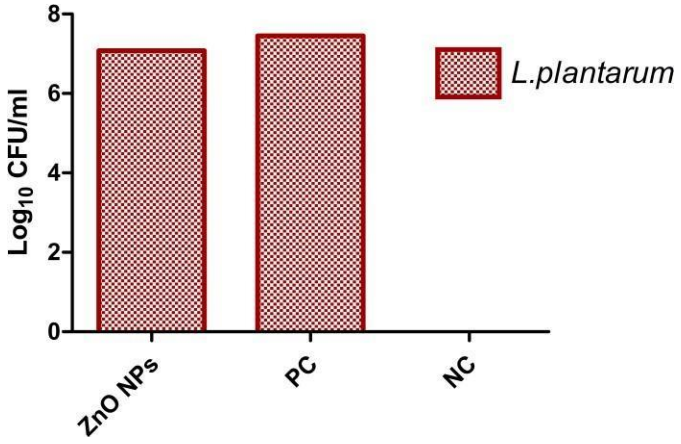

Fig. 10B. *In vitro* efficacy of green synthesized ZnO NPs on *L. plantarum* MTCC 5690
PC: Positive control, NC: Negative control

4.4.4. *In vitro* dose- and time-dependent extracellular killing kinetics of MDR-NTS strains treated with green synthesized ZnO NPs

The growth profile of individual isolates of MDR- NTS serotypes co-cultured with the green synthesized ZnO NPs at two different concentrations (MIC and MBC), along with their respective controls expressed as mean $\log_{10}$ CFU/mL at different time intervals is presented in Fig. 12.

In this experiment, all the six untreated MDR- NTS isolates (three each of *S.* Typhimurium and *S.* Enteritidis) exhibited an increasing growth pattern at 30, 60, 90, 120, 150, 180, 360 min and 24 h of incubation (Fig. 12). However, all the MDR-NTS isolates treated with meropenem (antibiotic control) exhibited no visible growth after 240 min of co-incubation. Moreover, all the MDR- NTS serotypes exhibited a progressive decline in the bacterial growth after 240 min of co-incubation with the MIC as well as MBC levels of green synthesized ZnO NPs (Fig. 12). Interestingly, none of the MDR- NTS serotypes (*S.* Typhimurium and *S.* Enteritidis) exhibited visible growth after 360 min of incubation with green synthesized ZnO NPs at both MIC as well as MBC values ($P< 0.001$).

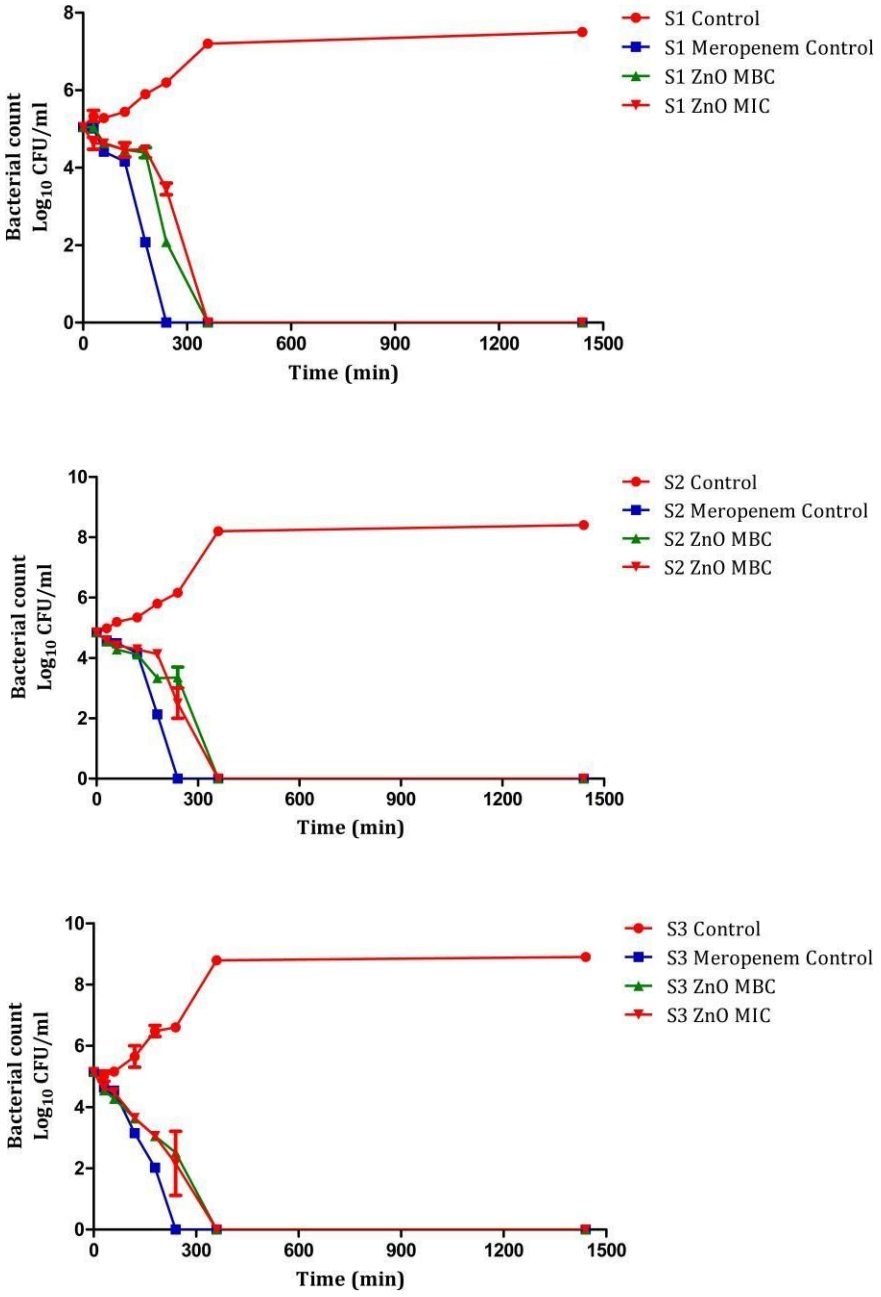

Fig 11.A. *In vitro* dose- and time- dependent extracellular killing kinetics of green synthesized ZnO NPs against MDR- *S*. Enteritidis

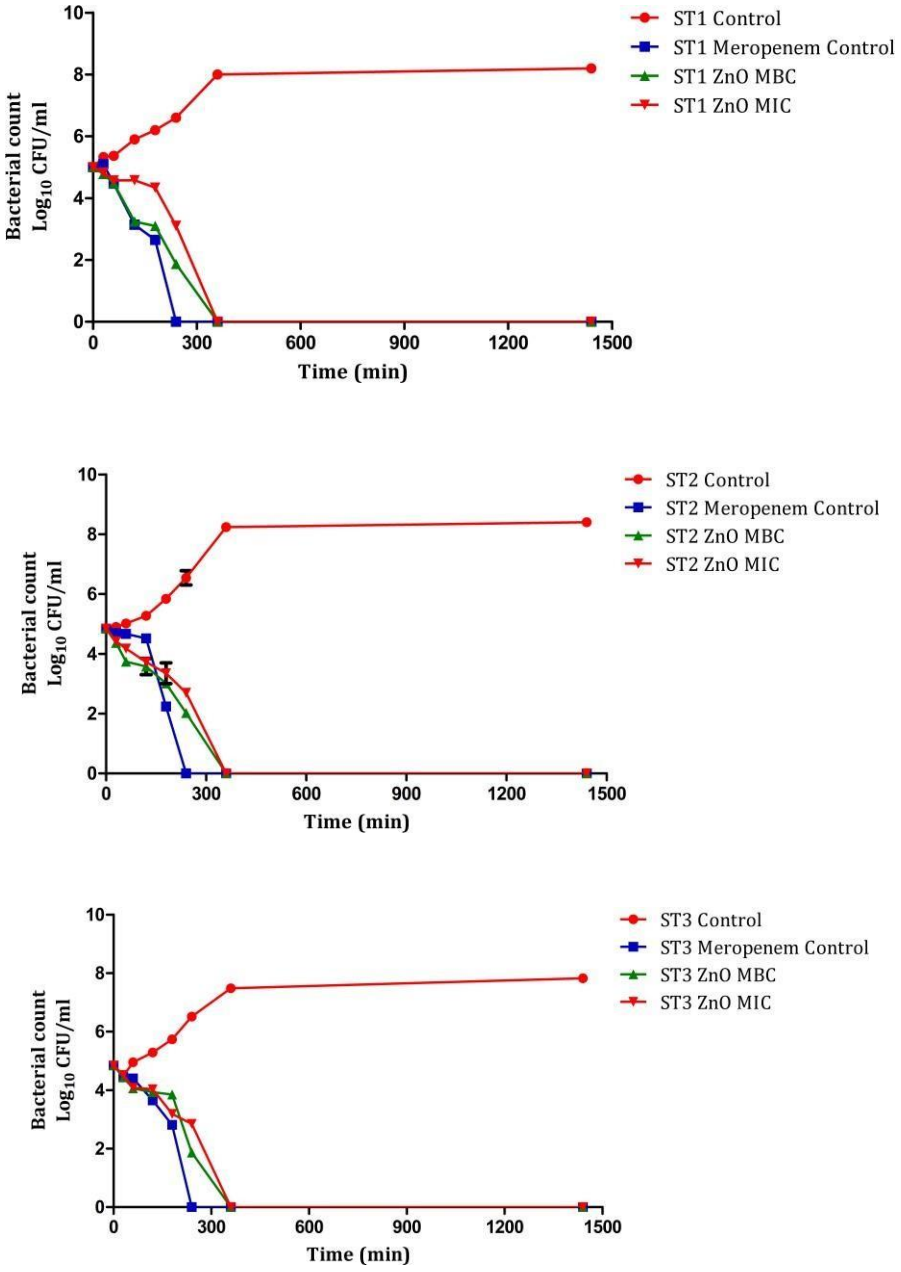

Fig 11.B. *In vitro* dose- and time- dependent extracellular killing kinetics of green synthesized ZnO NPs against MDR- *S*. Typhimurium

5. Discussion

5. DISCUSSION

Food-borne illnesses are considered as an emerging public health problem that results in considerable morbidity and mortality worldwide. In recent times, various bacterial pathogens, especially serovars of NTS constitute a major public health threat globally (Alghoribi *et al*., 2019). Generally, the NTS serotypes may infect and colonize the intestinal and/or reproductive tracts, constituting the environmental reservoirs. Moreover, the NTS strains form a part of the normal intestinal flora of food-producing animals and birds. The poultry products contaminated with various serotypesof NTS are often regarded as the source of the food-borne outbreak of salmonellosis in humans (Gal-Mor, 2019). The indiscriminate use of antimicrobials in livestock and poultry has led to the emergence of drug- resistant strains of pathogens, which were otherwise treated with empirical antimicrobial therapeutic approaches (Micoli *et al*., 2021). The emergence of MDR strains of NTS serovars has been well documented from various sources (Sharma *et al*., 2019; Tack *et al*., 2020).

The reduced pipeline of antimicrobial discovery amalgamated with the escalating trends in drug resistance patterns has forced the researchers to give more emphasis on novel alternative therapeutic strategies against MDR pathogens (Kumar *et al*., 2021). Among the various alternative approaches such as antimicrobial peptides, phage therapy, probiotics, CRISPR-Cas technology, phytochemicals, endolysins, and NPs reported so far, the use of NPs was found to be promising owing to their distinctive antimicrobial properties (Ahmad and Karla, 2020; Kumar *et al*., 2021; Streicher, 2021). In this study, the antimicrobial properties of ZnO NPs were investigated. The unique physicochemical properties of ZnO NPs, especially their large surface area-to-volume ratio, have attracted great interest in the recent past due to their tremendous scope for application in the field of biomedicine (Cherian *et al*.,

2019). Additionally, ZnO NPs possessed antibacterial properties and were approved as 'generally recognized as safe' by US Food and Drug Administration (FDA) and were employed to treat drug-resistant infections both in humans and animals (Yusof *et al*., 2019; Ameen *et al*., 2021).

Generally, ZnO NPs can be synthesized either by physical or chemical methods. Nevertheless, the hazardous chemicals employed during the process of synthesis of NPs can generate adverse environmental effects. Being eco-friendly, simple, inexpensive, and safe with minimal side effects, the green synthesis of ZnO NPs has gained wide attention (Yusof *et al*., 2020; Mohamed *et al*., 2021). Furthermore, the green synthesis of ZnO NPs employing plant extracts was found to be more efficient, as they do not require any sterile environment and culture media as in the case of the biosynthesis approach using microbes and fungi.

5.1. GREEN SYNTHESIS OF ZnO NPs

Since ancient times, *P. longum* has been recognized as an active ingredient of numerous ayurvedic medicinal preparations (Subramaniam *et al*., 2021). *P. longum* (commonly known as Indian long pepper or pippali) is an aromatic climber, which is extensively distributed in and around the sub-tropical as well as tropical regions of the world, including India (Jayapriya *et al*., 2019; Yadav *et al*., 2019; Huang *et al*., 2020). Being a rich source of bioactive constituents (such as tannins, dihydrostigmasterol, piperidine alkaloids, terpenines), the catkin, root, leaves, and stem of this plant have traditionally been used for the treatment of various ailments (Huang *et al*., 2020).

In the present study, the aqueous catkin extract of *P. longum* was used for the synthesis of ZnO NPs. The catkin extract of *P. longum* reduced the aqueous solution of 0.10 M Zinc acetate dihydrate (at a ratio of 1:4) to ZnO NPs at 60^{o}C under constant stirring for 2 h. The formation of brown-colored precipitate at the bottom of the beaker indicated the formation of ZnO NPs

(Fig. 1). The biosynthesis of ZnO NPs employing the *P. longum* catkin extract could be due to its capping and stabilizing action and the presence of electron-rich functional groups present in the aqueous extract. Moreover, the color change observed during the formation of ZnO NPs could be due to the excitation of SPR in the ZnO NPs (Singh *et al*., 2018; Dhandapani *et al*., 2020). The green synthesized ZnO NPs were further employed for their physicochemical characterization.

5.2. CHARACTERISATION OF ZnO NPs

Initially, UV- Vis spectroscopy confirmed the synthesis of ZnO NPs. The unique SPR property of noble metals strongly induces the absorption of incident light and can be monitored by UV- Vis spectroscopy (Sali *et al*., 2021). The green synthesized ZnO NPs produced in this study, revealed a progressive SPR band between 320 nm to 350 nm (Fig. 3), confirming its formation. The maximum absorbance peak was obtained at 340 nm, which isin accordance with the previously reported literature (Dulta *et al*., 2021; Joshi *et al*., 2021). The result confirmed that the bio- constituents present in the aqueous catkin extract of *P. longum* played an important role in the bio- reduction of Zn^{2+} (present in the Zinc acetate dihydrate) to Zn^{0} (ZnO NPs) ions(Sharmila *et al*., 2019).

The presence of chemical and functional groups of the green synthesized ZnO NPs was estimated by FTIR spectrum analysis (Rajendran *et al*., 2021). A prominent peak formed at 3640 cm^{-1} indicated the presence of O-H stretch and hydrogen-bonded functional groups either in alcohol, phenol, or water molecules in the extract (Ahmed *et al*., 2020). The peaks observed at 2850 cm^{-1}, 2100 $cm^{-1,}$ 1739 cm^{-1}, 1490 cm^{-1} were attributed to the presence of -CN stretching, C≡C terminal alkyne, C=O stretching and C-H bending, respectively. Moreover, the peaks observed at 870 cm^{-1} and 915 cm^{-1} were attributed to the presence of C-H bend in the alkane group and -C-O-C group (Vijayakumar *et al*., 2018; Nandiyanto *et al*., 2019; Prusty *et al*., 2019). All

these peaks observed confirmed the presence of phytochemical components associated with the green synthesized ZnO NPs (Fig. 4). The absorption peak obtained at 620 cm^{-1} revealed an inter-atomic vibration of metal oxides attributed to the presence of ZnO NPs, thereby confirming its formation (Pillai *et al*., 2020).

In order to determine the thermal stability and thermal degradation of green synthesized ZnO NPs under constant heating, thermogravimetric analysis (TGA) and differential thermogravimetry (DTG) was performed. The TGA data obtained in this study revealed an initial weight loss of around 6 per cent from 40 ^{o}C to 100 ^{o}C, supported by the DTG graph, with an exothermic peak observed at 200 ^{o}C. Further, progressive thermal degradation of the green synthesized ZnO NPs was observed between 250 ^{o}C and 400 ^{o}C that corresponded with a narrow endothermic peak at 330 ^{o}C. This increase in annealing temperature had resulted in a continuous weight loss of the green synthesized ZnO NPs. Furthermore, good thermal stability was noticed for annealing temperatures between 900 ^{o}C and 1300 ^{o}C (Fig. 5), as reported earlier (Khatami *et al*., 2018; Thi *et al*., 2020).

The PXRD analysis was carried out to confirm the formation of ZnO NPs and to verify their crystallinity. In the present study, the PXRD diffractogram was compared with the standard powder diffraction card of the Joint Committee on Powder Diffraction Standards (JCPDS), ZnO file No. 36-1451. The peaks observed in the PXRD pattern of the green synthesized ZnO NPs (Fig. 6) at 2θ values of 31.85^{o}, 34.50^{o}, 37.1^{o}, 51^{o}, 59^{o}, 64^{o}, 67.1^{o} and 77^{o} corresponded to the lattice planes (100), (002), (101), (102), (110), (103), (200), and (202), respectively (Sespasgozar *et al*., 2021). Hence, the observed sharp and intense peaks indicated that the green synthesized ZnO NPs exhibited hexagonal wurtzite crystalline structure (Hassan Basri *et al*., 2020; Iqbal *et al*., 2021). Moreover, as reported in the earlier studies (Jiang *et al*., 2018; Naseer *et al*., 2020), an average crystalline size of 14.54 nm was

estimated for the green synthesized ZnO NPs from the Debye Scherrer formula (Thi *et al*., 2020; Sali *et al*., 2021).

Furthermore, the shape and surface morphology of the biosynthesized ZnO NPs was determined by SEM imaging (Dandapani *et al*., 2020). The green synthesized ZnO NPs obtained in the present study appeared in a uniform manner, predominantly hexagonal, and a few of them in the form of cubes. The narrow space because of densification could be attributed to the agglomeration of synthesized NPs (Ahmed *et al*., 2020).

The sizes, as well as the crystalline nature of the green synthesized ZnO NPs, were ascertained using the TEM analysis. The reducing agents present in the extract play an important role in determining the size and shape of the biosynthesized NPs (Pillai *et al*., 2020). The TEM images of the biosynthesized ZnO NPs exhibited an almost hexagonal shape with a slight variation in thickness, which supported the results of SEM. Moreover, some of the particles were found agglomerated. Besides, the SAED patterns demonstrated hexagonal wurtzite crystallinity of ZnO NPs. Further, the TEM image demonstrated a spacing of lattice fringes for the biosynthesized ZnO NPs in the range of 0.24 nm that corresponded to the (101) plane (Lin *et al*., 2014). Intriguingly, the crystallinity of green synthesized ZnO NPs determined by SEM and TEM imaging matched with the data acquired from PXRD analysis.

5.3. *IN VITRO* ANTIMICROBIAL EFFICACY OF GREEN SYNTHESISED ZnO NPs

It is recognized that a reduction in the particle size increases strain-wise the antimicrobial activity due to a larger surface-to-volume ratio (Selim *et al*., 2020). In this study, the antibacterial activity of ZnO NPs was investigated against the characterized MDR field strains of NTS by the micro broth dilution technique (CLSI, 2019).

The MIC and MBC values of biosynthesized ZnO NPs against the tested pathogens (MDR- *S*. Typhimurium and *S*. Enteritidis) were found to be 125 µg/ml and 250 µg/ml, respectively (Table 3). The antibacterial effect of ZnO NPs might be either due to the bacterial outer membrane destabilization, induction of oxidative stress, disruption of ion movement, or the initiation of apoptosis (Dhandapani *et al*., 2020).

In the present study, a comparatively lower MIC, as well as MBC values of ZnO NPs, could be due to the presence of lipopolysaccharide in the cell wall of Gram-negative bacteria which might exert aversion towards NPs, thereby enabling resistance (Yusof *et al*., 2020).

5.4 *IN VITRO* STABILITY ASSAYS

5.4.1. Effect of high-end temperatures

The green synthesized ZnO NPs should be deemed thermostable to be used as feed ingredients since the animal feed processing involves various steps including mash preparation (45 - 55 °C), pelletization (around 80 °C), and finally steam sterilization at 100 °C. Further, a standard sterilization protocol should be followed for feed pellets in order to destroy the pathogens and to overcome post-processing contamination (Rebello *et al*., 2018).

In the present study, the green synthesized ZnO NPs were found to be variably stable at high-end temperatures (Table 4) and could withstand such temperatures employed for feed processing (Ebbensgaard *et al*., 2015).

5.4.2. Effect of protease enzymes (trypsin, lysozyme, and proteinase-K)

The stability of a therapeutic candidate is determined by various factors; proteases are among them. The changes induced on the surface of green synthesized NPs, as a result of the enzymatic metabolism, may result in aggregation and destabilization of NPs. Besides, protease-mediated degradation

may render the NPs inactive and subsequently could affect their therapeutic efficacy (Woods *et al*., 2020).

In the present study, the green synthesized ZnO NPs were found to be variably stable, as their MIC values remained more or less similar, although strain-wise variations were also observed (Table 5). This could be due to the destabilization of the bacterial cell membrane in presence of protease enzymes (Woods *et al*., 2020). Further, the protease stability of NPs could be improved by providing an energy barrier that might induce repulsion between these particles. However, the composition of the biological environment in the gastrointestinal tract may also result in variation in surface charge (Malhaire *et al*., 2016). The enzyme activity can be impeded by modifying the local pH of the environment exposed. Besides, non-ionic macromolecules like polyethylene glycol (PEG) polymers, mucoadhesive polymers like polyacrylate can also be used to reduce theinteraction between NPs and inhibitors present in biological fluids, and to limit the activity of endopeptidases (Malhaire *et al*., 2016; Woods *et al*., 2020).

5.4.3. Effect of physiological concentration of cationic salts

The fate of NPs is greatly affected by their interaction with the biological fluids. Following its entry into the biological system, these biofluids can significantly alter the colloidal stability and their antimicrobial properties (Muraleetharan *et al*., 2019). One of the main factors that limit the clinical translation of such NPs is the inactivation by cationic salts present in the biological system.

The green synthesized ZnO NPs tested in the present study retained their antimicrobial activity in presence of physiological concentrations of cationic salts (Table 6). The stability might be due to the functional groups present in the catkin extract used in the study. The nature of the capping agent used would heavily influence the stability of NPs during adverse conditions (Zhang *et al*., 2012).

5.4.4. Effect of pH

The large surface area and smaller size of the NPs might lead to the aggregation and destabilization of the NPs, which is the biggest challenge in the application of NPs (Marangon *et al*., 2021). Nevertheless, it is evident from the earlier reports that a change in the physicochemical conditions such as pH and ionic strength of the solution can affect the intrinsic properties of NPs, such as their size, stability, zeta potential, morphology, and shape of the synthesized NPs (Phongtongpasuk *et al*., 2019; Marangon *et al*., 2021). Besides, the pH has a great impact on the stability and aggregation of NPs, as it can alter the interactions between NPs (Chen *et al*., 2020).

In this study, it is noticeable that the antibacterial efficacy of green synthesized ZnO NPs has enhanced at the alkaline pH (Table 7). It was suggested by Ribut *et al*. (2018) that an increase in the pH would lead to the increased antibacterial activity of ZnO NPs. By increasing the pH of the solution, the electrostatic repulsive force between NPs increases, while low pH would lead to the agglomeration of NPs, thereby reducing its antibacterial activity (Peng *et al*., 2017). Furthermore, Chitra and Annadurai (2014) reported that those NPs synthesized at alkaline pH exhibited comparatively better antibacterial activitythan those NPs synthesized at acidic as well as neutral pH. In addition to this, smaller NPs exhibited more bactericidal effects and bacterial toxicity when compared to larger NPs, as they have a larger surface area (Zhang *et al*., 2016).

5.5. *IN VITRO* SAFETY ASSAYS OF GREEN SYNTHESIZED ZnO NPs

5.5.1. Haemolytic assay

The *in vitro* haemolytic assay is often employed as a versatile tool for carrying out the initial toxicity assessment of a therapeutic compound (Greco *et al*., 2020). The accumulation and extensive distribution of metal-based NPs over time in the biological system may lead to an adverse effect on the eukaryotic cells,though it has been found selectively toxic to bacterial cells (Sanchez-Lopez *et al*.,

2020). Furthermore, several factors including membrane composition, side chain associated with the NPs, incubation time, and the temperature would also affect the haemolytic property of compounds (Noudeh *et al*., 2011).

Classically, chicken erythrocytes are regarded as mammalian cell membrane models, mainly due to the presence of an intact as well as the transcriptionally inactive nucleus and other cell organelles (Babu *et al*., 2017). Hence, for clinical translation and to be used as a potential drug candidate, the cytotoxicity of NPs needs to be validated in suitable eukaryotic cells. In this study, the green synthesized ZnO NPs exhibited minimal haemolysis at 2X, 5X, and 10X MIC levels against chicken erythrocytes (Table 8). Moreover, dose- dependent haemolysis was observed in this study, as reported earlier (Andleeb *et al*., 2020). Besides, it is proposed that the ZnO NPs at very lower concentrations cannot produce toxicity in the biological system when compared to the bacterial cells (Siddiqi *et al*., 2018).

5.5.2. MTT cytotoxicity assay

Though *in vitro* haemolytic assay can successfully be employed for assessing the initial toxicity studies, additional cytotoxicity assays would deliver a strong foundation to the results of haemolytic studies and would further help in the evaluation of a drug candidate.

The present study revealed minimal cytopathic effect in the HEK cell lines, even at 1X, 5X, and 10X MIC levels. This low cytotoxicity obtained in the present study could be attributed to the presence of capping agents in the catkin extract associated with the surface of green synthesized ZnO NPs (Aldalbahi *et al*., 2020).

5.5.3. Effect of green synthesized ZnO NPs on commensal gut lactobacilli

Though the mechanism of action of ZnO NPs on the food-borne pathogenic bacteria was clearly understood, the investigation of its effect on

beneficial gut microflora is also equally important as they form an integral part of the body's innate defense system (Feng *et al*., 2017). Hence, in the present study, MIC dose of green synthesized ZnO NPs was treated with two commensal gut lactobacilli (*L. acidophilus*, and *L. plantarum*), to investigate adverse effects, if any.

In this study, *L. acidophilus* and *L. plantarum* revealed similar growth patterns in both treatment control (treated with green synthesized ZnO NPs) as well as the untreated control. Moreover, a non-significant ($P > 0.05$) antimicrobial efficacy was observed for the green synthesized ZnO NPs against the tested strains of *L. acidophilus* and *L. plantarum* (Fig.10).

Contrarily, several reports suggested a significant reduction in the number of beneficial gut lactobacilli following the treatment with ZnO NPs (Feng *et al.*, 2017; Kolba *et al*., 2020; Wang *et al*., 2021). However, in yet another study, the proportion of lactobacilli was found to increase after exposure to ZnO NPs (Xia *et al*., 2017). It could be well inferred from the findings of this study that various other factors such as the mode of synthesis of NPs, the conditions of exposure, size as well as the morphology of ZnO NPs could affect the efficacy of green synthesized NPs (Yoo *et al*., 2021).

5.6. *IN VITRO* DOSE- AND TIME- DEPENDENT EXTRACELLULAR KILLING KINETICS OF MDR-NTS STRAINS TREATED WITH GREEN SYNTHESIZED ZnO NPs.

The antibacterial activity of green synthesized ZnO NPs reported an increased bacterial inhibition with an increase in the concentration and incubation time without altering the mechanism of action (Siddiqi *et al*., 2018).

In the present study, no visible bacterial growth was observed in the ZnO NP-treated (MIC and MBC) groups after six h (Fig. 12). Moreover, meropenem-treated groups exhibited complete elimination of MDR-NTS strains after 240 min. This antibacterial activity of green synthesized ZnO NPs and meropenem might

be due to the peculiar cell wall structure of Gram-negative bacteria which possess a thin peptidoglycan layer and an outer membrane composed of lipopolysaccharides (Loo *et al*., 2018). The results suggested that the green synthesized ZnO NPs possess a broad spectrum of antibacterial activity, as it exerts a similar effect on all the tested MDR strains of *Salmonella* spp. (Loo *et al*.,2018). Moreover, the results of this study indicated that the green synthesized ZnO NPs has got a direct action on the bacterial cell before entering the stationary phase of growth, as they revealed a rapid as well as time-dependent bactericidal activity against the tested MDR-NTS strains, as reported earlier (Fahimmunisha *etal*., 2020).

In general, the increased antibacterial activity of NPs would be expected with increasing concentrations (Turleybekuly *et al*., 2019). However, from the obtained results of *in vitro* growth kinetic assay, it could be noted that both at MIC and MBC levels, the bacterial growth was inhibited after 360 min. Furthermore, the bacterial clearance of ZnO NPs was found to be independent of their concentration. Interestingly, the *in vitro* dose and time-dependent killing kinetics of green synthesized ZnO NPs were at par with the carbapenem antibiotic control (meropenem) used in this study.

In short, the green synthesized ZnO NPs from the aqueous extract of *P. longum* catkins could be considered as a promising drug candidate against the MDR- NTS strains; the study could further be extrapolated to a wide variety of food-borne pathogens. However, strategies need to be formulated to improve the antimicrobial efficacy of the green synthesized ZnO NPs, either by doping with other NPs or by optimizing different conditions employed for the synthesis. Additionally, the mechanistic studies of the ZnO NPs could be carried out in order to understand the detailed mechanism of action under varied host conditions. Furthermore, *in vivo* clinical studies should also be performed to validate the application of ZnO NPs in suitable target hosts.

6. Summary

6. SUMMARY

The emergence of drug-resistant pathogens, primarily due to the indiscriminate use of antibiotics, has been recognized as a potential threat to humans, animals as well as environment. Of late, an unusual emergence of AMR has been observed among the NTS strains; hence, the NTS strains have been listed as a priority pathogen by the WHO. The diminishing antibiotic discovery pipeline and lack of availability of newer classes of antibiotics along with the escalating trends in AMR have forced the researchers to shift their focus to alternative therapeutics. Hence, the present study was undertaken to evaluate the antibacterial potential of green synthesised ZnO NPs from the aqueous extract of *P. longum* catkin against the MDR-NTS isolates.

In the present study, three isolates each of MDR- *S.* Typhimurium and *S.* Enteritidis serotypes maintained in the laboratory repository of the Department of Veterinary Public Health, College of Veterinary and Animal Sciences, Pookode were revived and re-validated by employing genus- as well as serotype-specific PCR assays. Further, multi-drug resistance patterns of the test strains were also confirmed by employing antibiotic susceptibility testing.

The green synthesis of ZnO NPs was carried out from zinc acetate dihydrate (0.10 M) solution using the aqueous extract of the *P. longum* catkin. The biosynthesized ZnO NPs were physicochemically characterized by UV-Vis spectroscopy, FTIR, TGA, XRD, SEM, and TEM. The green synthesized ZnO NPs revealed a characteristic UV-Vis absorption peak at 340 nm. The FTIR spectroscopy confirmed specific functional groups associated with the green synthesized ZnO NPs. Additionally, TGA/DTA was performed to determine the thermal stability of ZnO NPs; progressive thermal degradation of the green synthesized ZnO NPs was observed between 250 ^{o}C and 400 ^{o}C. However, they exhibited good thermal stability for annealing temperatures between 900 ^{o}C and 1300 ^{o}C. The XRD studies exhibited a hexagonal wurtzite crystalline structure for

the green synthesized ZnO NPs. Moreover, an average crystallite size of 14.54 nm was estimated for the green synthesised ZnO NPs from the Debye- Scherrer formula.

The morphological studies of the green synthesized ZnO NPs carried out using SEM revealed a predominant hexagonal shape. The shape and crystalline nature of ZnO NPs were further confirmed using TEM analysis. The SAEDpatterns demonstrated hexagonal wurtzite crystallinity of ZnO NPs and TEMrevealed space lattice fringes in the range of 0.24 nm. The green synthesized ZnO NPs were then explored for their *in vitro* antibacterial efficacy against the MDR- NTS strains.

Initially, the minimum inhibitory concentration (MIC; 125 μg/mL), as well as minimum bactericidal concentration (MBC; 250 μg/mL) of green synthesized ZnO NPs, were determined by employing the micro broth dilution technique.

The green synthesised ZnO NPs were also investigated for their *in vitro* stability to high-end temperatures (70 °C and 90 °C), proteases (trypsin, lysozyme, and proteinase-K), the physiological concentration of cationic salts (150 m*M* NaCl and 2 m*M* $MgCl_2$), and pH (four, six, and eight). At MIC (1X) levels, for S3 and S2, the antimicrobial activity of green synthesized ZnO NPs remained the same at 70 °C. However, at 70 °C, with all the remaining strains tested (S1, ST1, ST2, and ST3), a two-fold increase in the MIC levels wasobserved. Additionally, a three- to four-fold increase in the MBC values was observed for ZnO NPs until 30 min. In contrast, the green synthesised ZnO NPs were found stable even after incubation at 90 °C, since they retained their MIC values with the tested MDR- NTS strains. Alike at 70 °C, a three to four-fold increase in the MBC values was observed upon incubation at 90 °C for five, 15, and 30 min.

Irrespective of treatment with proteases (trypsin, lysozyme, and proteinase-K), the green synthesized ZnO NPs were found variably stable; however, slight strain-wise variation was exhibited. Besides, the green synthesised

ZnO NPs tested were found to be stable at physiological concentrations of cationic salts and different pH, as they retained their antimicrobial activity (MIC and MBC values). Interestingly, the MIC value of ZnO NPs was reduced to half atpH eight.

In vitro safety assays of green synthesized ZnO NPs were carried out by employing a haemolytic assay using chicken erythrocytes as well as MTT cytotoxicity assay using epithelial HEK cell lines. Minimal haemolysis (less than two per cent) was exhibited by the green synthesised ZnO NPs at 2X, 5X, and 10X MIC levels. Moreover, the green synthesized ZnO NPs did not exhibit any cytopathic effect at 1X, 5X, and 10X MIC levels in the *in vitro* MTT cytotoxicity assay.

The adverse effect of green synthesised ZnO NPs on the commensal gut lactobacilli was investigated by broth microdilution method using *L. acidophilus* and *L. plantarum*. In the present study, *L. acidophilus* and *L. plantarum* revealed a similar growth pattern in both treatment control (treated with green synthesised ZnO NPs) and the untreated control. Overall, a non-significant ($P > 0.05$) antimicrobial efficacy was observed for the green synthesised ZnO NPs against *L. acidophilus* and *L. plantarum*.

Further, the *in vitro* dose- and time-dependent extracellular killing kinetics of MDR-NTS strains treated with green synthesised ZnO NPs was assessed in comparison with the carbapenem antibiotic, meropenem. All the six untreated MDR- NTS isolates (three each of *S.* Typhimurium and *S.* Enteritidis) exhibited an increasing growth pattern at 30, 60, 90, 120, 150, 180, 360 min, and 24 h of incubation. Irrespective of the MIC and MBC levels, green synthesised ZnO NPs completely inhibited the MDR- NTS counts treated with meropenem (antibiotic control) at 240 min of co-incubation. Moreover, all the MDR- NTS serotypes exhibited a progressive decline in the bacterial growth after 360 min of co-incubation with the MIC as well as MBC levels of green synthesised ZnO NPs.

To conclude, the biosynthesised ZnO NPs were found to exhibitantibacterial activity against the tested MDR-NTS strains and was found stable and safe. Overall, the study demonstrated a facile, eco-friendly method for the synthesis of ZnO NPs, which could be employed as a potential antimicrobial alternative candidate. However, strategies need to be formulated to improve the antimicrobial efficacy of the green synthesized ZnO NPs, either by doping with other NPs or by optimizing different conditions employed for the synthesis. Additionally, the mechanistic studies of the ZnO NPs could be carried out to understand the detailed mechanism of action under varied host conditions. Furthermore, *in vivo* clinical studies should also be performed to validate the application of ZnO NPs in suitable target hosts.

7. References

7. REFERENCES

Adhikari, S., Saud, B., Paudel, G. and Bajracharya, D. 2019. Emergence of Antimicrobial Drug Resistant Bacteria in Nepal: A Current Scenario. *Proteomics Bioinformatics Curr. Res*. **1**: 31-33.

Ahmad, M. and Khan, A.U. 2019. Global economic impact of antibiotic resistance: A review. *J. global Antimicrob. Resist.* **19**: 313-316.

Ahmad, W. and Kalra, D. 2020. Green synthesis, characterization and antimicrobial activities of ZnO nanoparticles using *Euphorbia hirta* leaf extract. *J. King Saud Univ. Sci*. **32**: 2358-2364.

Akbar, A., Sadiq, M.B., Ali, I., Muhammad, N., Rehman, Z., Khan, M.N., Muhammad, J., Khan, S.A., Rehman, F.U. and Anal, A.K. 2019. Synthesis and antimicrobial activity of zinc oxide nanoparticles against foodborne pathogens *Salmonella* Typhimurium and *Staphylococcus aureus*. *Biocatal. Agric. Biotechnol.* **17**: 36-42.

Akbar, S., Tauseef, I., Subhan, F., Sultana, N., Khan, I., Ahmed, U. and Haleem, K.S. 2020. An overview of the plant-mediated synthesis of zinc oxide nanoparticles and their antimicrobial potential. *Inorg. Nano-Met. Chem*. **50:** 257-271.

Alam, M.M., Islam, M., Wahab, A. and Billah, M. 2019. Antimicrobial resistance crisis and combating approaches. *J. Med.* **20**: 38-45.

Alavi, M. and Rai, M. 2019. Recent advances in antibacterial applications of metal nanoparticles (MNPs) and metal nanocomposites (MNCs) against multidrug-resistant (MDR) bacteria. *Expert Re.v Anti-Infect.*

Albert, M.J., Bulach, D., Alfouzan, W., Izumiya, H., Carter, G., Alobaid, K., Alatar, F., Sheikh, A.R. and Poirel, L. 2019. Non-typhoidal *Salmonella* blood stream infection in Kuwait: Clinical and microbiological characteristics. *PLoS Negl. Trop. Dis.* **13:** e0007293.

Aldalbahi, A., Alterary, S., Ali Abdullrahman Almoghim, R., Awad, M.A., Aldosari, N.S., Fahad Alghannam, S., Nasser Alabdan, A., Alharbi, S., Ali Mohammed Alateeq, B., Abdulrahman Al Mohsen, A. and Alkathiri, M.A. 2020. Greener synthesis of zinc oxide nanoparticles: Characterization and multifaceted applications. *Molecules*. **25**: 4198.

Aldrich, C., Hartman, H., Feasey, N., Chattaway, M.A., Dekker, D., Al-Emran, H.M., Larkin, L., McCormick, J., Sarpong, N., Le Hello, S. and Adu-Sarkodie, Y. 2019. Emergence of phylogenetically diverse and fluoroquinolone resistant *Salmonella* Enteritidis as a cause of invasive nontyphoidal *Salmonella* disease in Ghana. *PLoS Negl. Trop. Dis.* **13:** e0007485.

Al-Fahad, A.J., Aldossary, A.M., Alshehri, A.A., Alomary, M.N., Almughem, F.A., Alyahya, S. and Tawfik, E.A. 2021. Microbial Nanotechnology in Treating Multidrug-Resistance Pathogens. *Microb. Nanotechnol. Green Synthesis. Appl*. **25**: 191-216.

Alghamdi, S. 2021. The role of vaccines in combating antimicrobial resistance (AMR) bacteria. *Saudi J. Biol. Sci.* **28**: 7505-7510.

Alghoribi, M.F., Doumith, M., Alrodayyan, M., Al Zayer, M., Köster, W.L., Muhanna, A., Aljohani, S.M., Balkhy, H.H. and Desin, T.S. 2019. *S.* Enteritidis and *S.* Typhimurium harboring SPI-1 and SPI-2 are the predominant serotypes associated with human salmonellosis in Saudi Arabia. *Front. Cell. Infect. Microbiol.* **9**: 187p.

Ali, J., Mazumder, J.A., Perwez, M. and Sardar, M. 2021. Antimicrobial effect of ZnO nanoparticles synthesized by different methods against food borne pathogens and phytopathogens. *Mater. Today. Proc.* **36**: 609-615.

Ali, T., Sarwar, A., Sattar, M.M.K., Tariq, M. and Ali, M.A. 2020. Salmonella Enteritidis: a major threat for disease and food poisoning. *Pakistan J. Sci.* **72**.

Alkasir, M., Samadi, N., Sabouri, Z., Mardani, Z., Khatami, M. and Darroudi, M. 2020. Evaluation cytotoxicity effects of biosynthesized zinc oxide nanoparticles using aqueous *Linum usitatissimum* extract and investigation of their photocatalytic activityackn. *Inorg. Chem. Commun.* **119**: 108066p.

Allaker, R.P. and Yuan, Z. 2019. Nanoparticles and the control of oral biofilms. In *Nanobiomater. Clinic. Dent.* **21**: 243-275

Al-Mnaser, A.A. and Woodward, M.J. 2020. Sub-lethal concentrations of phytochemicals (Carvacrol and Oregano) select for reduced susceptibility mutants of *Escherichia coli* O23: H52. *Polish J. Microbiol.* **69**: 121p.

Al-Mohaithef, M., Hazazi, A., Chandramohan, S. and Edrees, H.H. 2019. Assessing physician knowledge and attitude on food borne illnesses in Kingdom of Saudi Arabia. *Int.J. Med.Res.Hlth. Sci.* **8**: 80-87.

Al-Seghayer, M.S. and Al-Sarraj, F.M. 2021. The Outbreak of Foodborne Disease by Pathogenic Enterobacteriaceae Antimicrobial Resistance-A Review. *Asian Food Sci. J* .91-99.

Ameen, F., Dawoud, T. and AlNadhari, S. 2021. Ecofriendly and low-cost synthesis of ZnO nanoparticles from *Acremonium potronii* for the photocatalytic degradation of azo dyes. *Environ. Res.* **202**: 111700.

Anand, T., Virmani, N., Kumar, S., Mohanty, A.K., Pavulraj, S., Bera, B.C., Vaid, R.K., Ahlawat, U. and Tripathi, B.N. 2020. Phage therapy for treatment of virulent *Klebsiella pneumoniae* infection in a mouse model. *J. Glob. Antimicrob. Resist.* **21**: 34-41.

Andleeb, S., Tariq, F., Muneer, A., Nazir, T., Shahid, B., Latif, Z., Abbasi, S.A.,ul Haq, I., Majeed, Z., Khan, S.U.D. and Khan, S.U.D. 2020. In vitro bactericidal, antidiabetic, cytotoxic, anticoagulant, and hemolytic effect of green-synthesized silver nanoparticles using *Allium sativum* clove extract incubated at various temperatures. *Green Process. Synth.* **9**: 538- 553.

Angel Villegas, N., Silvero Compagnucci, M.J., Sainz Ajá, M., Rocca, D.M., Becerra, M.C., Fabián Molina, G. and Palma, S.D. 2019. Novel antibacterial resin-based filling material containing nanoparticles for the potential one-step treatment of caries. *J. hlthcare. Engng.* **12**: 32-35.

Aquib, M., Farooq, M.A., Banerjee, P., Akhtar, F., Filli, M.S., Boakye-Yiadom, K.O., Kesse, S., Raza, F., Maviah, M.B., Mavlyanova, R. and Wang, B. 2019. Targeted and stimuli–responsive mesoporous silica nanoparticles for drug delivery and theranostic use. *J. Biomed. Mater. Res. Part A.* **107**: 2643-2666.

Arya, S.S., Sharma, M.M., Das, R.K., Rookes, J., Cahill, D. and Lenka, S.K. 2019. Vanillin mediated green synthesis and application of goldnanoparticles for reversal of antimicrobial resistance in *Pseudomonas aeruginosa* clinical isolates. *Heliyon*. **5**: e02021.

Awwad, A.M., Amer, M.W., Salem, N.M. and Abdeen, A.O. 2020. Green synthesis of zinc oxide nanoparticles (ZnO-NPs) using *Ailanthus altissima* fruit extracts and antibacterial activity. *Chem. Int*. **6**: 151-159.

Aygün, A., Atalay, E., Yassin, S., Khan, A. and Şen, F. 2019. Graphene-Based Nanomaterials for Hydrogen Storage. *Graphene Functionalization Strategies*. **2**: 229-245.

Aygün, A., Gülbağça, F., Nas, M.S., Alma, M.H., Çalımlı, M.H., Ustaoglu, B., Altunoglu, Y.C., Baloğlu, M.C., Cellat, K. and Şen, F. 2020. Biological synthesis of silver nanoparticles using Rheum ribes and evaluation of their anticarcinogenic and antimicrobial potential: a novel approach in phytonanotechnology. *J.Pharm.Biomed. Anal.* **179**: 113012p.

Babu, E.P., Subastri, A., Suyavaran, A., Premkumar, K., Sujatha, V., Aristatile, B., Alshammari, G.M., Dharuman, V. and Thirunavukkarasu, C. 2017. Size dependent uptake and hemolytic effect of zinc oxide nanoparticles on erythrocytes and biomedical potential of ZnO-ferulic acid conjugates. *Sci. Rep.* **7:** 1-12.

Basavegowda, N. and Baek, K.H. 2021. Multimetallic Nanoparticles as Alternative Antimicrobial Agents: Challenges and Perspectives. *Molecules*. **26:** 912.

Bauer, A.W., Kirby, W.M.M., Sherries, J.C., Tuck, M. 1966. Antibiotic susceptibility testing by a standardized disc diffusion method. *Am. J. Clin. Pathol*. **45**: 493-496.

Bloomfield, S.J., Benschop, J., Midwinter, A.C., Biggs, P.J., Marshall, J.C., Hayman, D.T., Carter, P.E., Price-Carter, M., Toombs-Ruane, L., Gray, H. and Burgess, S. 2021. Genomic and phenotypic comparison of two *Salmonella* Typhimurium strains responsible for consecutivesalmonellosis outbreaks in New Zealand. *Int. J. Med. Microbiol.* 151534p.

Boone, K., Wisdom, C., Camarda, K., Spencer, P. and Tamerler, C. 2021. Combining genetic algorithm with machine learning strategies for designing potent antimicrobial peptides. *BMC bioinformatics*. **22**: 1-17.

Borrelli, L., Varriale, L., Dipineto, L., Pace, A., Menna, L.F. and Fioretti, A. 2021. Insect Derived Lauric Acid as Promising Alternative Strategy to Antibiotics in the Antimicrobial Resistance Scenario. *Frontiers. Microbiol.* **12**: 330p.

CDC. 2019. https://www.cdc.gov/drugresistance/pdf/threats-report/2019-ar-threats-report-508.pdf.

CDC. 2020. https://www.cdc.gov/salmonella/backyardpoultry-05.

CLSI [Clinical and Laboratory Standards Institute]. 2019. Performance Standards for Antimicrobial Susceptibility Testing. (29th Ed.). Wayne, USA, 241.

Chang, Y.J., Chen, Y.C., Chen, N.W., Hsu, Y.J., Chu, H.H., Chen, C.L. and Chiu, C.H. 2021. Changing Antimicrobial Resistance and Epidemiology of Non-Typhoidal *Salmonella* Infection in Taiwanese Children. *Frontiers. Microbiol.* **12**: 634p.

Chee, E. and Brown, A.C. 2020. Biomimetic antimicrobial material strategies for combating antibiotic resistant bacteria. *Biomatr. Sci*. **8**: 1089-1100.

Chen, S., Li, Q., McClements, D.J., Han, Y., Dai, L., Mao, L. and Gao, Y. 2020. Co-delivery of curcumin and piperine in zein-carrageenan core-shell nanoparticles: Formation, structure, stability and in vitro gastrointestinal digestion. *Food Hydrocolloids*. **99**: 105334p.

Cherian, T., Ali, K., Fatima, S., Saquib, Q., Ansari, S.M., Alwathnani, H.A., Al-Khedhairy, A.A., Al-Shaeri, M. and Musarrat, J. 2019. *Myristica fragrans* bio-active ester functionalized ZnO nanoparticles exhibit

antibacterial and antibiofilm activities in clinical isolates. *J. Microbiol. Methods*. **166**: 105716.

Chitra, K. and Annadurai, G. 2014. Antibacterial activity of pH-dependent biosynthesized silver nanoparticles against clinical pathogen. *BioMedRes. Int.* **22:** 12-14.

Chiu, C.H. and Su, L.H. 2019. *Salmonella*, Non-Typhoidal Species (*S.* Choleraesuis, *S.* Enteritidis, *S.* Hadar, S. Typhimurium). *Infect. Dis. Antimicrob. Agents.* **21**.

Czyżowska, A., Dyba, B., Rudolphi-Szydło, E. and Barbasz, A. 2021. Structural and biochemical modifications of model and native membranes of human immune cells in response to the action of zinc oxide nanoparticles. *J. Appl. Toxicol.* **41**: 458-469.

Dhandapani, K.V., Anbumani, D., Gandhi, A.D., Annamalai, P., Muthuvenkatachalam, B.S., Kavitha, P. and Ranganathan, B. 2020. Green route for the synthesis of zinc oxide nanoparticles from *Melia azedarach* leaf extract and evaluation of their antioxidant and antibacterial activities. *Biocatal. Agric. Biotechnol*. **24:** 101517.

Dulta, K., Ağçeli, G.K., Chauhan, P., Jasrotia, R. and Chauhan, P.K. 2021. A novel approach of synthesis zinc oxide nanoparticles by *Bergenia ciliata* rhizome extract: antibacterial and anticancer potential. *J. Inorg. Organomet. Polym. Mater*. **31**: 180-190.

da Silva, A.P.S., Ferreira, B.S., Favarim, H.R., Silva, M.F.F., Silva, J.V.F., dos Anjos Azambuja, M. and Campos, C.I. 2019. Physical properties of medium density fiberboard produced with the addition of ZnO nanoparticles. *BioResour*. **14**: 1618-1625.

Dewi, G., Nair, D.V., Peichel, C., Johnson, T.J., Noll, S. and Johny, A.K. 2021. Effect of lemongrass essential oil against multidrug-resistant *Salmonella* Heidelberg and its attachment to chicken skin and meat. *Poultry Sci.* **100**: 101116p.

Ebbensgaard, A., Mordhorst, H., Overgaard, M.T., Nielsen, C.G., Aarestrup, F.M. and Hansen, E.B. 2015. Comparative evaluation of the antimicrobial activity of different antimicrobial peptides against a range of pathogenic bacteria. *PloS one*, **10***:* e0144611.

Ehuwa, O., Jaiswal, A.K. and Jaiswal, S. 2021. *Salmonella*, Food Safety and Food Handling Practices. *Foods*. **10**: 907p.

Etter, A.J., West, A.M., Burnett, J.L., Wu, S.T., Veenhuizen, D.R., Ogas, R.A. and Oliver, H.F. 2019. *Salmonella enterica* subsp. enterica serovar Heidelberg food isolates associated with a Salmonellosis outbreak have enhanced stress tolerance capabilities. *Appl. Environ. Microbiol.* **85**: e01065-19.

Fahimmunisha, B.A., Ishwarya, R., AlSalhi, M.S., Devanesan, S., Govindarajan, M. and Vaseeharan, B. 2020. Green fabrication, characterization and antibacterial potential of zinc oxide nanoparticles using *Aloe socotrina* leaf extract: A novel drug delivery approach. *J.Drug. Delivery Sci.Technol.* **55***:* 101465p.

Feng, Y., Min, L., Zhang, W., Liu, J., Hou, Z., Chu, M., Li, L., Shen, W., Zhao, Y. and Zhang, H. 2017. Zinc oxide nanoparticles influence microflora in ileal digesta and correlate well with blood metabolites. *Frontiers. Microbiol.* **8**: 992p.

Fernando, S.S.N., Gunasekara, T.D.C.P. and Holton, J. 2018. Antimicrobial Nanoparticles: applications and mechanisms of action.

Forouhar, M. and Harzandi, N. 2019. Molecular Survey of Quinolone Resistance in *Salmonella* spp. Isolated From Poultry Products in Karaj, Iran. *Int J Enteric Pathog*, **7**: 55-59.

Gal-Mor, O. 2019. Persistent infection and long-term carriage of typhoidal and nontyphoidal *Salmonellae*. *Clin. Microbiol. Rev.* **32**: e00088-18.

Ghosh, C., Sarkar, P., Issa, R. and Haldar, J. 2019. Alternatives to conventional antibiotics in the era of antimicrobial resistance. *Trends. Microbiol.* **27**: 323-338.

Ghotekar, S. 2019. A review on plant extract mediated biogenic synthesis of CdO nanoparticles and their recent applications. *Asian. J. Green Chem.* **3:** 187-200.

Gondil, V.S. and Chhibber, S. 2021. Bacteriophage and Endolysin Encapsulation Systems: A Promising Strategy to Improve Therapeutic Outcomes. *Frontiers. Pharmacol.* **12**: 1113p.

Gour, A. and Jain, N.K, 2019. Advances in green synthesis of nanoparticles. *Artificial. Cells. Nanomed. Biotechnol.*, **47**: 844-851.

Gourama, H. 2020. Foodborne pathogens. *Food Safety Engng.* **23***:* 25-49

Gourkhede, D.P., Wankhade, P.R., Sirsant, B., Kandhan, S., Sakhare, D.T. and Talokar, A.J. 2021. Antimicrobial Resistance in Bacteria-Its Origin and Evolution: A Review. *J. Livestock Res.* **11**: 14-24.

Greco, I., Molchanova, N., Holmedal, E., Jenssen, H., Hummel, B.D., Watts, J.L., Håkansson, J., Hansen, P.R. and Svenson, J. 2020. Correlation between hemolytic activity, cytotoxicity and systemic in vivo toxicity of synthetic antimicrobial peptides. *Sci. Rep.* **10**: 1-13.

Gupta, N., Rai, D.B., Jangid, A.K. and Kulhari, H. 2019. Use of nanotechnology in antimicrobial therapy. *Methods Microbiol.* **46**: 143-172.

Gupta, P.K. 2020. Poisonous foods and food poisonings. *Prob. Solving Quest. Toxicol.* **43***:* 229-238

Gymoese, P., Kiil, K., Torpdahl, M., Østerlund, M.T., Sørensen, G., Olsen, J.E., Nielsen, E.M. and Litrup, E. 2019. WGS based study of the population structure of *Salmonella enterica* serovar Infantis. *BMC genomics*. **20**: 1-11.

Hassan, A., Alsaihati, A., Al Shammari, M., Sharroufna, M., Alaithan, H. and Aljubran, S. 2019. *Erythema nodosum*: A Manifestation of Salmonella Infection. *Case Rep. Gastroenterol.* **13**: 456-461.

Hassan Basri, H., Talib, R.A., Sukor, R., Othman, S.H. and Ariffin, H. 2020. Effect of synthesis temperature on the size of ZnO nanoparticles derived from pineapple peel extract and antibacterial activity of ZnO–starch nanocomposite films. *Nanomaterials*. **10:** 1061.

Hill-Cawthorne, G., Negin, J., Capon, T., Gilbert, G.L., Nind, L., Nunn, M., Ridgway, P., Schipp, M., Firman, J., Sorrell, T.C. and Marais, B.J. 2019. Advancing Planetary Health in Australia: focus on emerging infections and antimicrobial resistance. *BMJ Global Hlth.* **4:** e001283.

Huang, H., Shan, K., Liu, J., Tao, X., Periyasamy, S., Durairaj, S., Jiang, Z. and Jacob, J.A. 2020. Synthesis, optimization and characterization of silver nanoparticles using the catkin extract of *Piper longum* for bactericidal effect against food-borne pathogens via conventional and mathematical approaches. *Bioorg. Chem*. **10:** e104230.

Iqbal, Y., Malik, A.R., Iqbal, T., Aziz, M.H., Ahmed, F., Abolaban, F.A., Ali, S.M. and Ullah, H. 2021. Green synthesis of ZnO and Ag-doped ZnO

nanoparticles using *Azadirachta indica* leaves: Characterization and their potential antibacterial, antidiabetic, and wound-healing activities. *Mater. Lett.* **305**: 130671.

Jamila, N., Khan, N., Bibi, A., Haider, A., Khan, S.N., Atlas, A., Nishan, U., Minhaz, A., Javed, F. and Bibi, A. 2020. *Piper longum* catkin extract mediated synthesis of Ag, Cu, and Ni nanoparticles and their applications as biological and environmental remediation agents. *Arabian J. Chem.* **13***:* 6425-6436.

Jayappa, M.D., Ramaiah, C.K., Kumar, M.A.P., Suresh, D., Prabhu, A., Devasya, R.P. and Sheikh, S. 2020. Green synthesis of zinc oxide nanoparticles from the leaf, stem and in vitro grown callus of *Mussaenda frondosa* L.: characterization and their applications. *Appl. Nanosci.* **10**: 3057-3074.

Jayapriya, M., Dhanasekaran, D., Arulmozhi, M., Nandhakumar, E., Senthilkumar, N. and Sureshkumar, K. 2019. Green synthesis of silver nanoparticles using *Piper longum* catkin extract irradiated by sunlight: antibacterial and catalytic activity. *Res. Chem. Intermed*. **45**: 3617-3631.

Jiang, J., Pi, J. and Cai, J. 2018. The advancing of zinc oxide nanoparticles for biomedical applications. *Bioinorg Chem and Appl.* **2018***: 1-18*

Jin, D., Kao, C.Y., Darby, J. and Palmer, S. 2020. *Salmonella* Typhimurium myopericarditis: A case report and review of literature. *Wld. J. Cardiol.* **12**: 67p.

Jin, S.E. and Jin, H.E.,2021. Antimicrobial activity of zinc oxide nano/microparticles and their combinations against pathogenic microorganisms for biomedical applications: From physicochemical characteristics to pharmacological aspects. *Nanomaterals.* **11**: 263p.

Jyoti, A., Agarwal, M. and Tomar, R.S. 2020. Synergistic effect of Zinc Oxide Nanoparticles and Guava Leaf extract for Enhanced antimicrobial activity against Enterotoxigenic *Escherichia coli*. *J. Biochem. Technol*, **11**: 17-23.

Joshi, L.P., Khatri, B.V., Gyawali, S., Gajurel, S. and Chaudhary, D.K. 2021. Green Synthesis of Zinc Oxide Nanoparticles Using *Ixora coccinea* Leaf Extract for Ethanol Vapour Sensing. *J. Phys. Sci.* **32**: 15-26.

Kebede, T., Gadisa, E. and Tufa, A. 2021. Antimicrobial activities evaluation and phytochemical screening of some selected medicinal plants: A possible alternative in the treatment of multidrug-resistant microbes. *Plos one*. **16**: e0249253.

Khatami, M., Alijani, H.Q., Heli, H. and Sharifi, I. 2018. Rectangular shaped zinc oxide nanoparticles: Green synthesis by Stevia and its biomedical efficiency. *Ceramics Int.* **44**: 15596-15602.

Khoobchandani, M., Katti, K.K., Karikachery, A.R., Thipe, V.C., Bloebaum, P.L. and Katti, K.V. 2019. Targeted phytochemical-conjugated gold nanoparticles in cancer treatment. In: Khoobchandani, M. and Saxena, A. (eds.), Biotechnology Products. in Everyday Life. EcoProduction, USA, pp. 37-52.

Kolba, N., Guo, Z., Olivas, F.M., Mahler, G.J. and Tako, E., 2020. Intra-amniotic administration (Gallus gallus) of TiO2, SiO2, and ZnO nanoparticlesaffect brush border membrane functionality and alters gut microflorapopulations. *Food. Chem. Toxicol.* **135**: 110896p.

Kumar, P.M., Anandkumar, R., Sudarvizhi, D., Mylsamy, K. and Nithish, M. 2020. Experimental and theoretical investigations on thermal conductivity of the paraffin wax using CuO nanoparticles. *Mater. Today. Proc.* **22**: 1987-1993.

Kumar, M., Sarma, D.K., Shubham, S., Kumawat, M., Verma, V., Nina, P.B., Jp, D., Kumar, S., Singh, B. and Tiwari, R.R. 2021. Futuristic Non-antibiotic Therapies to Combat Antibiotic Resistance: A Review. *Frontiers. Microbiol.* **12**: 16.

Lee, C.M., Lee, M.S., Yang, T.L., Lee, K.L., Yen, T.Y., Lu, C.Y., Hsueh, P.R., Lee, P.I., Chen, J.M., Huang, L.M. and Chang, L.Y. 2021. Clinical features and risk factors associated with bacteremia of nontyphoidal salmonellosis in pediatric patients, 2010–2018. *J. Formosan Med. Assoc.* **120**: 196-203.

Lee, H. and Yoon, Y. 2021. Etiological agents implicated in foodborne illness world wide. *Food Sci. Ani. Resour.* **41**: 1p.

Lee, N.Y., Ko, W.C. and Hsueh, P.R. 2019. Nanoparticles in the treatment of infections caused by multidrug-resistant organisms. *Frontiers Pharmacol.* **10**: 1153p.

Leshkasheli, L., Kutateladze, M., Balarjishvili, N., Bolkvadze, D., Save, J., Oechslin, F., Que, Y.A. and Resch, G. 2019. Efficacy of newly isolated and highly potent bacteriophages in a mouse model of extensively drug-resistant *Acinetobacter baumannii* bacteraemia. *J. Global. Antimicrobe. Resist.* **19**: 255-261.

Li, Y., Pei, X., Bai, L., Yan, L., Yang, S., Zhang, H., Yan, J., Zhan, L., Lan, G., Li, N. and Yang, D. 2021. The China National Foodborne Pathogen Surveillance System: Twenty Years of Experience and Achievements. *Foodborne Path. Dis.* **18**: 519-527.

Lin, C.D., Kou, Y.Y., Liao, C.Y., Li, C.H., Huang, S.P., Cheng, Y.W., Liao, W.C., Chen, H.X., Wu, P.L., Kang, J.J. and Lee, C.C., 2014. Zinc oxide nanoparticles impair bacterial clearance by macrophages. Nanomedicine. **9**: 1327-1339.

Loo, Y.Y., Rukayadi, Y., Nor-Khaizura, M.A.R., Kuan, C.H., Chieng, B.W., Nishibuchi, M. and Radu, S. 2018. In vitro antimicrobial activity of green synthesized silver nanoparticles against selected gram-negative foodborne pathogens. *Frontiers. Microbiol.* **9**: 1555p.

Lu, J., Xu, H., Xia, J., Ma, J., Xu, J., Li, Y. and Feng, J. 2020. D-and unnatural amino acid substituted antimicrobial peptides with improved proteolytic resistance and their proteolytic degradation characteristics. *Frontiers. Microbiol.* **11:** 2-7.

Luvsansharav, U.O., Vieira, A., Bennett, S., Huang, J., Healy, J.M., Hoekstra, R.M., Bruce, B.B. and Cole, D. 2020. Salmonella serotypes: A novel measure of association with foodborne transmission. *Foodborne Path. Dis.* **17**: 151-155.

MacDonald, E., White, R., Mexia, R., Bruun, T., Kapperud, G., Brandal, L.T., Lange, H., Nygård, K. and Vold, L. 2019. The role of domestic reservoirs in domestically acquired *Salmonella* infections in Norway: Epidemiology of salmonellosis, 2000–2015, and results of a national prospective case–control study, 2010–2012. *Epidemiol. Infect.*147.

Mahmoud, A.E.D., Al-Qahtani, K.M., Alflaij, S.O., Al-Qahtani, S.F. and Alsamhan, F.A. 2021. Green copper oxide nanoparticles for lead, nickel, and cadmium removal from contaminated water. *Sci. Rep.* **11**: 1-13.

Makvandi, P., Wang, C.Y., Zare, E.N., Borzacchiello, A., Niu, L.N. and Tay, F.R. 2020. Metal-based nanomaterials in biomedical applications: Antimicrobial activity and cytotoxicity aspects. *Advanced Functional. Mater.* **30**: 1910021.

Malhaire, H., Gimel, J.C., Roger, E., Benoit, J.P. and Lagarce, F. 2016. How to design the surface of peptide-loaded nanoparticles for efficient oral bioavailability. *Adv. Drug. Delivery Rev.* **106**: 320-336.

Mandakini, R., Dutta, T.K., Roychoudhury, P., Subudhi, P.K., Samanta, I. and Bandyopadhayay, S. 2019. Isolation, identification and molecular characterization of multidrug-resistant *Escherichia coli* recovered from pigs of Arunachal Pradesh, India. *Indian J. Anim. Hlth*. **58:** 153-168.

Marangon, C.A., Vigilato Rodrigues, M.A., Vicente Bertolo, M.R., Amaro Martins, V.D.C., de Guzzi Plepis, A.M. and Nitschke, M. 2021. The effects of ionic strength and pH on antibacterial activity of hybrid biosurfactant-biopolymer nanoparticles. *J. Appl. Polym. Sci.* **139**: 51437.

Marchello, C.S., Fiorino, F., Pettini, E., Crump, J.A. and Vacc-iNTS Consortium Collaborators. 2021. Incidence of non-typhoidal *Salmonella* invasive disease: A systematic review and meta-analysis. *J. Infect.*

Medalla, F., Gu, W., Friedman, C.R., Judd, M., Folster, J., Griffin, P.M. and Hoekstra, R.M. 2021. Increased Incidence of Antimicrobial-Resistant Nontyphoidal *Salmonella* Infections, United States, 2004–2016. *Emerg. Infect. Dis.* **27**: 1662p.

Merah, A., Abidi, A., Merad, H., Gherraf, N., Iezid, M. and Djahoudi, A. 2019. Comparative Study of the Bacteriological Activity of Zinc Oxide and Copper Oxide Nanoparticles. *Acta Scientifica Naturalis*. **6**: 63-72.

Micoli, F., Bagnoli, F., Rappuoli, R. and Serruto, D. 2021. The role of vaccines in combatting antimicrobial resistance. *Nat. Rev. Microbiol.* **19**: 287-302.

Miles, A.A., Misra, S.S. and Irwin, J.O. 1938. The estimation of the bactericidal power of the blood. *Epidemiol. Infect.* **38**: 32-749.

Miri, A., Mahdinejad, N., Ebrahimy, O., Khatami, M. and Sarani, M. 2019. Zinc oxide nanoparticles: Biosynthesis, characterization, antifungal and cytotoxic activity. *Mater. Sci. Eng.* **104**: 109981p.

Mohamed, H.Y., Ismael, E., Elaasser, M.M. and Khalil, M.M. 2021. Green synthesis of zinc oxide nanoparticles using *Portulaca oleracea* (Regla seeds) extract and its biomedical applications. *Egyptian J. Chem.* **64**: 661-672.

Mohamed, M.F., Abdelkhalek, A. and Seleem, M.N. 2016. Evaluation of short synthetic antimicrobial peptides for treatment of drug-resistant and intracellular *Staphylococcus aureus*. *Sci. Rep.* **6**: 1-14.

Mohan, A., Munusamy, C., Tan, Y.C., Muthuvelu, S., Hashim, R., Chien, S.L., Wong, M.K., Khairuddin, N.A., Podin, Y., Lau, P.S.T. and Ng, D.C.E. 2019. Invasive *Salmonella* infections among children in Bintulu,Sarawak, Malaysian Borneo: a 6-year retrospective review. *BMC Infect. Dis.* **19:** 1-11.

Mohd Yusof, H., Rahman, A., Mohamad, R., Hasanah Zaidan, U. and Samsudin, A.A. 2021. Antibacterial Potential of Biosynthesized Zinc Oxide Nanoparticles against Poultry-Associated Foodborne Pathogens: An In Vitro Study. *Animals*. **11**: 2093p.

Morgado, M.E., Jiang, C., Zambrana, J., Upperman, C.R., Mitchell, C., Boyle, M., Sapkota, A.R. and Sapkota, A. 2021. Climate change, extreme events,and increased risk of salmonellosis: foodborne diseases active surveillance network (FoodNet), 2004-2014. *Environ. Hlth.* **20**: 1-11.

Mosmann, T. 1983. Rapid colorimetric assay for cellular growth and survival: application to proliferation and cytotoxicity assays. *J. Immunol. Methods. 65*(1-2), pp.55-63.

Mourdikoudis, S., Pallares, R.M. and Thanh, N.T. 2018. Characterization techniques for nanoparticles: comparison and complementarity upon studying nanoparticle properties. *Nanoscale*. **10**: 12871-12934.

Mughini-Gras, L., van Hoek, A.H., Cuperus, T., Dam-Deisz, C., van Overbeek, W., van den Beld, M., Wit, B., Rapallini, M., Wullings, B., Franz, E. and van der Giessen, J. 2021. Prevalence, risk factors and genetic traits of *Salmonella* Infantis in Dutch broiler flocks. *Vet. Microbiol.* **258**: 109120p.

Mulani, M.S., Kamble, E.E., Kumkar, S.N., Tawre, M.S. and Pardesi, K.R. 2019. Emerging strategies to combat ESKAPE pathogens in the era of antimicrobial resistance: a review. *Frontiers Microbiol.* **10**: 539p.

Muraleetharan, V., Mantaj, J., Swedrowska, M. and Vllasaliu, D. 2019. Nanoparticle modification in biological media: implications for oral nanomedicines. *RSC Adv.* ***9*****:** 40487-40497.

Nair A, Balasaravanan T, Malik SS, Mohan V, Kumar M, Vergis J, Rawool DB. 2015. Isolation and identification of *Salmonella* from diarrheagenic infants and young animals, sewage waste and fresh vegetables. Vet.World. **8**: 669.

Nair, S., Day, M., Godbole, G., Saluja, T., Langridge, G.C., Dallman, T.J. and Chattaway, M. 2020. Genomic surveillance detects *Salmonella enterica* serovar Paratyphi A harbouring bla CTX-M-15 from a traveller returning from Bangladesh. *Plos one*. **15**: .e0228250.

Nandiyanto, A.B.D., Oktiani, R. and Ragadhita, R. 2019. How to read and interpret FTIR spectroscope of organic material. Indones. J. Sci. Tech. **4:** 97-118.

Naseer, M., Aslam, U., Khalid, B. and Chen, B. 2020. Green route to synthesize Zinc Oxide Nanoparticles using leaf extracts of Cassia fistula and Melia azadarach and their antibacterial potential. *Sci. Rep.* **10**: 1-10.

NCCLS [National Committee for Clinical Laboratory Standards]. 1999. Methods for determining bactericidal activity of antimicrobial agents; approved guidelines. Wayne, USA, 19:14

Nisar, P., Ali, N., Rahman, L., Ali, M. and Shinwari, Z.K. 2019. Antimicrobial activities of biologically synthesized metal nanoparticles: an insight into the mechanism of action. *JBIC Journal of Biological Inorg. Chem.* **24**: 929-941.

Nityasree, B.R., Chalannavar, R.K., Kouser, S., Divakar, M.S., Gani, R.S., Sowmyashree, K. and Malabadi, R.B. 2021. Bioinspired synthesis of zinc oxide nanoparticles by using leaf extract of *Solanum lycopersicum* L. for larvicidal activity of *Aedes aegypti* L. *Adv. Nat. Sci. Nanosci. Nanotech.* **12**: 015009p.

Noudeh, G.D., Sharififar, F., Behravan, E., Mohajeri, E. and Alinia, V. 2011. Medicinal plants as surface activity modifiers. *J. Med. Plant. Res.* **5**: 5378-5383.

Ojemaye, M.O., Adefisoye, M.A. and Okoh, A.I. 2020. Nanotechnology as a viable alternative for the removal of antimicrobial resistance determinants from discharged municipal effluents and associated watersheds: A review. *J. Environ. Mgmt.* **275**: 111234p.

Ouali, B.E.F., Chiou, T.H., Chen, J.W., Lin, I.C., Liu, C.C., Chiang, Y.C., Ho, T.S. and Wang, H.V. 2021. Correlation Between PathogenicDeterminants Associated with Clinically Isolated Non-Typhoidal *Salmonella*. *Pathogens*. **10**: 74p.

Pal, M., Teashal, B.M., Gizaw, F., Alemayehu, G. and Kandi, V., 2020. Animals and Food of Animal Origin as a Potential Source of Salmonellosis: A Review of the Epidemiology, Laboratory Diagnosis, Economic Impact and Public Health Significance. *Am. J. Microbiol. Res.* **8**: 48-56.

Park, J.B., Kang, J.H. and Song, K.B. 2019. Clove bud essential oil emulsion containing benzethonium chloride inactivates *Salmonella* Typhimurium and Listeria monocytogenes on fresh-cut pak choi during modified atmosphere storage. *Food Control*. **100**: 17-23.

Park, S.E., Pham, D.T., Pak, G.D., Panzner, U., Espinoza, L.M.C., von Kalckreuth, V., Im, J., Mogeni, O.D., Schutt-Gerowitt, H., Crump, J.A. and Breiman, R.F. 2021. The genomic epidemiology of multi-drug resistant invasive non-typhoidal Salmonella in selected sub-Saharan African countries. *BMJ. Global. Hlth.* **6**: e005659.

Peng, C., Shen, C., Zheng, S., Yang, W., Hu, H., Liu, J. and Shi, J. 2017. Transformation of CuO nanoparticles in the aquatic environment: influence of pH, electrolytes and natural organic matter. *Nanomaterials*. **7**: 326p.

Phongtongpasuk, S., Norasingsatorn, T. and Yongvanich, N. 2019. Effect of pH on the Environmentally Friendly Fabrication of Silver Nanoparticles Using Rambutan Peel Extract. *Key. Engng. Mater*. **824**: 149-155.

Pillai, A.M., Sivasankarapillai, V.S., Rahdar, A., Joseph, J., Sadeghfar, F., Rajesh, K. and Kyzas, G.Z. 2020. Green synthesis and characterization of zinc oxide nanoparticles with antibacterial and antifungal activity. J. Mol. Struct. **1211**: 28107.

Prasad, E.R. and Sivakumar, S.R. 2020. Zinc oxide nanoparticles (ZnO-NPs) via green approach for enhanced antimicrobial activity against food-borne pathogen (F-BP) bacteria.Parishodh J. **9:** 562-576

Prusty, K., Barik, S. and Swain, S.K. 2019. A corelation between the graphene surface area, functional groups, defects, and porosity on the performance of the nanocomposites. Functionalized Graphene Nanocomposites and their Derivatives. **21**: 265-283.

Pulford, C.V., Perez-Sepulveda, B.M., Rodwell, E.V., Weill, F.X., Baker, K.S. and Hinton, J.C., 2019. *Salmonella* enterica serovar Panama, anunderstudied serovar responsible for extraintestinal salmonellosis worldwide. *Infect. Immun.* **87**: e00273-19.

Raina, S.K., 2019. State of the globe: Antimicrobial resistance: Need for de-compartmentalization of action. *J. global Infect. Dis.***11**: 133p.

Rajendran, N.K., George, B.P., Houreld, N.N. and Abrahamse, H. 2021. Synthesis of Zinc Oxide Nanoparticles Using *Rubus fairholmianus* Root Extract and Their Activity against Pathogenic Bacteria. Molecules. **26**: 3029.

Ralte, R., Kumar, V., Wani, M.Y., Randhawa, S.N.S., Malik, A. and Kaur, N. 2019. Antimicrobial resistance profile of livestock and poultry of North- western Punjab. *Int. J. Curr. Microbiol. Appl. Sci*, **8**: 1250-1259.

Ramya, V., Kalaiselvi, V., Kannan, S.K., Shkir, M., Ghramh, H.A., Ahmad, Z., Nithiya, P. and Vidhya, N. 2021. Facile Synthesis and Characterization of Zinc Oxide Nanoparticles Using *Psidium guajava* leaf Extract and Their Antibacterial Applications. *Arab. J. Sci. Eng.* **34**: 1-10.

Rebello, S., Anoopkumar, A.N., Puthur, S., Sindhu, R., Binod, P., Pandey, A. and Aneesh, E.M. 2018. Zinc oxide phytase nanocomposites as contributory tools to improved thermostability and shelflife. *Bioresour. Technol. Rep*. **3**: pp.1-6.

Rezasoltani, S., Yadegar, A., Hatami, B., Aghdaei, H.A. and Zali, M.R. 2020. Antimicrobial resistance as a hidden menace lurking behind the COVID-

19 outbreak: the global impacts of too much hygiene on AMR. *Frontiers. Microbiol.* **11**.

Ribut, S.H., Abdullah, C.A.C., Mustafa, M., Yusoff, M.Z.M. and Azman, S.N.A. 2018. Influence of pH variations on zinc oxide nanoparticles and their antibacterial activity. *Mater. Res. Express*. **6**: 025016p.

Rodrigues, G.L., Panzenhagen, P., Ferrari, R.G., Dos Santos, A., Paschoalin, V.M.F. and Conte-Junior, C.A. 2020. Frequency of antimicrobial resistance genes in *Salmonella* From Brazil by in silico whole-genome sequencing analysis: An overview of the last four decades. *Frontiers. Microbiol.* **11**: 1864p.

Saharan, V.V., Verma, P. and Singh, A.P. 2020. High prevalence of antimicrobial resistance in *Escherichia coli*, *Salmonella* spp. and *Staphylococcus* aureus isolated from fish samples in India. *Aquacult. Res.* **51**: 1200-1210.

Sakarikou, C., Kostoglou, D., Simões, M. and Giaouris, E. 2020. Exploitation of plant extracts and phytochemicals against resistant *Salmonella* spp. in biofilms. *Food Res. Int.* **128***:* 108806p.

Salama, A., Almaaytah, A. and Darwish, R.M. 2021. The Design of Alapropoginine, a Novel Conjugated Ultrashort Antimicrobial Peptide with Potent Synergistic Antimicrobial Activity in Combination with Conventional Antibiotics. *Antibiotics*. **10**: 712p.

Sali, R.K., Pujar, M.S., Patil, S. and Sidarai, A.H. 2021. Green Synthesis of ZnO and Ag-ZnO Nanoparticles using *Macrotyloma uniflorum*: Evaluation of Antibacterial Activity. *Adv. Mater. Lett.* **12**: 1-7.

Sambrook, J. 2001. Preparation and analysis of Eukaryotic Genome DNA. *Mol. Cloning: Lab. Manual*. **1**: 6-1.

Samir, S. 2021. Bacteriophages as Therapeutic Agents: Alternatives to Antibiotics. *Recent Patents. Biotechnol*. **15**: 25-33.

Sánchez-López, E., Gomes, D., Esteruelas, G., Bonilla, L., Lopez-Machado, A.L., Galindo, R., Cano, A., Espina, M., Ettcheto, M., Camins, A. and Silva, A.M. 2020. Metal-based nanoparticles as antimicrobial agents: an overview. *Nanomaterials*. **10**: 292p.

Sanjukta, R., Surmani, H., Mandakini, K., Milton, A., Das, S., Puro, K., Ghatak, S., Shakuntala, I. and Sen, A. 2019. Characterization of MDR and ESBL-producing *E. coli* strains from healthy swine herds of north-eastern India. *Ind. J. Ani. Sci.* **89**: 625-631.

Selim, Y.A., Azb, M.A., Ragab, I. and Abd El-Azim, M.H. 2020. Green synthesis of zinc oxide nanoparticles using aqueous extract of *Deverra tortuosa* and their cytotoxic activities. Sci. Rep. **10:** 1-9.

Sen, K., Berglund, T., Patel, N., Chhabra, N., Ricci, D.M., Dutta, S. and Mukhopadhyay, A.K. 2021. Genotypic analyses and antimicrobial resistance profiles of *Campylobacter jejuni* from crows (Corvidae) of United States and India reflect their respective local antibiotic burdens. *J. Appl. Microbiol.*

Sepasgozar, S.M.E., Mohseni, S., Feizyzadeh, B. and Morsali, A. 2021. Green synthesis of zinc oxide and copper oxide nanoparticles using *Achillea nobilis* extract and evaluating their antioxidant and antibacterial properties. *Bulletin. Mater. Sci.* **44**: 1-13.

Shah, R., Pathan, A., Vaghela, H., Ameta, S.C. and Parmar, K. 2019. Green synthesis and characterization of copper nanoparticles using mixture (*Zingiber officinale, Piper nigrum* and *Piper longum*) extract and its antimicrobial activity. *Chem. Sci.* **8***:* 63-69.

Sharmila, G., Thirumarimurugan, M. and Muthukumaran, C. 2019. Green synthesis of ZnO nanoparticles using *Tecoma castanifolia* leaf extract: characterization and evaluation of its antioxidant, bactericidal and anticancer activities. Microchem. J. **145**: 578-587

Sharma, J., Kumar, D., Hussain, S., Pathak, A., Shukla, M., Kumar, V.P., Anisha, P.N., Rautela, R., Upadhyay, A.K. and Singh, S.P. 2019. Prevalence, antimicrobial resistance and virulence genes characterization of nontyphoidal *Salmonella* isolated from retail chicken meat shops in Northern India. *Food Control.* **102**: 104-111.

Sharma, N.C., Kumar, D., Sarkar, A., Chowdhury, G., Mukhopadhyay, A.K. and Ramamurthy, T. 2019. Prevalence of MDR *Salmonellae* with increasing frequency of *S.* Kentucky and *S.* Virchow serovars among hospitalized diarrheal cases in and around Delhi, India. *Jap. J. Infect. Dis.*.

Sharma, P., Kumari, B., Dahiya, S., Kulsum, U., Kumar, S., Manral, N., Pandey, S., Kaur, P., Sood, S., Das, B.K. and Kapil, A. 2019. Azithromycin resistance mechanisms in typhoidal *Salmonellae* in India: A 25 years analysis. *The Ind. J. Med. Res.* **149**: .404p.

Siddiqi, K.S., ur Rahman, A. and Husen, A. 2018. Properties of zinc oxide nanoparticles and their activity against microbes. *Nanoscale Res. Lett.***13**: 1-13.

Singh, A., Singh, N.A., Afzal, S., Singh, T. and Hussain, I. 2018. Zinc oxide nanoparticles: a review of their biological synthesis, antimicrobial activity, uptake, translocation and biotransformation in plants. *J. Mater. Sci.* **53**: 185-201.

Situmeang, B., Ibrahim, A.M., Bialangi, N., Musa, W.J. and Silaban, S. 2019. Antibacterial activity and phytochemical screening of Kesambi

(Sapindaceae) against *Eschericia coli* and *Staphylococcus aureus*. *J. Pendidikan Kimia*. **11**: 14-17.

Sivagami, K., Vignesh, V.J., Srinivasan, R., Divyapriya, G. and Nambi, I.M. 2020. Antibiotic usage, residues and resistance genes from food animals to human and environment: An Indian scenario. *J. Environ. Chem. Eng.* **8**: 102221p.

Srivastava, P., Shukla, M., Kaul, G., Chopra, S. and Patra, A.K. 2019. Rationally designed curcumin based ruthenium (II) antimicrobials effective against drug-resistant *Staphylococcus aureus*. *Dalton Trans.* **48**: 11822-11828.

Stanaway, J.D., Parisi, A., Sarkar, K., Blacker, B.F., Reiner, R.C., Hay, S.I., Nixon, M.R., Dolecek, C., James, S.L., Mokdad, A.H. and Abebe, G. 2019. The global burden of non-typhoidal *Salmonella* invasive disease: a systematic analysis for the Global Burden of Disease Study 2017. *Lancet.Infect. Dis*. **19**: 1312-1324.

Streicher, L.M. 2021. Exploring the future of infectious disease treatment in a post-antibiotic era: A comparative review of alternative therapeutics. *J. Glob. Antimicrob. Resist.*

Subramaniam, K., Subramanian, S.K., Bhargav, S., Parameswari, R., Praveena, R., Ravikumar, R., Yuvaraj, E. and Kumar, V.M. 2021, April. Review on potential antiviral and immunomodulatory properties of *Piper longum*. *Mater. Sci. Eng.* **1145**: 012099p

Sultana, N.A., Zilani, M.N.H., Taraq, K.T.M. and Al-Din, M.K. 2019. Phytochemical, antibacterial and antioxidant activity of piper longum leaves. *Pharmacol. OnLine*. **1**: 27-35.

Suman Kumar, M., Ramees, T.P., Dhanze, H., Gupta, S., Dubal, Z.B. and Kumar, A. 2021. Occurrence and antimicrobial resistance of *Campylobacter*

isolates from broiler chicken and slaughter house environment in India. *Ani.l Biotechnol.* 1-9.

Tack, B., Vanaenrode, J., Verbakel, J.Y., Toelen, J. and Jacobs, J. 2020. Invasive non-typhoidal *Salmonella* infections in sub-Saharan Africa: a systematic review on antimicrobial resistance and treatment. *BMC Med.* **18**: 1-22.

Taneja, N. and Sharma, M. 2019. Antimicrobial resistance in the environment: The Indian scenario. *The Ind. J. Med. Res.* **149**: 119p.

Tewabe, A., Marew, T. and Birhanu, G. 2021. The contribution of nano-based strategies in overcoming ceftriaxone resistance: a literature review. *Pharmacol. Res. Perspectives*. **9**: e00849.

Thapa, S.P., Shrestha, S. and Anal, A.K., 2020. Addressing the antibiotic resistance and improving the food safety in food supply chain (farm-to- fork) in Southeast Asia. *Food Control*. **108**: 106809p.

Thi, T.U.D., Nguyen, T.T., Thi, Y.D., Thi, K.H.T., Phan, B.T. and Pham, K.N. 2020. Green synthesis of ZnO nanoparticles using orange fruit peel extract for antibacterial activities. *RSC Adv*. **10**: 23899-23907.

Trecarten, S., Zu'bi, F., Beaiti, M. and Papanikolaou, F. 2019. Case–Neonatal epididymo-orchitis: An unusual manifestation of salmonellosis. *Canadian Urolog. Ass. J.* **13:** 303p.

Turlybekuly, A., Pogrebnjak, A.D., Sukhodub, L.F., Sukhodub, L.B.,Kistaubayeva, A.S., Savitskaya, I.S., Shokatayeva, D.H., Bondar, O.V., Shaimardanov, Z.K., Plotnikov, S.V. and Shaimardanova, B.H. 2019. Synthesis, characterization, in vitro biocompatibility and antibacterial properties study of nanocomposite materials based on hydroxyapatite- biphasic ZnO micro-and nanoparticles embedded in Alginate matrix. *Matr. Sci. Engng.* **104**: 109965p.

Ude, I.U., Moses, I.B., Okoronkwo, C., Ovia, K., Okafor, C., Chukwunwejim, C.R., Okata-Nwali, O.D., Iroha, C.S., Akuma, S., Peter, I.U. and Uzoeto, H.O. 2021. Phytochemical properties and antimicrobial activity of *Buchholzia coriacea* and *Psychotria microphylla* leaf extracts onbacterial pathogens isolated from aquatic environments in Nigeria. *Med. Plants Res.* **15**: 232-240.

Umavathi, S., Mahboob, S., Govindarajan, M., Al-Ghanim, K.A., Ahmed, Z., Virik, P., Al-Mulhm, N., Subash, M., Gopinath, K. and Kavitha, C. 2021.Green synthesis of ZnO nanoparticles for antimicrobial and vegetative growth applications: A novel approach for advancing efficient high quality health care to human wellbeing. *Saudi J. Biol.l Sci.* **28**: 1808- 1815.

Varghese, B., Kurian, M., Krishna, S. and Athira, T.S. 2020. Biochemical synthesis of copper nanoparticles using *Zingiber officinalis* and *Curcuma longa*: Characterization and antibacterial activity study. *Mater. Today: Proc.* **25**: 302-306.

Vergis, J., Malik, S.V.S., Pathak, R., Kumar, M., Sunitha, R., Barbuddhe, S.B. and Rawool, D.B. 2019. Efficacy of indolicidin, cecropin a (1-7)-melittin (CAMA) and their combination against biofilm-forming multidrug-resistant enteroaggregative *Escherichia coli*. *Probiotics Antimicrob. Proteins*. p. 1-11.

Viana, C., Sereno, M.J., Pegoraro, K., Yamatogi, R.S., Call, D.R., dos Santos Bersot, L. and Nero, L.A. 2019. Distribution, diversity, virulence genotypes and antibiotic resistance for *Salmonella* isolated from a Brazilian pork production chain. *Int. J. Food Microbiol.* **310**: 108310p.

Vico, J.P., Lorenzutti, A.M., Zogbi, A.P., Aleu, G., Sanchez, I.C., Caffer, M.I., Rosmini, M.R. and Mainar-Jaime, R.C. 2020. Prevalence, associated risk factors, and antimicrobial resistance profiles of non-typhoidal Salmonella

in large scale swine production in Córdoba, Argentina. *Res. Vet. Sci.* **130**: 161-169.

Vidayanti, I.N., Sukon, P., Khaengair, S., Pulsrikarn, C. and Angkittitrakul, S. 2021. Prevalence and antimicrobial resistance of *Salmonella* spp. isolatedfrom chicken meat in upper northeastern Thailand. *Vet. Int. Sci.* **19**.

Vijayakumar, S., Mahadevan, S., Arulmozhi, P., Sriram, S. and Praseetha, P.K. 2018. Green synthesis of zinc oxide nanoparticles using *Atalantia monophylla* leaf extracts: Characterization and antimicrobial analysis. *Mater. Sci. Semicond. Process*. **82**: 39-45.

Vijayakumar, S., Divya, M., Vaseeharan, B., Ranjan, S., Kalaiselvi, V., Dasgupta, N., Chen, J. and Durán-Lara, E.F. 2020. Biogenic Preparation and Characterization of ZnO Nanoparticles from Natural Polysaccharide *Azadirachta indica*. L.(neem gum) and its Clinical Implications. *J. Cluster Sci.* 1-11.

Vijilvani, C., Bindhu, M.R., Frincy, F.C., AlSalhi, M.S., Sabitha, S., Saravanakumar, K., Devanesan, S., Umadevi, M., Aljaafreh, M.J. and Atif, M., 2020. Antimicrobial and catalytic activities of biosynthesized gold, silver and palladium nanoparticles from *Solanum nigurum* leaves. *J Photochem. Photobiol. B: Biol.* **202**: 111713p.

Vinay, S.P. and Chandrasekhar, N. 2021. Structural and biological investigation of green synthesized silver and zinc oxide nanoparticles. *J. Inorg. Organometallic Polym. Mater.* **31**: 552-558.

Viswanathan, A., Rangasamy, J. and Biswas, R., 2019. Functionalized antibacterial nanoparticles for controlling biofilm and intracellularinfections. *Surface Modification Nanoparticles Targeted Drug Delivery*. **23**: 183-206.

Wang, J., Li, J., Liu, F., Cheng, Y. and Su, J. 2020. Characterization of *Salmonella enterica* isolates from diseased poultry in northern China between 2014 and 2018. *Pathogens*, **9**: 95.

Wang, M., Li, Y., Yang, J., Shi, R., Xiong, L. and Sun, Q. 2021. Effects of food-grade inorganic nanoparticles on the probiotic properties of *Lactobacillus plantarum* and *Lactobacillus fermentum*. *LWT*. **139**: 110540p.

WHO. 2017. https://www.who.int/health-topics/foodborne-diseases

WHO. 2020. https://www.who.int/activities/estimating-the-burden-of-foodborne-diseases

Wilson, C.N., Pulford, C.V., Akoko, J., Perez Sepulveda, B., Predeus, A.V., Bevington, J., Duncan, P., Hall, N., Wigley, P., Feasey, N. and Pinchbeck, G. 2020. Salmonella identified in pigs in Kenya and Malawi reveals the potential for zoonotic transmission in emerging pork markets. *PLoS Neglect. Trop. Dis.* **14**: e0008796.

Windiasti, G., Feng, J., Ma, L., Hu, Y., Hakeem, M.J., Amoako, K., Delaquis, P. and Lu, X. 2019. Investigating the synergistic antimicrobial effect of carvacrol and zinc oxide nanoparticles against *Campylobacter jejuni*. *Food Control*. **96***:* 39-46.

Woods, A., Andrian, T., Sharp, G., Bicer, E.M., Vandera, K.K.A., Patel, A., Mudway, I., Dailey, L.A. and Forbes, B. 2020. Development of new in vitro models of lung protease activity for investigating stability of inhaled biological therapies and drug delivery systems. *Eur. J. Pharmaceutics. Biopharmaceutics*. **146**: 64-72.

Wyres, K.L., Nguyen, T.N., Lam, M.M., Judd, L.M., van Vinh Chau, N., Dance, D.A., Ip, M., Karkey, A., Ling, C.L., Miliya, T. and Newton, P.N. 2020. Genomic surveillance for hypervirulence and multi-drug resistance in

invasive Klebsiella pneumoniae from South and Southeast Asia. *Genome Med.* **12**: 1-16.

Xia, T., Lai, W., Han, M., Han, M., Ma, X. and Zhang, L. 2017. Dietary ZnO nanoparticles alters intestinal microbiota and inflammation response in weaned piglets. *Oncotarget*, **8**: 64878p.

Xu, J., Li, Y., Wang, H., Zhu, M., Feng, W. and Liang, G. 2021. Enhanced Antibacterial and Anti-Biofilm Activities of Antimicrobial Peptides Modified Silver Nanoparticles. *Int. J. Nanomed.* **16**: 4831p.

Yadav, V., Krishnan, A. and Vohora, D. 2020. A systematic review on Piper longum L.: Bridging traditional knowledge and pharmacological evidence for future translational research. *J. Ethnopharmacol.* **247***:* 112255p.

Yanagimoto, K., Yamagami, T., Uematsu, K. and Haramoto, E. 2020. Characterization of *Salmonella* isolates from wastewater treatment plant influents to estimate unreported cases and infection sources of salmonellosis. *Pathogens*. **9**: 52p.

Yang, Y., Ashworth, A.J., Willett, C., Cook, K., Upadhyay, A., Owens, P.R., Ricke, S.C., DeBruyn, J.M. and Moore Jr, P.A. 2019. Review of antibiotic resistance, ecology, dissemination, and mitigation in US broiler poultry systems. *Frontiers Microbiol.* **10**: 2639p.

Yaqoob, A.A. and Ibrahim, M.N.M. 2019. A review article of nanoparticles; synthetic approaches and wastewater treatment methods. *Int. Res. J. Eng. Technol*, **6**: 1-7.

Yoo, A., Lin, M. and Mustapha, A. 2021. Zinc Oxide and Silver Nanoparticle Effects on Intestinal Bacteria. *Materials*, **14**: 2489p.

Yusof, H.M., Mohamad, R., Zaidan, U.H. and Samsudin, A.A. 2020. Biosynthesis of zinc oxide nanoparticles by cell-biomass and supernatant of *Lactobacillus plantarum* TA4 and its antibacterial and biocompatibility properties. *Sci. Rep*. **10**: 1-13.

Yusof, H.M., Mohamad, R. and Zaidan, U.H. 2019. Microbial synthesis of zinc oxide nanoparticles and their potential application as an antimicrobial agent and a feed supplement in animal industry: a review. *J. Ani. Sci. Biotechnol.***10**: 1-22.

Zhang, X., Servos, M.R. and Liu, J. 2012. Ultrahigh nanoparticle stability against salt, pH, and solvent with retained surface accessibility via depletion stabilization. *J. Am. Chem. Soc.* **134**: 9910-9913.

Zhang, X.-F., Liu, Z.-G., Shen, W., and Gurunathan, S. 2016. Silver nanoparticles: synthesis, characterization, properties, applications, and therapeutic approaches. *Int. J. Mol. Sci.* **17**:1534.

Zohra, T., Numan, M., Ikram, A., Salman, M., Khan, T., Din, M., Farooq, A., Amir, A. and Ali, M. 2021. Cracking the Challenge of Antimicrobial Drug Resistance with CRISPR/Cas9, Nanotechnology and Other Strategies in ESKAPE Pathogens. *Microorganisms*. **9**: 954p.

Annexures and appendix

ANNEXURE

COMPOSITION OF REAGENTS

Buffered Peptone Water (HiMedia)	**g/L**
Casein enzyme hydrosylate	10.00
Sodium chloride	5.00
Disodium hydrogen phosphate 12 H_2O	9.00
Monopotassium hydrogen phosphate	1.50

Final pH (at 25ºC), 7.0±0.2

Mueller Hinton Agar	**g/L**
Beef infusion	300.0
Casein acid hydrosylate	17.5
Starch	1.5
Agar	7.0

Final pH (at 25ºC), 7.3±0.2

Nutrient Broth	**g/L**
Peptic digest of animal tissue	5.0
Sodium chloride	5.0
Beef extract	1.5
Yeast extract	1.5

Final pH (at 25ºC), 7.4±0.2

Normal Saline Solution (NSS)	**g/L**
Sodium chloride	8.5
Distilled water	1000ml

EMB Agar	**g/L**

Peptic digest of animal tissue	10.000
Dipotassium phosphate	2.000
Lactose	5.000
Sucrose	5.000
Eosin – Y	0.400
Methylene blue	0.065
Agar	13.500

Final pH (at 25ºC), 7.2±0.2

XLD Agar	**g/L**
Yeast extract	3.00
L-Lysine	5.00
Lactose monohydrate	7.50
Sucrose	7.50
Xylose	3.50
Sodium chloride	5.00
Sodium deoxycholate	2.50
Sodium thiosulphate	6.80
Ferric ammonium citrate	0.80
Phenol red	0.08
Agar	13.50

Final pH (at 25ºC), 7.2±0.2

EFFICACY OF GREEN SYNTHESISED ZINC OXIDE NANOPARTICLES AGAINST MULTI-DRUG RESISTANT NON-TYPHOIDAL *SALMONELLA* SPP.

VARSHA UNNI

(19-MVP-33)

ABSTRACT

Submitted in partial fulfilment of the requirement for the degree of

MASTER OF VETERINARY SCIENCE

(Veterinary Public Health)

2021

Faculty of Veterinary and Animal Sciences

Kerala Veterinary and Animal Sciences University

DEPARTMENT OF VETERINARY PUBLIC HEALTH

COLLEGE OF VETERINARY AND ANIMAL SCIENCES

POOKODE, LAKKIDI P.O., WAYANAD 673 576

KERALA, INDIA

ABSTRACT

In the recent wake of antimicrobial resistance, nanotechnology has received remarkable attention and has been considered as a promising interventional tool for treating the drug resistant pathogens. The present study evaluated the antibacterial efficacy of green synthesised Zinc Oxide nanoparticles (ZnO NPs) against multi-drug resistant non-typhoidal *Salmonella* spp. (MDR-NTS). The synthesis and characterisation of ZnO NPs was attempted using the aqueous extract of *Piper longum* catkin. Initially, the characterisation of green synthesised ZnO NPs was performed by UV- Vis spectroscopy, Fourier transform infra- red spectroscopy (FTIR), Thermogravimetric analysis (TGA) and differential thermogravimetric analysis (DTA), powder X-ray diffraction (PXRD), Scanning electron microscopy (SEM) and Transmission electron microscopy (TEM). The green synthesised ZnO NPs exhibited an absorbance peak at 340 nm by UV- Vis spectroscopy, which was confirmed by FTIR analysis. The TGA/DTA revealed a progressive thermal degradation of the ZnO NPs between 250^{o}C and 400^{o}C, however, a good thermal stability was exhibited for annealing temperatures between 900^{o}C and 1300^{o}C. The ZnO NPs exhibited a hexagonal wurtzite crystalline structure by PXRD analysis, which was further confirmed by SEM and TEM. This study evaluated the *in vitro* antibacterial efficacy of ZnO NPs against MDR- NTS strains (*S. enterica* Typhimurium and *S.* Enteritidis (n= 3 for each serotype). The minimum inhibitory concentration (MIC; 125 μg/ml) and minimum bactericidal concentration (MBC; 250 μg/ml) of ZnO NPs was determined by employing microbroth dilution technique. Later, ZnO NPs was also tested for its stability (high- end temperatures, physiological concentration of cationic salts, proteases and pH); safety (chicken RBCs; HEK cell lines) and effect on gut beneficial lactobacilli (*Lactobacillus acidophilus* and *L. plantarum*). In general, the ZnO NPs tested stable at MIC concentration; however, a three to four- fold rise in the MBC value was observed. Besides, ZnO NPs were tested safe with chicken RBCs and HEK cell

lines at MIC (1X, 2X, 5X and 10X) levels; moreover, the beneficial gut lactobacilli were not inhibited. Furthermore, the *in vitro* time- kill kinetic assay of MDR-NTS strains treated with ZnO NPs revealed a complete clearance after 360 min. To conclude, the biosynthesised ZnO NPs was found to exhibit antibacterial activity against the tested MDR-NTS, found stable and safe. Overall, the study demonstrated facile, eco-friendly method for the synthesis of ZnO NPs, which could be employed as a potential antimicrobial alternative candidate.

Acad. Form No.19

KERALA VETERINARY AND ANIMAL SCIENCES UNIVERSITY
Faculty of Veterinary and Animal Sciences
PROGRAMME OF RESEARCH WORK FOR THESIS FOR MASTERS DEGREE

1. Title of thesis:

Efficacy of green synthesised Zinc oxide nanoparticles against multi-drug resistant non-typhoidal *Salmonella* spp.

2.(a)Title of the departmental/KVASU research project of which this forms a part:

Exploiting encapsulated nanoparticle conjugated phytochemicals to combat antimicrobial resistance in poultry

(b) Code No. if any, and order by which the departmental/KVASU research project is approved:

No. KVASU/DAR/R1/35474/2019 dtd. 03/01/2020

3. a) Name of student:

Varsha Unni

b) Admission No.:

19-MVP-33

c) Name of the Discipline:

Veterinary Public Health

4. a) Name of Major Advisor (Guide):

Dr. Jess Vergis

b) Designation:

Assistant Professor,
Department of Veterinary Public Health,
College of Veterinary and Animal Sciences, Pookode, Wayanad- 673 576

5. Objectives of the study:

1. Synthesis and characterisation of green synthesised Zinc oxide nanoparticles (ZnO NPs)
2. Antibacterial activity of green synthesised ZnO NPs against multi-drug resistant non-typhoidal *Salmonella* spp. (MDR- NTS)

6. Practical/Scientific utility:

Salmonellosis, caused by non-typhoidal *Salmonella* spp. (NTS), constitutes the major cause for gastroenteritis worldwide. The most common broad- host range NTS serotypes of public health significance include *S.* Typhimurium and *S.* Enteritidis. Of late, multi-drug resistance has been observed widely among the NTS serotypes.

With the dwindling pipeline in the discovery of effective antibiotics, research has now been targeted towards alternate therapeutic strategies to combat antimicrobial resistance. Nanoparticle- based therapeutics targeting multi-drug resistant (MDR) pathogens has gained attention in the recent past. Hence, the present study is envisaged with an objective to investigate the antimicrobial efficacy of green synthesised ZnO NPs against MDR-NTS strains.

7. Important publications on which the study is based:

Andino and Hanning (2015) reported that *Salmonella* serovars typically produced gastroenteritis and occasionally systemic infections.

Mizan *et al*. (2015) observed that majority of the food-borne outbreaks of salmonellosis have been linked to surface colonisation, thereby troubling food industries as well as clinical settings.

Ramesh *et al*. (2015) found that the green synthesised ZnO NPs were effective against *S*. Paratyphi compared to the standard tablet.

Dobrucka and Długaszewska (2016) noticed that the green synthesised ZnO NPs possessed better antibacterial properties against *Pseudomonas aeruginosa* than the antibiotic, gentamicin.

Antibiotic resistant strains of *Salmonella* spp. have been isolated globally from human patients as well as from animals (both apparently healthy and clinically ill), animal food products, seafoods and fresh produce resulted in consecutive outbreaks within the community (Nair *et al*., 2018).

Horizontal gene transfer, particularly by way of conjugation, was identified as the major factor responsible for antibiotic resistance among NTS strains (Shi *et al*., 2018).

Haubert *et al*. (2019) evaluated the antibiotic susceptibility of 26 *Salmonella* spp. from food and associated sources wherein, 10 isolates (38.50 per cent) presented a phenotypic resistance profile, while 7 isolates (26.90 per cent) exhibited multi- drug resistance pattern.

Gour and Jain (2019) reported that the green synthesis could culminate in the development of safe, eco-friendly NPs and would have wide acceptance in nanotechnology.

Sakarikou *et al*. (2019) observed that the small size of nanoparticles not only allowed the direct transport of compounds into the site of infection, but also enhanced their antimicrobial efficacy by increasing the contact area to volume ratio.

Varghese *et al*. (2020) reported that ZnO NPs, due to the generation of reactive oxygen species on the oxide surface, were resistant to microorganisms.

8. Outline of the technical programme:

The MDR-NTS isolates (*S*. Typhimurium and *S*. Enteritidis; n= 3 for each serotypes) maintained in the Zoonoses laboratory of Department of Veterinary Public Health, CVAS, Pookode will be used for the study.

The isolates will be revived and re-validated using PCR assay (Nair *et al*., 2015) and antibiotic susceptibility testing (CLSI, 2019).

Green synthesis of ZnO NPs will be carried out as per Khoobchandani *et al*. (2019) using the dried spike extract of Indian long pepper (*Piper longum*). In order to characterise the synthesised ZnO NPs, UV- Vis spectrophotometry, Fourier-transform infrared spectroscopy (FTIR), dynamic light scatter (DLS) and scanning electron microscopy (SEM) will be performed (Khoobchandani *et al*., 2019).

The minimum inhibitory concentration (MIC) as well as minimum bactericidal concentration (MBC) of ZnO NPs against MDR-NTS isolates will be determined (CLSI, 2019).

The green synthesised ZnO NPs will be tested for its stability at high-end temperatures (70^{o}C and 90^{o}C), proteases(proteinase-K and trypsin) and physiological concentration of cationic salts (150 mM sodium chloride and 2 mM magnesium chloride) as per Vergis *et al*. (2019).

In order to ensure safety of the ZnO NPs, haemolytic assay and cytotoxicity assays using human epithelial (HEp-2) cell lines will be performed (Vergis *et al*., 2019). Further, the ZnO NPs will be tested for its activity against commensal gut lactobacilli (Vergis *et al*., 2019).

In vitro time- and concentration-dependent killing kinetics of MDR-NTS strains treated with green synthesised ZnONPs will be performed (Vergis *et al*., 2019).

The green synthesised ZnO NPs, if found effective *in vitro*, will be tested *in vivo* in *Galleria mellonella* larvae (Vergis *et al*., 2019) and further confirmed in Swiss albino mice (Kumar *et al*., 2016) model for its antimicrobial efficacy.

For *G. mellonella* larval experiments, the following groups will be formed for each MDR-NTS serotypes with 40 final instar larvae (approximately 200 to 250 mg) per group: Group I (infected group), Group II (ZnO NP treatment group), Group III (PBS control), Group IV (ZnO NP control) and Group V (*P. longum* control). The larvae of groups I and II will be infected with cocktail of MDR-NTS strains; group II will be administered MIC dose of ZnO NPs (10 µL); group III will be injected with sterile PBS (10 µL) whereas, groups IV and V will be administered with ZnO NPs and *P. longum* extract (10 µL), respectively. The larvae will then be observed for their melanisation and survival till 120 h post-infection.

For *in vivo* mice experiments, weaned Swiss albino mice (n=72) of three to four

weeks of age weighing approximately 18 to 20 g will be used. The mice for each MDR- NTS serotypes will be grouped as follows: 12mice each in infected group (Group I) and treatment group (Group II) as well as four mice each in phosphate buffered saline (PBS)control (Group III), ZnO NP control (Group IV) and *P. longum* extract control (Group V). Mice of groups I and II will be infected orallywith MDR-NTS strains (cocktail of MDR-NTS strains) using 22 gauge (G) feeding needles, whereas mice of group III will be fedorally with sterile PBS. Similarly, mice of groups II and IV will be fed orally with ZnO NP, while those of group V with *P. longum* extract using 22 G feeding needle. The mice will be monitored for its clinical signs and survivability.

The results obtained will further be analysed using relevant statistical tools (SPSS version 24.0).

9. Main items of observations to be made:

1. Absorbance of ZnO NPs
2. Hydrodynamic size, functional groups and morphology of ZnO NPs
3. MIC and MBC values of ZnO NPs
4. *In vitro* temperature, protease and cationic salt stability of ZnO NPs
5. *In vitro* haemolysis and cytotoxicity percentage of ZnO NPs
6. *In vitro* time- and concentration-dependent log reduction in MDR-NTS counts treated with ZnO NPs
7. *In vivo* survival rate of infected larvae and Swiss albino mice treated with ZnO NPs

10. Facilities required:

(a) Existing:

Work will be commenced with the existing facilities available in the Department of Veterinary Public Health, other Departments and Central Instruments Laboratory of College of Veterinary and Animal Sciences, Pookode and Mannuthy.

(b) Additional facilities required:

Chemicals and Biologicals

11. Duration of study:

Four semesters

12. Financial estimate:

Cost of chemicals, biologicals and contingencies	: Rs. 25,000

Total	: Rs. 25,000

Signature of student

Project coordination group to which the proposal is to be placed: Animal Biotechnology

Signature of Major Advisor

Place: Pookode

Date: 05.03.2020

Name and signature of members ofAdvisory Committee:

1. Dr. Jess Vergis
   Assistant Professor
2. Dr. Latha C.
   Professor and Head
3. Dr. Prejit
   Assistant Professor and Head (i/C)
4. Dr. Lijo John
   Assistant Professor

APPENDIX-I

References:

Andino, A. and Hanning, I. 2015. *Salmonella enterica*: survival, colonization, and virulence differences among serovars. *Sci. Wld. J.* **2015**: 1-16.

CLSI [Clinical and Laboratory Standards Institute]. 2019. *Performance Standards for Antimicrobial Susceptibility Testing.* (29th Ed.). Wayne, USA, 241p.

Dobrucka, R. and Długaszewska, J. 2016. Biosynthesis and antibacterial activity of ZnO nanoparticles using *Trifolium pratense* flower extract. *Saudi J. Biol. Sci.* **23**: 517-523.

Gour, A. and Jain, N.K. 2019. Advances in green synthesis of nanoparticles. *Artif. cells Nanomed. Biotechnol.* **47**: 844-851.

Haubert, L., Zehetmeyr, M.L., Pereira, Y.M.N., Kroning, I.S., Maia, D.S.V., Sehn, C.P. and da Silva, W.P. 2019. Tolerance to benzalkonium chloride and antimicrobial activity of *Butia odorata* Barb. Rodr. extract in *Salmonella* spp. isolates from food and food environments. *Food Res. Int.* **116**: 652– 659.

Khoobchandani, M., Katti, K.K., Karikachery, A.R., Thipe, V.C., Bloebaum, P.L. and Katti, K.V. 2019. Targeted phytochemical-conjugated gold nanoparticles in cancer treatment. In: Khoobchandani, M. and Saxena, A. (eds.), *Biotechnology Products. in Everyday Life*. EcoProduction, USA, pp. 37-52.

Kumar, M., Dhaka, P., Vijay, D., Vergis, J., Mohan, V., Kumar, A., Kurkure, N.V., Barbuddhe, S.B., Malik, S.V.S. and Rawool, D.B. 2016. Antimicrobial effects of *Lactobacillus plantarum* and *Lactobacillus acidophilus* against multidrug-resistant enteroaggregative *Escherichia coli*. *Int. J. Antimicrob. Agents.* **48**: 265-270.

Mizan, M.F.R., Jahid, I.K. and Ha, S.D. 2015. Microbial biofilms in seafood: a food-hygiene challenge. *Food Microbiol.* **49**: 41-55.

Nair, A., Balasaravanan, T., Malik, S.V.S., Mohan, V., Kumar, M., Vergis, J. andRawool, D.B. 2015. Isolation and identification of *Salmonella* from diarrheagenic infants and young animals, sewage waste and fresh vegetables. *Vet. Wld.* **8**: 669-673.

Nair, D., Venkitanarayanan, K. andKollanoor J.A. 2018. Antibiotic-resistant *Salmonella* in the food supply and the potential role of antibiotic alternatives for control. *Foods,* **7**: 167.

Ramesh, M., Anbuvannan, M. and Viruthagiri, G. 2015. Green synthesis of ZnO nanoparticles using *Solanum nigrum* leaf extract and their antibacterial activity. *Mol. Biomol. Spect.* **136**: 864-870.

Sakarikou, C., Kostoglou, D., Simões, M. and Giaouris, E. 2019. Exploitation of plant extracts and phytochemicals against resistant *Salmonella* spp. in biofilms. *Food Res. Int.* **128***:* 1-63.

Shi, H., Zhou, X., Zou, W., Wang, Y., Lei, C., Xiang, R., Zhou, L., Liu, B., Zhang, A. and Wang, H. 2018. Co-occurrence of biofilm formation and quinolone resistance in *Salmonella enterica* serotype Typhimurium carrying an IncHI2-type *oqx*AB-positive plasmid. *Microb. Pathog.* **123**: 68-73.

Varghese, R.J., Zikalala, N. and Oluwafemi, O.S. 2020. Green synthesis protocol on metal oxide nanoparticles using plant extracts. *Colloidal Metal Oxide Nanoparticles*. Elsevier, USA, 82p.

Vergis, J., Malik, S.V.S., Pathak, R., Kumar, M., Sunitha, R., Barbuddhe, S.B. and Rawool, D.B. 2019. Efficacy of indolicidin, cecropin a (1-7)-melittin (CAMA) and their combination against biofilm-forming multidrug-resistant enteroaggregative *Escherichia coli*. *Probiotics Antimicrob. Proteins.* p. 1-11.

APPENDIX II

Time frame of work

Semester I

1. Collection of literature
2. Preparation of research proposal
3. Revival of MDR-NTS serotypes

Semester II

1. Maintenance of MDR-NTS serotypes
2. PCR-based re-validation of MDR-NTS serotypes
3. Antibiotic susceptibility testing of the revived MDR-NTS serotypes

Semester III

1. Maintenance of MDR-NTS serotypes
2. Synthesis and characterisation of ZnO NPs
3. *In vitro* safety, stability and killing kinetic assays of ZnO NPs
4. *In vivo* antimicrobial assays of ZnO NPs

Semester IV

1. Analysis of data and interpretation of results
2. Preparation and submission of thesis

CERTIFICATE

Certified that the research project has been formulated observing the stipulations laid down under the Prevention of Cruelty to animals Act (Amendment, 1998).

Place: Pookode
Date: 05.03.2020

Dr. Jess Vergis
Major Advisor

Curriculum vitae

CURRICULUM VITAE

Name	-	Varsha Unni
D. O. B	-	12-02-1994
Nationality	-	Indian
Father's name	-	V Unnikrishnan Nair
Name	-	V Usha Devi
Address	-	Ambattu Cheruthana PO, Karuvatta Alappuzha (Dist), Kerala, Pin -690517
E-mail	-	varshaunni888@gmail.com

Academic qualification

Qualification	University/board	Institution	OGPA	Year of passing
BVSc &AH	Kerala Veterinary and Animal Sciences University, Pookode, Wayanad, Kerala	College of Veterinary and Animal Sciences, Mannuthy, Thrissur	8.518	2019
MVSc	Kerala Veterinary and Animal Sciences University, Pookode, Wayanad, Kerala	College of Veterinary and Animal Sciences, Pookode, Wayanad	Ongoing	
PGDOH	Kerala Veterinary and Animal Sciences University, Pookode, Wayanad, Kerala	Centre for One Health Education, Advocacy, Research and Training, Pookode, Wayanad	8.58	2022

Membership in professional bodies : Kerala State Veterinary Council (KSVC)

Member of World Veterinary Poultry Association(WVPA), Indian Branch